

# **ANALYSIS OF SHOWER COOLING TOWERS**

A major project report submitted

In partial fulfillment of the requirements for the award of the degree of

**MASTER OF ENGINEERING**

**(Thermal Engineering)**

By

**MANISH PAL**

**ME (part time)**

**University Roll No.12631**

Under the able guidance of

**Dr. S.S. Kachhwaha**

**Prof. R.S. Mishra**



**Department of Mechanical Engineering,  
Delhi College of Engineering, Delhi - 110 042**

**University of Delhi**

**Session 2006-09**

**Department of Mechanical Engineering,  
Delhi College of Engineering, Delhi- 110042**



**CERTIFICATE**

This is to certify that the Major project entitled “**Analysis of shower cooling towers**” which is being submitted by Shri MANISH PAL, is the authentic record of student’s own work carried out by him under our guidance and supervision for partial fulfillment of the award of the degree of Master of Engineering (Thermal Engineering), Department of Mechanical Engineering, Delhi College of Engineering, University of Delhi.

The matter embodied in this project has not been submitted for the award of any other degree.

**(Prof. R.S.Mishra)**  
Professor  
Department of Mechanical Engg.  
Delhi College of Engineering, Delhi

**(Dr. S.S. Kachhwaha)**  
Assistant Professor  
Department of Mechanical Engg.  
Delhi College of Engineering, Delhi

## ACKNOWLEDGEMENT

It is a great pleasure to have the opportunity to extend my heartiest felt gratitude to everybody who helped me throughout the course of this major project.

It is distinct pleasure to express my deep sense of gratitude and indebtedness to my learned supervisors **Dr. S.S. Kachhwaha**, Assistant Professor and **Dr. R.S. Mishra**, Professor, in the Department of Mechanical Engineering, Delhi College of Engineering for their invaluable guidance, encouragement, and patient review. Their continuous inspiration only has enabled me to complete this major project.

I would also like to take this opportunity to present my sincere regards to my teachers for their kind support and encouragement.

I am thankful to my family members, friends and colleagues for their unconditional support and motivation.

**MANISH PAL**

**College Roll No.15/Thr /2006**

**University Roll No. 12631**

# CONTENTS

	Page No.
<b>Certificate</b>	I
<b>Acknowledgement</b>	III
<b>contents</b>	IV
<b>Abstract</b>	V
<b>Nomenclature</b>	VI
<b>List of Figures</b>	VII
<b>List of Tables</b>	VIII
<b>1. INTRODUCTION</b>	
1.1 Air water interaction	1
1.2 Type of Cooling towers	2
1.2.1 Pact Cooling Tower (PCT)	2
1.2.2 Limitations of PCT	4
1.2.3 Shower Cooling Tower(SCT)	4
1.2.3.1 Shower ventilation cooling tower	5
1.2.3.2 General shower cooling tower	12
1.2.3.3 Advantage of shower cooling tower	13
1.3 Motivation	14
1.4 Organization of report	15
<b>2. LITERATURE REVIEW</b>	
2.1 Summary	16

2.2	Conclusion	21
2.3	Objective of the present work	21
<b>3</b>	<b>MATHEMATICAL MODEL FORMULATION</b>	
3.1	Introduction	22
3.2	Heat and mass transfer formulation in downdraft Shower cooling tower	22
3.2.1	Conservation of mass for water droplet	25
3.2.2	Conservation of momentum for water droplet	27
3.2.3	Conservation of energy for water droplet	30
3.2.4	Thermal balance equations in Shower Cooling Tower	34
3.2.5	Mass balance equation in Shower Cooling Tower	37
3.2.6	Heat transfer on the wall of the Tower	37
3.2.7	Multi Droplet Diameter model based on Rosin- Rammler distribution	39
3.2.8	Total number of equations due to distribution of droplet diameter	42
3.3	Heat and mass transfer formulation in Counter flow Shower cooling tower	44
3.3.1	Governing equations in counter flow for unsaturated air	45
3.3.2	Governing equations in counter flow for supersaturated air	47
3.4	Exergy formulations	49
3.5	Exergy Destruction	59

<b>4. SIMULATION STUDIES AND DISCUSSIONS</b>	
4.1 Simulation studies for parallel flow downdraft SCT	<b>61</b>
4.1.1 Boundary conditions	<b>61</b>
4.1.2 Simulation procedure	<b>62</b>
4.1.3 Model validation	<b>65</b>
4.1.4 Parametric study	<b>68</b>
4.1.5 Exergy analysis	<b>81</b>
4.2 Simulation studies for Counter flow cooling tower	<b>88</b>
4.2.1 Simulation procedure	<b>88</b>
4.2.2 Boundary conditions	<b>90</b>
4.2.3 Model validation	<b>90</b>
4.2.4 Parametric study	<b>91</b>
<b>5. CONCLUSION AND FUTURE SCOPE OF WORK</b>	
5.1 Conclusion	<b>95</b>
5.2 Future Scope	<b>96</b>
Appendix	<b>97</b>
Reference	<b>108</b>

## Abstract

Cooling towers are heat exchangers that are used to dissipate large heat load to the atmosphere. In conventional tower due to salt deposition on the packing and subsequent blockage, the use of tower packing is not practical. A cooling tower without packing is an ideal choice to overcome it; hence a type of evaporative cooling tower without fill is described briefly in this report. A SHOWER COOLING TOWER can be used for comfort air cooling in buildings or in power & process industry where circulating water cooling is main criterion. Both the applications i.e. Dwindraft cooling tower and general shower cooling tower are analyzed in this report.

A computer program is developed in MATLAB software to solve design and performance analysis problems of mechanical draft shower cooling towers. Various subroutines to calculate mean temperature, specific heat of water, vapor pressure, humidity ratio, latent heat, enthalpy for dry air and air-water vapor mixture, Lewis number etc. were made using the respective equations and then introduced in the main programs to calculate the required parameters by the use of ordinary differential equation solver **ode45**.

The various input are provided to program and results are checked for validation by the experimental data for down draft shower cooling tower as well as counter flow cooling tower

**Key words:** Cooling tower, Heat transfer, Lewis number, water outlet temperature.

## List of figures

<b>Figure No.</b>	<b>Title</b>
Figure 1.1	Conventional pact cooling tower
Figure 1.2	Direction of air flow in PDESCT
Figure 1.3	Nozzle configuration and water supply
Figure 1.4	Section of the shower tower design and perspective section
Figure 1.5	schematic section of an active downdraft evaporative shower cooling tower and temperature profile
Figure 1.6	Schematic representation of General shower cooling tower
Figure 3.1	Schematic representation of downward vertical parallel flow
Figure 3.2	Control volume for mass flow along length $dz$
Figure 3.3	Schematic of forces acted on the water droplet sprayed downward at an angle $\theta$
Figure 3.4	Velocity vector diagram of water droplet and air
Figure 3.5	Energy exchange at the water droplet level
Figure 3.6	Control volume of vertical downward parallel flow
Figure 3.7	A typical Rosin-Rammler distribution curve for droplet diameter range
Figure 3.8	Control volume in counter flow shower cooling tower
Figure 3.9	Schematic representation of counter flow shower cooling tower
Figure4.1.	Flow chart of numerical solution
Figure 4.2	Flow chart of mathematical model



- Figure 4.3**      **Variation of rate of flow of water with height of the tower**
- Figure 4.4**      **Variation of rate of water vapor added in air with height of the tower**
- Figure 4.5**      **Net enthalpy with height of tower**
- Figure 4.6**      **Air temperature along tower height**
- Figure 4.7**      **Specific humidity along tower height**
- Figure 4.8**      **Air temperature and Specific humidity along tower height**
- Figure 4.9**      **Air temperature and Specific humidity along tower height**
- Figure4.10**      **Air temperature and Specific humidity along tower height for multi droplet model**
- Figure 4.11**      **Retention Time of Different sized droplets (10 droplets)**
- Figure 4.12**      **Air temperature and Specific humidity along tower height ( $t_w=18^0\text{C}$ )**
- Figure 4.13**      **Air temperature along tower height ( $t_w=20^0\text{C}$ )**
- Figure 4.14**      **Air temperature along tower height( $t_w=25^0\text{C}$ )**
- Figure 4.15**      **Water temperature variations**

- Figure 4.16** Water temperature distributions among droplets
- Figure 4.17** Droplet trajectories of 15 droplets at an angle  $54^{\circ}$  from horizontal
- Figure 4.18** Droplet trajectories of 15 droplets at an angle  $70^{\circ}$  from horizontal,
- Figure 4.19** Absolute Speed of Droplets with height  $\theta=54^{\circ}$
- Figure 4.20** Absolute Speed of Droplets with height  $\theta=54^{\circ}$ ,  $u_d=6\text{m/s}$
- Figure 4.21** Air temperature and specific humidity along tower height
- Figure 4.22** Exergy and mass flow rate of water
- Figure 4.23** Convective exergy of air
- Figure 4.24** Evaporative Exergy of Air
- Figure 4.25** Exergy Destruction
- Figure 4.26** Flow chart of numerical solution of counter flow
- Figure 4.27** Influence of initial velocity and diameter on the outlet temperature for air velocity  $0.97\text{m/s}$
- Figure 4.28** Effect of mean diameter on the retention time of the water droplet
- Figure 4.29.** Effect of mean diameter and air velocity on the outlet water

## **List of Tables**

<b>Table No.</b>	<b>Title</b>
<b>Table 4.1</b>	<b>Field testing and result</b>
<b>Table 4.2</b>	<b>Initial conditions used for simulation program.</b>
<b>Table 4.3</b>	<b>Effect on exit air by variation in inlet droplet diameter</b>
<b>Table 4.4</b>	<b>Effect of variation in inlet water temperature on air outlet condition</b>
<b>Table 4.5</b>	<b>Effect of variation of projection angle on air outlet properties</b>
<b>Table 4.6</b>	<b>Field testing and result for counter flow</b>

## 1.1 Air water interaction

The use of water to control the air properties (DBT, WBT or RH), is not an innovative technique. Historical use of evaporation cooling to cool incoming air is well known in old civilization. The heat transfer takes place between air and water in two modes:

### a) Convective heat transfer

Here the heat transfer takes place due to the temperature gradient exists between air and water. The temperature of air and water raised or lower by this mode of heat transfer only until a thermal equilibrium reached.

### b) Evaporative heat transfer

In evaporative heat transfer air is passed through a continuously recirculation water sprays, the water soon attain a temperature equal to WBT of incoming air which remains constant as long as WBT of incoming air does not change. Hence evaporation of water takes places due to the higher vapor pressure of spray water than the vapor in the air adding moisture to the air stream. Since water temperature is lower than DBT of air (water temperature being equal to WBT of air), there is some sensible cooling caused drop in the DBT of air. But sensible heat lost by the air is equal to latent heat gain by the addition of water vapor to the air. As the total heat content does not change, WBT of air remain same while the DBT of air drops down, and RH goes up.

Air water interactions caused by water spray in air are employed in the following applications:

- 1) **Cooling tower** which is a heat rejection device, which extracts waste heat to the atmosphere through the cooling of a working fluid to near the wet-bulb air temperature. Cooling towers are used to cool water as in conventional pact Cooling Tower (PCT) and general Shower cooling tower (SCT).
- 2) In **Air conditioning** to reduce DBT and increase RH of incoming air if air is hot and dry, Downdraft shower cooling tower provides comfort condition in a large semi enclosed inhabited space [1].
- 3) **Gas turbine power plant** to enhance performance of plant by fogging of intake air .

## 1.2 Type of Cooling Towers

Cooling towers as per their construction and applications can be classified as

- 1) Pact Cooling Tower ( **PCT**)
- 2) Shower Cooling Tower (**SCT**)

### 1.2.1 Pact Cooling Tower

Figure 1.1 represents a conventional pact cooling tower which is an enclosed structure with internal means to distribute the warm water fed to it over a labyrinth-like packing or “fill.” The fill provides a vastly expanded air-water interface for heating of the air and evaporation to take place. The water is cooled as it descends through the fills by gravity while in direct contact with air that passes over it. The cooled water is then collected in a cold water basin below the fill from which it is pumped back through the process to absorb more heat. The heated and moisture laden air leaving the fill is

discharged to the atmosphere at a point remote enough from the air inlet to prevent its being drawn back into the cooling tower.

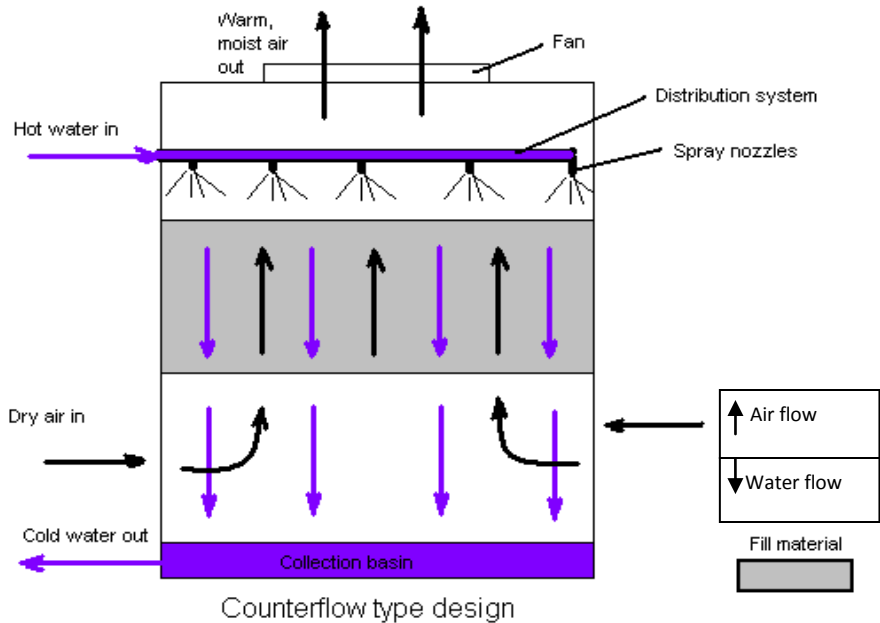


**Figure 1.1 Conventional pact cooling tower**

The fill may consist of multiple, mainly vertical, wetted surfaces upon which a thin film of water spreads (film fill), or several levels of horizontal splash elements which create a cascade of many small droplets that have a large combined surface area (splash fill).

When air circulation through the cooling tower is by natural convection, the cooling tower is called a natural draft cooling tower. When the air circulation through the cooling tower is by the action of a fan or blower, the cooling tower is called a mechanical draft cooling tower. Mechanical draft cooling towers may be further classified as

- (a) Induced draft cooling towers,
- (b) Forced draft cooling towers,

### **1.2.2 Limitation of pack cooling tower**

In the conventional cooling tower (PCT), fills which acts as media to distribute the water current & provide great surface area for contact between the air and water are subjected to fouling during operation, which reduces the tower's efficiency and capability with time. On the other hand, the existence of the fills increases the draught drag extremely, which is the main part of its power consumption. So the general disadvantages are

- 1) Lower temperature drop of air and water.
- 2) Higher power consumption and noise of the motor.
- 3) Fills are easy to get blocked.
- 3) Unstable cooling effect.
- 4) Difficulty for the fills to be replaced and cleaned.
- 5) Electric fan is easy to be damaged.

### **1.2.3 Shower cooling tower (SCT)**

In view of the disadvantage of the conventional packed cooling tower (PCT), a new type of shower cooling tower (SCT) is developed in which the fills are eliminated completely and thin water droplets replace the fills as the mode of mass transfer. In SCT the circulating water is separated into small droplets in spray distribution water zone and the drenching zone in which normal heat transfer can be accomplished without fill and the circulating water can be cooled to the anticipated temperature.

The selection of a shower cooling tower depends on the desired consumer's requirement whether it would be used to cool incoming air or to cool circulating water.

Based on the applications, the shower cooling tower is classified as:

1. Shower ventilation cooling tower
2. General shower cooling tower

### **1.2.3.1 Shower ventilation cooling tower**

The shower ventilation cooling tower is used to cool the air to provide comfort conditions for occupants.

The *principle* of evaporative cooling is based on the relatively large amount of energy required to convert water from its liquid form into its gaseous form, vapor. While the heat energy required to raise the temperature of water by 1°C is a mere 4.18 kJ/kg, the specific latent heat of vaporization is 2257kJ/kg. In the case of an evaporative cooling system, this energy is supplied primarily by the intake air, whose heat content and capacity to hold vapor are indicated by its dry bulb temperature and relative humidity. The combined high temperature and low humidity typical of daytime summer air in hot climate provide promising conditions for the efficient, large-scale utilization of the evaporative process for cooling of inhabited spaces.

With respect to the drawing air through the tower it is further classified as

- a) Passive down draft evaporative shower tower (Natural draft)
- b) Active down draft evaporative shower tower (force draft)



### **c) Passive Down Draft Evaporative Shower Cooling Tower (PDESCT)**

In this system, the ambient air enters the tower at the top, is cooled by the evaporation of water, and leaves the tower at the bottom (Fig. 1.2). The exit air, with a lower dry-bulb temperature and a higher relative humidity than that of the ambient, is supplied into the lowest part of a building complex, thus providing cooling for the occupants of the space. The thermal force driving the air through a PDESCT is created by the introduction of water at the top of the tower. Initial cooling may be caused by the evaporation of water in the form of a fine spray. The water drops fall through the tower, so that the air inside it remains moist - close to saturation, if sufficient water is provided. Since the density of a gas is inversely proportional to its temperature, the cooler air inside the cool tower is denser than the ambient air. The force driving the air through the tower may be calculated by integrating this density difference along the height of the tower and multiplying by the acceleration due to gravity [1]. The magnitude of the thermos phonic force thus depends on the temperature difference between the air at the inlet at the top of the tower and the outlet at the bottom. This difference is greatest if the ambient air is warm and very dry; if enough water is added to the airflow to produce saturation conditions throughout the length of the tower; and if the height of the tower is large.

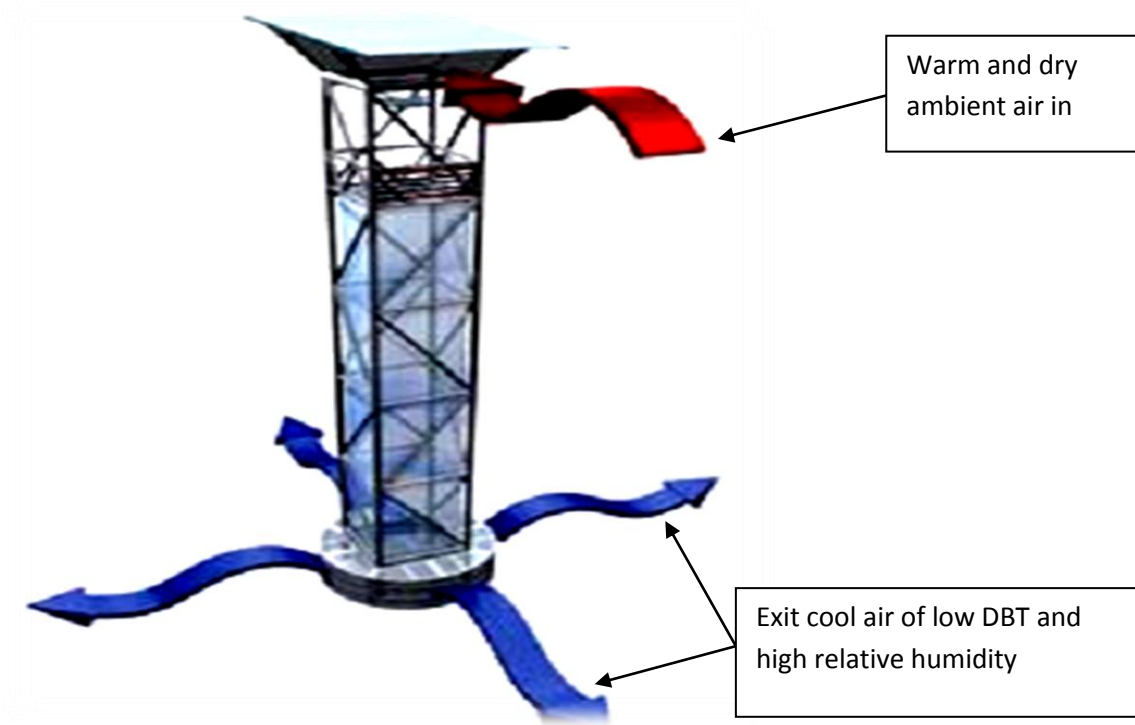


**Fig.1.2 Direction of air flow in PDESCT [2]**

In fig 1.3 a plan view of nozzle configuration is shown, a metal rings supports the header pipes containing the spray nozzles. A heavy duty piping runs up to the headers from a valve arrangement below the tower as shown in fig. 1.4. The valve arrangement includes a water meter and a filter. Water is supplied via a flexible hose connected to an outlet in the floor bellow the tower. In PDESCT two types of nozzles are used, a single high flow nozzle with large orifice and a pin to break up the water stream, and 9 nozzles with the mist generated by the smaller diameter of the orifice to distribute the spray

better. The nozzles are arranged so that water can be supplied in steps of 1, 3 or 6 nozzles or any addition of that number as per requirement.

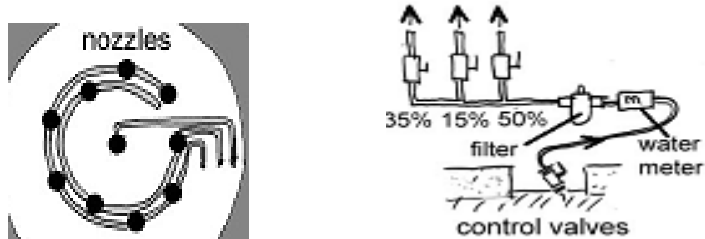


**Fig 1.3 Nozzle configuration and water supply [3]**

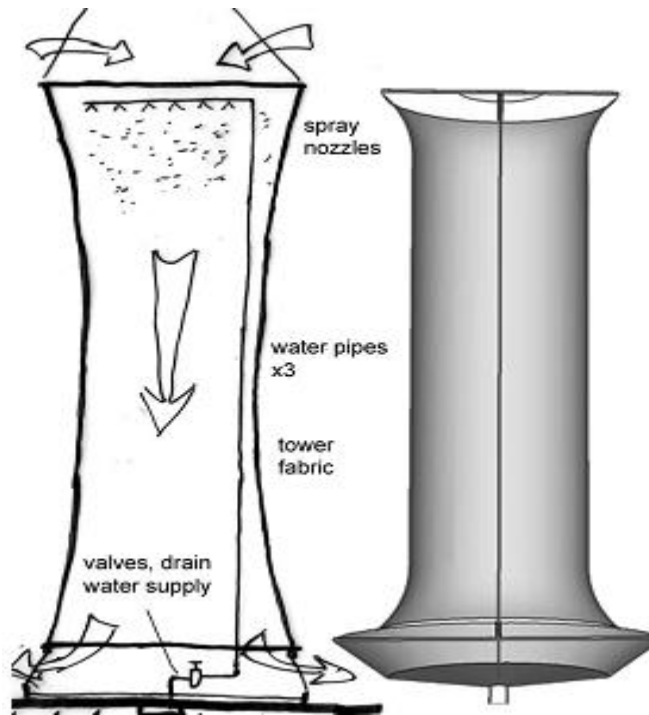


**Fig. 1.4 Section of the shower tower design and perspective section [3]**

In Fig. 1.4 elevated section of the PDESCT tower is shown, the special design facilitates to force the air to change direction at bottom of the tower and water droplets that have not evaporated are dropped out onto the periphery to drain via the floor drain adjacent to the water supply [3].

### **b) Active downdraft evaporative shower cooling tower**

In PDESCT maximum cooling occurs if the air is brought to saturation but the air cannot be cooled by evaporation beyond the thermodynamic wet-bulb temperature. Once this temperature is reached, the only means of increasing the cooling output of an evaporative cool tower of a given height is to increase the air flow rate, while maintaining the outlet temperature at the dew point.

Increasing the cooling output of a down-draft evaporative cooling tower of moderate height thus requires a larger flow rate than can be attained by free convection alone. This implies the utilization of a mechanical fan to force air through the tower. Such type of forced draft cooling towers is known as *active downdraft evaporative shower cooling tower*.

In Fig. 1.5 a schematic diagram of an active downdraft evaporative shower cooling tower is shown, in which mechanical forced air flow is utilized .The tower has a steel pipe frame structure and lightweight rigid envelope. A propeller fan at the top of the tower introduced ambient air into the tower at a measured rate ( $\text{m}^3/\text{hr}$ ).The air stream passes through a spray of water droplets, which are directed downwards

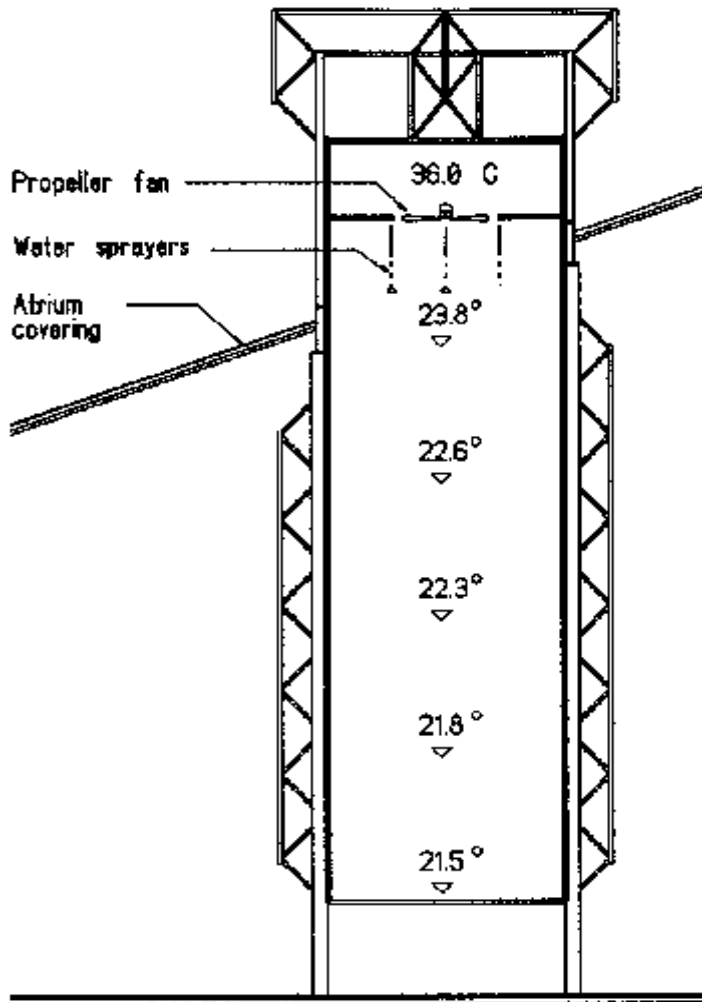


**Fig 1.5 schematic section of an active downdraft evaporative shower cooling tower and temperature profile [4]**

together with the air. A typical temperature profile a particular summer daytime operation is also depicted, which shows decrease in air temperature by about 15°C by this cooling tower.

By Monitoring temperature and humidity by electronic sensors at its inlet and outlet, the airflow rate for each system can be calculated according to measured airspeeds and the effective opening area of the air supply system. Based on the

temperature differential and rate of airflow through the system, the capacity for air cooling, or maximum cooling power ( $P_{max}$ ) of each system (PDESCT and ADESCT) can be calculated by the relation [4],

$$P = \rho A u C_p \Delta t \text{-----} (1)$$

In which:

$P$ = cooling power (Kw)

$A$ = cross- sectional area of entry (fan) opening ( $m^2$ )

$u$ =velocity of air flow (m/s)

$\Delta t$ = maximum temperature differential between entry and exit air ( $^{\circ}C$ )

$C_p$ = specific heat of air (kJ/kg  $^{\circ}C$ )

$\rho$  = Density of air ( $kg/m^3$ )

Calculation of the cooling power for each system is further modified [4], to normalize for varying ambient conditions, yielding an overall cooling performance factor ( $P_{norm}$ )

$$P_{norm} = P (\omega_s - \omega)_1 / (\omega_s - \omega) \text{-----} (2)$$

Where  $P$  is cooling power (kW) [Eq. (1)],  $\omega$  the moisture content of ambient air (kg/kg dry air),  $\omega_s$  the moisture content of ambient air at saturation (kg/kg dry air), and  $(\omega_s - \omega)_1$  the difference between  $\omega_s$  and  $\omega$  at the given hour for the reference configuration.

### 1.2.3.2 General Shower Cooling Tower (GSCT)

The general shower cooling tower is used for evaporative cooling of water by direct contact with air. Because of heat and mass transfer between the air and the water, the water temperature is reduced, while the air enthalpy is increased. The water is sprayed through pressurized nozzles and flows downward, opposite to the air flow which enters from bottom and lift upward.

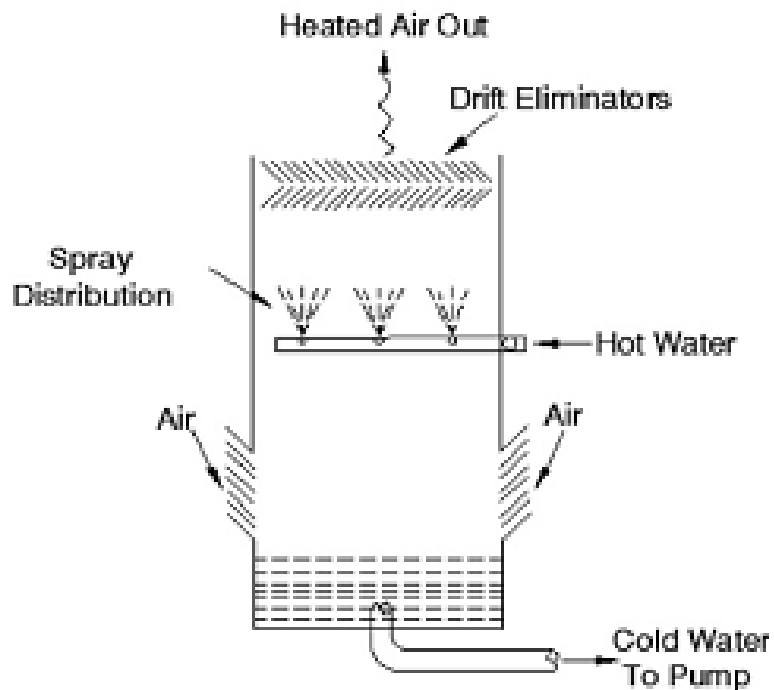


Fig 1.6 Schematic representation of General shower cooling tower

The cooling principle is identical to that of shower ventilation cooling tower (evaporative cooling) however the ways of making water droplets are different. In order to attained adequate heat exchange the diameter of the falling droplets must be small

enough to increase the interface area of water and the air, which makes the distribution system the critical point in designing a general shower cooling tower.

The following approaches are used to design a GSCT;

- 1) Increasing the contact area of the air and water.
- 2) Enhance the movement of the air and water.
- 3) Prolong the contact time of the air and water to enhance the cooling ability.

Under these conditions, the pressure energy of the water is used in the SCT device by means of a nozzle to release the energy. The water through the nozzle forms the thin fog grain, bubble. The air extracted from outside the tower is swirl to increase the cooling time of the water and the evaporative quantity of the water high.

### **1.2.3.3 Advantages of shower cooling tower over Pact cooling tower**

a) CONTACT TYPES: In PCT water is sprayed over fills of wood, PVC, RCC or FRP. Thin film is made of water over the fills. In SCT, an efficient low pressure atomization device replaces the conventional fills, so the resistance of the cooling medium in the tower decreases considerably as spray cooling is superior to film cooling. This is the first ground reality due to which SCT gives better efficiency than PCT with fills.

b) CONTACT TIME: Finite time interval is required for mass transfer i.e. water to evaporate. Contact time depends upon height of fills, height with which water falls. In SCT complete height of tower is acting as a fill height. Moreover the water droplets motion is may be in two directions: first they are introduced upward by the nozzles (Fig.1.6), and after the vertices are reached, they fall vertically downward at the same time an air stream rises uniformly in vertical. Thus, the cooling takes places during



upward and downward motion of drops. Compared with the PCT, the duration of heat transfer between the water and air in the counter flow SCT is longer, and hence, the effect on the temperature drop is better. This is the second ground reality due to which SCT give better results.

3. RGL: The water sprayed in the form of thin droplets exchanges heat with the cool air, enlarging the contact area with the cool air, so the ratio of the mass flow of dry air to water (RGL) increases sharply.

4. RELIABILITY: The synchronous reliability of SCT components is better, so the operation duration without repair can extend up to 5 years, and the operational life span can be extended up to 15 years.

### **1.3 Motivation**

In conventional pact cooling tower the heat and mass transfer phenomenon is well understood. Therefore *experimental* or *simulation* studies are easily available and literature is in abundance. On the other hand SCT is a new field of study and a limited research work has been done.

In case of downdraft cooling tower, which are basically used for air cooling and humidification to enhance comfort in hot and dry climate, the simplicity and the nature of location where it has traditionally been used seem to have discourage into scientific enquiry. However, in present scenario due to energy scarcity and environmental issues, there is renewed interest in this technology.

Its simplicity, size, saving in installation and operational cost motivate to undergo an in depth study to correlate heat and mass transfer analysis of SCT working process and factors affecting its performance and development of a simulation model.

## 1.4 Organization of report

This report is organized by chapter wise as follow:

Chapter1: deals with basic principle of air water interaction, working and limitation of pact cooling tower (PCT), description of ventilation downdraft and shower cooling tower and their superiority over PCT.

Chapter2: deals with literature review, conclusion and objective of this work

Chapter3: deals with mathematical formulation on droplet level as well as system level, both for parallel downward flow and counter flow, Formulation also includes energy analysis

Chapter4: consist with simulation studies, results and discussion.

Chapter5: covers with conclusion and future scope.

### LITERATURE REIVEW

#### 2.1. Literature Summary

Many works have been presented related to the performance of shower cooling tower. Various conventional methods have been proposed by different research scientists to make the design process of shower cooling tower more efficient and the product performance better. Below are presented the brief literature reviews of such works:

Givoni [1] developed a kind of passive downdraft SCT used for cooling building in 1995 which consists of an open shaft with showers at the top and a collecting pond at the bottom. A pond at the bottom of the shaft collects the sprayed water for re-circulation by a small pump. He introduced the system and performed a test to analyze thermal performance.

Carew and Joubert [2] present the design and testing results of a prototype passive downdraft evaporative cooling tower PDEC installed and tested to guide the design of a permanent tower intended as a cost effective approach to the Miele show room in Johannesburg. The prototype shower tower consists of a tube of elasticized fabric suspended from the roof structure with a metal hoop at the top and bottom to hold the shape. Water is vaporized at the top of the tower using micronized spray nozzles to produce an evaporative cooling effect. This tower is unusual from other towers in that it recycles air from the room and fresh air is not introduced directly via the tower.

Webster and Mannison [3], of Charles Sturt university (Australia) developed an innovative approach of cooling using four down draught passive evaporative shower towers to provide cooling. This unique project, by using thermal modeling and hydraulic engineering is strategically important in demonstrating a low energy, low water use, and healthy cooling system that has strong commercial potential.

Pearlmutter et al. [4], developed an direct evaporative cooling tower (DECT) at Sede-Boqer in the arid Negev Highlands of southern Israel, which is a particular application of evaporative cooling which has been developed to provide cooling for a relatively large, semi-enclosed inhabited space. The DECT is an energy-efficient and cost-effective means for improving interior comfort in hot dry regions. In this system, the ambient air enters the tower at the top by a propeller fan, is cooled by the evaporation of water, and leaves the tower at the bottom. The exit air, with a lower dry-bulb temperature and a higher relative humidity than that of the ambient, is supplied into the lowest part of the central covered courtyard of the multi-use building complex, thus providing cooling for the occupants of the space.

Jaber and Webb [5] developed the necessary equations to apply the e-NTU method directly to counter flow or cross flow cooling towers. The e-NTU method is based on the some simplifying assumptions as the Merkel method. Kloppers et al. [6] investigated the critical differences in the heat and mass transfer analyses and solution techniques of the Merkel and Poppe methods using enthalpy diagrams and psychometric charts. They made a detailed derivation of the heat and mass transfer equations of evaporative

cooling in wet-cooling towers and derived the governing equations of Poppe method from first principles.

Kloppers et al. [7] investigated the performance evaluation of the Merkel, e-NTU and Poppe methods for a certain fill material at different operating and ambient conditions. Kloppers et al. [8] investigated the effect of the Lewis factor (which relates the relative rates of heat and mass transfer in wet cooling towers) on the performance prediction of natural draft and mechanical draft wet-cooling towers and also investigated the relation of the Lewis factor to the Lewis number. Kloppers et al. [9] proposed a new form of empirical equation that correlates fill loss coefficient data more effectively when compared to other forms of empirical equation commonly found in literature.

Naphon [10] investigated both experimental and theoretical results of the heat transfer characteristics of the cooling tower and found that there is a reasonable agreement from the comparison between the measured data and predicted results in his model. Kachhwaha et al. [11] carried out heat and mass transfer analysis of a counter flow wet cooling tower. Sutherland [12] compared accurate analysis of mechanical draft counter flow cooling tower, including water loss by evaporation, with the approximate common method based on enthalpy driving force (Merkel method) for wide range of inlet water and air conditions. A few theoretical and experimental works have been reported on the heat transfer characteristics.

Qureshi et al. [13] modeled three zones of the cooling tower; namely, spray zone, packing and rain zones and the developed models of these zones were validated against experimental data. Furthermore, fouling in cooling tower fills as well as its

modelling strategy is explained and incorporated in the cooling tower model to study performance evaluation problems.

Qureshi et al [14] did a second-law based performance evaluation of cooling towers and evaporative heat exchangers. A parametric study was carried out to determine the variation of second-law efficiency as well as exergy destruction as a function of various input parameters such as inlet wet bulb temperature.

Xiaoni et al [15] , based on the kinetic model and mass and heat transfer model, in his paper developed a one-dimensional model for studying the motional process and evaporative cooling process occurring at the water droplet level in the SCT. The finite difference approach was used for three motional processes to obtain relative parameters in each different stage, and the possibility of the droplets being entrained outside the tower is fully analyzed. The accuracy of his model was checked by practical operational results from a full scale prototype in real conditions, and some exclusive factors that affect the cooling characteristics for the SCT are analyzed in detail. His study provides the theoretical foundation for practical application of the SCT in industry.

Xiaoni et al. [16] in another paper, derive a new model without applying the assumptions made in the earlier work. According to the condition of the outlet air, the governing equations considered two cases, including the supersaturated and unsaturated states. This model predicted the performance of a full scale SCT with different conditions for validation. The differences in the heat and mass transfer analyses of the two models were described at different atmospheric conditions.

Muangnoi et al [17] did an exergy analysis on the performance of a counter flow wet cooling tower. The results revealed that the cooling process due to thermodynamic irreversibility perform poorly at the bottom and gradually improve along the height of the tower. The results also showed that the lowest exergy destruction is located at the top of the tower. The model was also validated against experimental data.

Muangnoi et al [18] in another paper studied the effects of inlet relative humidity and inlet temperature on the performance of counter flow wet cooling tower based on exergy analysis. They analyzed the influence of the ambient temperature and humidity on the performance of a counter flow wet cooling tower according to the second law, exergy analysis, of thermodynamics.

Bejan and Moran[19,20] showed that for any system that undergoes a psychometrics process such as in cooling tower operation, the total exergy can be split into thermo-mechanical and chemical components.

Viljoen [21] in his M.Sc. thesis studied the heat transfer and drop size distribution in the spray zone theoretically as well as experimentally. He compares the experimental data with Rosin-Rammler distribution curve and found satisfactory results

Terblanche et al [22] measured the drop size distribution photographically below three different counter flow fills (cross fluted film, trickle and fiber cement).The data for each test case is presented as a cumulative mass distribution curve, Sauter mean diameter, Rosin – Rammler curve and Rosin- Rammler function.

Suresh Kumar et al [23] measured the drop size distribution with different nozzle angles, the affect of inlet air velocity on projection angle its result on DBT and RH.

## **2.2 Conclusion**

Although a lot of work has been done in the field of conventional cooling towers, there is very little information in the area of shower cooling towers. The works of Xiaoni et al[15,16] involve analysis of simple models of shower cooling towers. These models involve certain assumptions which may deviate the predictions from practical results. Some factors such as consideration of the two dimensional droplet trajectories, distribution of diameter of droplets in the shower, heat transfer after the droplets hit the wall may effect the predictions in bringing them closer to the practical results and therefore more accurate modeling is needed for accurate prediction.

## **2.3 Objectives of the present work**

The objective of the present work is to develop a simple and numerically efficient mathematical model for droplet air interaction in downward vertical parallel flow as well as counter flow configuration with mono and multi droplet diameter distribution.



---

### Mathematical Model Formulation

#### 3.1 Introduction

It is essential to investigate the theoretical background of the processes that take place in the SCT at the droplet level. The various aspects of mass balance and energy transfers are discussed in the following sections in detail. This involves the study of SCT in the following two configurations:

- Downward vertical parallel flow
- Counter flow

The Cooling towers are used to extract waste heat from water to atmosphere. An energy analysis alone is not sufficient to describe some important viewpoints on energy utilization and the quality of energy involved. Hence an exergy analysis is required. This is also covered in this work. Exergy can be defined as the maximum useful work obtainable when a system reaches the restricted dead state, referred to as '0' state. It can be understood as the quality of energy or availability of energy.

#### 3.2 Heat and Mass Transfer Formulation in Vertical Downward Parallel Flow Shower Cooling Towers:

A single water drop in a non saturated environment experiences heat, mass and momentum transfer processes as following

( i ) The temperature gradient at the drop-air interface provokes a net heat transfer from the air to the drop surface if the air is warmer (High DBT and low relative Humidity) than the drop.

( ii ) The concentration of water vapor near the water surface gives way to water diffusion from the drop surface to the non-saturated air. This water diffusion needs a previous evaporation of water from the drop; due to the latent energy of this phase change, this mass transfer is strongly coupled to the heat transfer.

( iii ) If there is a relative movement between the drop of water and the surrounding air, a transfer of momentum between them will occur. This transfer of momentum tends to increase the rate of both the heat and mass transfer.

Thus the physical action of water drops falling through the interior air of the cooling tower may accelerate the cooling process.

The first two phenomena have opposite effects on the thermal state of a typical drop of water drop. The heat transfer tends to *increase* the drop temperature, whereas the latent energy absorbed by the evaporated water (mass transfer) causes a *decrease in* the temperature of the drop. An equilibrium is reached when the drop is cooled to the wet bulb temperature .The latent energy required to evaporate more water, reducing the size of the drop, is supplied by the surrounding air, so the latter is cooled .Thus the evaporation of a drop of occurs in two stages: first it is cooled to the equilibrium temperature, and second, its radius decreases.

Figure 3.1 represents the schematic diagram of *Downward Vertical Parallel Flow* configuration. The ambient air enters at the top by the help of a propeller fan, is cooled by the evaporation of water, and leaves the tower at the Bottom.

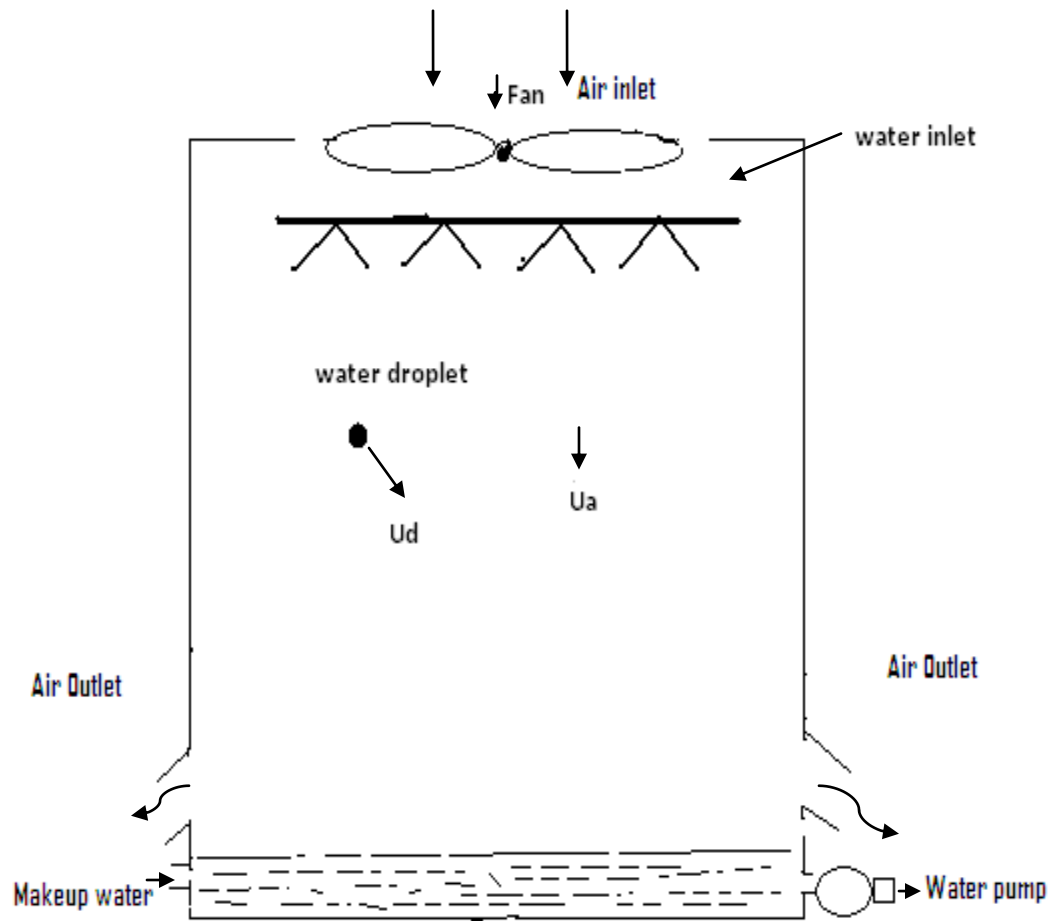


**Figure 3.1 Schematic representation of downward vertical parallel flow**

Before going to the mathematical formulation some critical simplifying assumptions are given below

- 1) The water droplet is spherical and its diameter is small enough that the drop temperature is uniform.
- 2) All water droplets have a uniform diameter and motion track.
- 3) The possibility of collision or scattering of the water droplet during the motion process is ignored.

- 4) The circumgyration, libration, non uniformity of internal flow and temperature distribution are ignored.
- 5) Steady state condition prevails.

### 3.2.1 Conservation of mass for water droplets

A control volume for air water droplet is shown in Figure 3.2

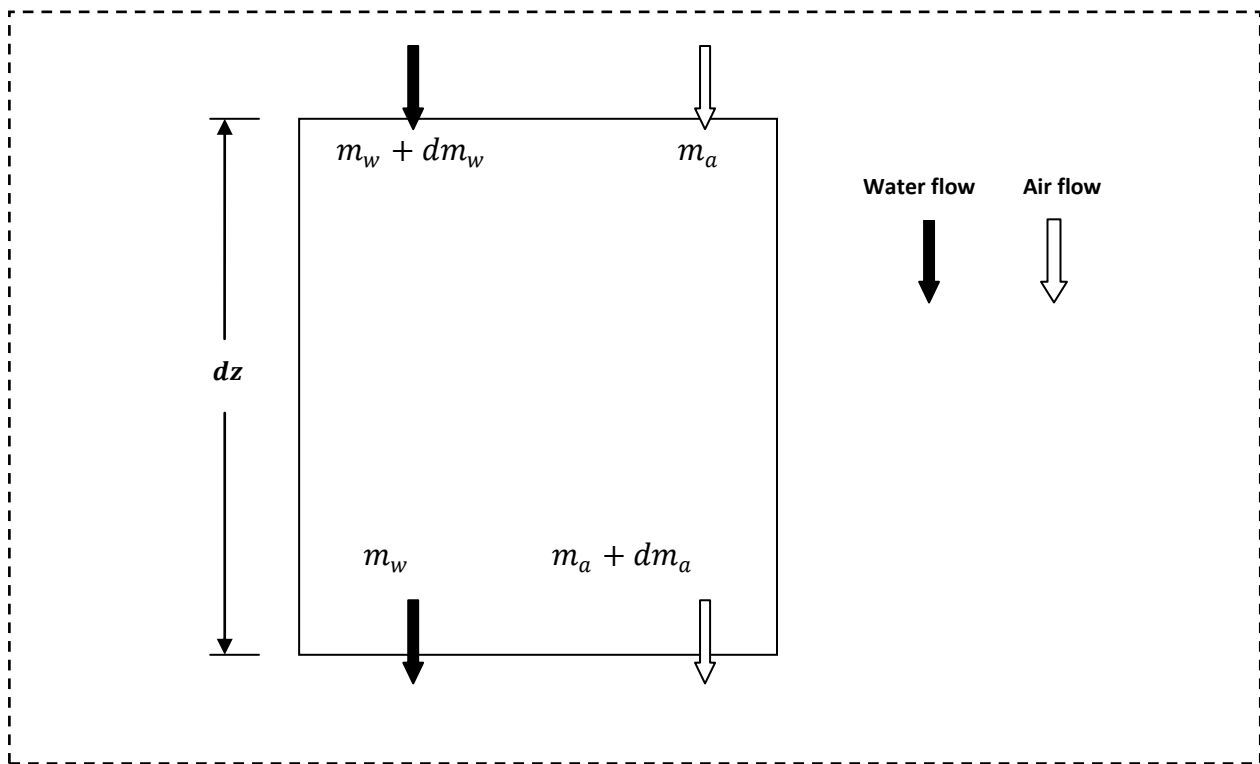


**Fig. 3.2 Control volume for mass flow along length dz**

Let

$m_w$  = mass flow rate of water

$dm_w$  = Water evaporation rate along length dz

$$(m_{w\ in}) = (m_{w\ out}) + \frac{dm_w}{dz} dz \quad (3.1)$$

$$\text{But } (m_w) = N_d \cdot m_d \quad (3.2)$$

where

$N_d$  = Number of droplet moving to control volume over length  $dz$

$m_d$  = Mass of a single droplet

$$\text{i.e. } dm_w = N_d \frac{dm_d}{dt} \quad (3.3)$$

The water evaporation rate of single droplet associated with mass transfer

$$\frac{dm_d}{dt} = -h_d (\omega_{sw} - \omega_a) A_d \quad (3.4)$$

where  $h_d$  = mass transfer coefficient in Kg/ms

$\omega_{sw}$  = Specific humidity of saturated air on droplet surface in kg of water vapor / kg of dry air

$\omega_a$  = Specific Humidity of air in kg / kg of dry air

$A_d = \pi d^2$ , Area of water droplet( $m^2$ )

$$\frac{dm_d}{dz} \cdot \frac{dz}{dt} = -h_d (\omega_{sw} - \omega_a) A_d$$

$$\frac{dm_d}{dz} = -\frac{h_d}{u_{dz}} (\omega_{sw} - \omega_a) A_d \quad (3.5)$$

where  $u_{dz} = \frac{dz}{dt}$  (component of droplet velocity in z direction)

$$\text{since } m_d = \frac{1}{6} \pi d_d^3 \rho_w \quad (3.6)$$

$$\frac{1}{6} \pi \rho_w \frac{d}{dz} (d_d^3) = -\frac{h_d}{u_{dz}} (\omega_{sw} - \omega_a) \pi d_d^2$$

or

$$\frac{d(d_d)}{dz} = -\frac{2h_d}{u_{dz} \rho_w} (\omega_{sw} - \omega_a) \quad (3.7)$$

### 3.2.2 Conservation of momentum for water droplet

In the downward motion process of a water droplet sprayed from the nozzle (Fig.3.3), the forces acting on the droplet moving with a certain velocity ( $u_d$ ) are the body force due to gravity,  $G_d$ , buoyancy force,  $F_b$ , and aerodynamic drag force,  $R_d$  due to the relative air velocity.

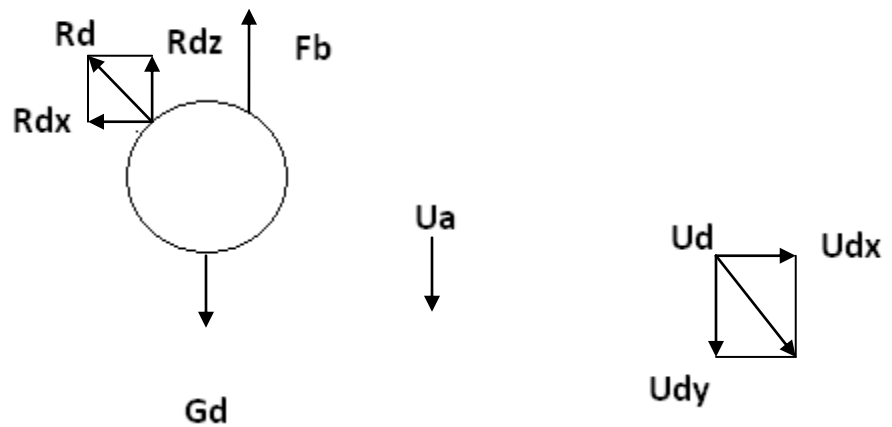


Fig 3.3 Schematic of forces acted on the water droplet sprayed downward at an angle  $\theta$

The forces can be expressed as

Gravity

$$G_d = m_d g = \frac{\pi d_d^3 \rho_w g}{6} \quad (3.8)$$

Buoyancy

$$F_b = \frac{\pi d_d^3 \rho_a g}{6} \quad (3.9)$$

$$\text{Resistance } R_d = \frac{\pi C_d \rho_a u^2 d_d^2}{8} \quad (3.10)$$

Figure 3.4 shows a relative velocity vector diagram of water droplet and air motion. Let  $u$  be the relative velocity of the droplet with respect to air. Consider the components of the

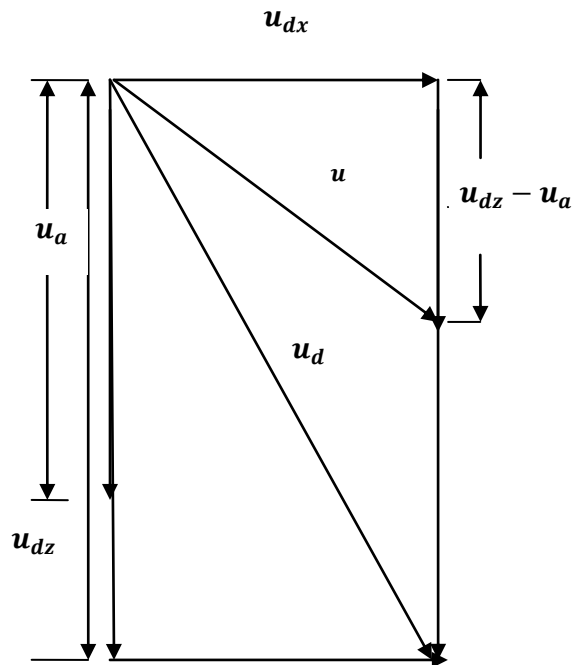


Fig 3.4 Velocity vector diagram of water droplet and air

absolute velocity of droplet ( $u_d$ ) in horizontal ( $u_{dx}$ ) and vertical direction ( $u_{dz}$ ). If  $u_a$  is the velocity of air as shown in Figure 3.3, then being  $\theta$  is an angle of action of  $u_d$  from horizontal

$$u_{dx} = u_d \cos \theta$$

$$u_{dz} = u_d \sin\theta$$

$$u = \sqrt{(u_{dz} - u_a)^2 + u_{dx}^2} \quad (3.11)$$

$u$  is the relative velocity of droplet with respect to air

And  $\theta = \tan^{-1} \left( \frac{u_{dz}}{u_{dx}} \right)$  is its angle from horizontal

where

$\rho_a$  is the density of air

$C_d$  is the drag coefficient (see **article 4** of appendix for discussion on drag coefficient),

$d_d$  is the droplet diameter

Now the resistive force acts in the direction of the relative velocity of the droplet w. r. t. air. Therefore resolving the forces in the  $x$  and  $z$  directions respectively we get

$$R_x = R \left( \frac{u_{dx}}{u} \right)$$

$$R_z = R \left( \frac{u_{dz} - u_a}{u} \right)$$

Therefore



$$R_x = \frac{1}{8} \pi \rho_a C_d u d_d^2 u_{dx} \quad (3.12)$$

$$R_z = \frac{1}{8} \pi \rho_a C_d u d_d^2 (u_{dz} - u_a)$$

Also  $\frac{dx}{dz} = \frac{dx}{dt} \frac{dt}{dz} = \frac{u_{dx}}{u_{dz}}$

Conserving momentum using the above equations

$$\frac{du_{dz}}{dz} = \left[ g(\rho_w - \rho_a) - \frac{3(C_d \rho_a u (u_{dz} - u_a))}{4d_d} \right] \frac{1}{\rho_w u_{dz}} \quad (3.13)$$

And

$$\frac{du_{dx}}{dz} = - \left[ \frac{3(C_d \rho_a u u_{dx})}{4d_d \rho_w u_{dz}} \right] \quad (3.14)$$

### 3.2.3 Conservation of Energy for water droplet

As shown in Fig.4.5 heat rejected from the water droplets includes convective heat and evaporative heat. The water droplets lose heat to the air at expense of the internal energy and energy balance on control surface surrounding the water droplet yields,

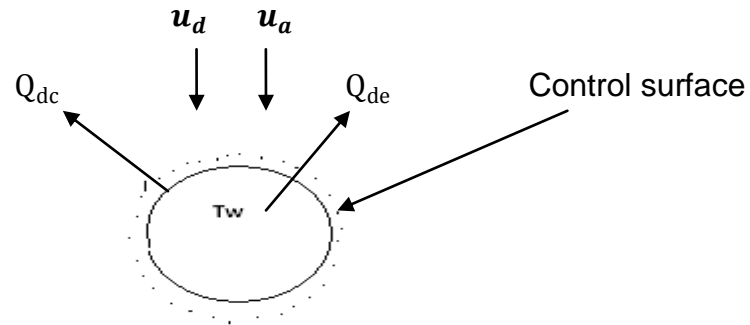


Fig. 3.5 Energy exchange at the water droplet level

$$\frac{dU_d}{dt} = -(Q_{dc} + Q_{de}) \quad (3.15)$$

$$U_d = m_d c_{pw} T_w, \text{ is the energy of the droplet} \quad (3.16)$$

$$Q_{dc} = h_c A_d (T_w - T_a), \text{ is the convective heat transfer} \quad (3.17)$$

$$Q_{de} = h_d A_d (w_{sw} - w_a) i_v, \text{ is the evaporative heat transfer} \quad (3.18)$$

and

$m_d$  = mass of single drop

$c_{pw}$  = specific heat of water

$w_{sw}$  = specific humidity of saturated water

$w_a$  = specific humidity of air

$T_w$  = bulk temperature of water

$T_a$  = temperature of air

$h_d$  = mass transfer coefficient

$h_c$  = convective heat transfer coefficient

$A_d$  = surface area of droplet

$i_v$  = enthalpy of evaporation

Also,

$$dU_d = m_d c_{pw} dT_w \quad (3.19)$$

Therefore,

$$m_d c_{pw} \frac{dT_w}{dt} = -[h_c (T_w - T_a) + h_d (w_{sw} - w) i_v] A_d \quad (3.20)$$

Rearranging using article 1 in the appendix,

$$\frac{dT_w}{dt} = -\frac{6h_d}{\rho_w c_{pw} d_d} \left[ \frac{h_c}{h_d} (T_w - T_o) + (w_{sw} - w_a) i_v \right] \quad (3.21)$$

where

$\rho_w$  = density of water

$d_d$  = diameter of droplet

Using articles 2 & 3 from the appendix,

$$\frac{dT_w}{dt} = - \frac{6h_d [Le_f (i_{masw} - i_{ma}) + (1 - Le_f)(w_{sw} - w)i_v]}{c_{pw} d_d \rho_w} \quad (3.22)$$

where,

$Le_f$ , is the Lewis factor.

$i_{masw}$ , is the enthalpy of saturated air evaluated at the local bulk water temperature;  $T_w$  the bulk temperature of water droplet.

$i_{ma}$ , is the enthalpy of the air-water vapor mixture per unit mass of dry air.

Now,

$$\frac{dT_w}{dt} = \frac{dT_w}{dz} \frac{dz}{dt} = u_{dz} \left[ \frac{dT_w}{dz} \right] = - \frac{6h_d [Le_f (i_{masw} - i_{ma}) + (1 - Le_f)(w_{sw} - w)i_v]}{c_{pw} d_d \rho_w} \quad (3.23)$$

Therefore,

$$\frac{dT_w}{dz} = - \frac{6h_d [Le_f (i_{masw} - i_{ma}) + (1 - Le_f)(w_{sw} - w)i_v]}{u_{dz} c_{pw} d_d \rho_w} \quad (3.24)$$

### 3.2.4 Thermal balance equations in the SCT

The previous analysis represents a water droplet model. But in order to predict the total amount of the heat rejected, it is better to consider the large number of water droplets falling in the SCT. Moreover, it also requires to consider that the air and water conditions change from top to bottom

The following analysis considers the property variations in the vertical direction. The SCT of height  $H$  is divided into  $n$  sections of finite thickness  $dz$  and finite volume  $dV$ . The water is assumed to be distributed evenly in the form of water droplets with average diameter  $d_d$ . The positive direction is taken from top to bottom of the tower.

Considering an elementary control volume in the parallel flow cooling tower (Fig. 3.6), the evaporation of the downward water occurs at the air-water interface.

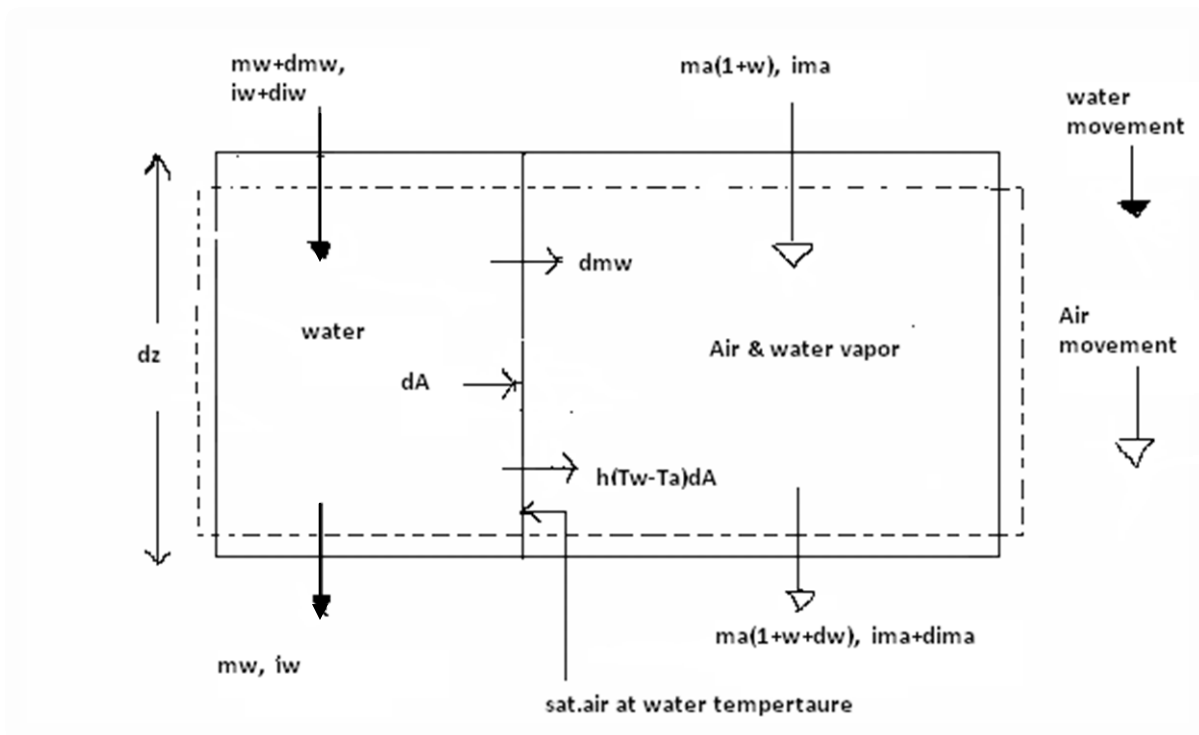


Fig. 3.6 Control volume of vertical parallel flow Shower Cooling Tower

The total enthalpy transfer at the air-water interface consists of an enthalpy transfer associated with the mass transfer due to the difference in vapor concentration between the saturated air and mean stream air, and the sensible heat transfer due to the difference in temperature.

A mass balance in the control volume in the Figure 3.6 yields

$$dm_w = m_a dw \quad (3.25)$$

The energy balance in the control volume of the SCT in Fig 3.6 is as follows

$$m_a di_{ma} = m_w di_w + i_w dm_w \quad (3.26)$$

Rearranging using above two equations

$$dT_w = \frac{m_a}{m_w} \left( \frac{di_{ma}}{c_{pw}} - T_w dw \right) \quad (3.27)$$

Energy balance at the water and air interface yields

$$dQ = dQ_c + dQ_e \quad (3.28)$$

where

$$dQ_c = h(T_w - T_a) dA, \quad (3.29)$$

is the sensible heat transfer due to difference in temperature

and

$$dQ_e = i_v h_d (w_{sw} - w_a) dA, \quad (3.30)$$

is the enthalpy transfer due to the difference in vapor concentration between the saturated air at the interface and the mean stream air.

Using above relations and **Article 2** from appendix we get,

$$dQ = \left[ \frac{h(T_w - T_a) + i_v h_d (w_{sw} - w_a) dA}{C_{pma}} \right] + i_v h_d (w_{sw} - w_a) dA \quad (3.31)$$

$$dQ = \left[ \frac{h}{C_{pma}} (i_{masw} - i_{ma}) + \left( h_d - \frac{h}{c_{pma}} \right) i_v (w_{sw} - w_a) \right] dA \quad (3.32)$$

The enthalpy transfer to the air stream is

$$\begin{aligned} di_{ma} &= \frac{dQ}{m_a} \\ &= \frac{h_d}{m_a} \left[ Le_f (i_{masw} - i_{ma}) + (1 - Le_f) i_v (w_{sw} - w) \right] dA \end{aligned} \quad (3.33)$$

The number of droplets in the control volume with a section height  $dz$  is

$$N_d = \frac{m_w dz}{m_d u_{dz}} \quad (3.34)$$

So the transverse area for it is expressed as

$$dA = \frac{m_w dz \pi d_d^2}{m_d u_{dz}} = \frac{6m_w dz}{\rho_w u_d d_{dz}} \quad (3.35)$$

Substitute Eq. (3.35) into Eq. (3.33) we get

$$\left( di_{ma} \right)_{control\ volume} = \left( \frac{m_w}{m_a} \right) \frac{6h_d}{\rho_w u_{dz} d_d} \left[ Le_f (i_{masw} - i_{ma}) + (1 - Le_f) i_v (w_{sw} - w_a) \right] dz \quad (3.36)$$

### 3.2.5. Mass balance equation in the SCT

Writing a mass balance equation for the control volume (Fig. 3.6)

$$dm_w = m_a d\omega \quad (3.37)$$

But

$$dm_w = N_d \frac{dm_d}{dt} \quad (3.38)$$

Where  $\frac{dm_d}{dt}$  = water evaporation rate of a single droplet [=  $h_d(\omega_{sw} - \omega_a)A_d$ ]

Substituting  $N_d = \frac{m_w dz}{m_a u_d}$ ,  $A_d = \pi d_d^2$ ,  $m_d = \frac{1}{6} \pi d_d^3 \rho_w$  and rearranging equations (3.37) and (3.38) yields.

$$dw_a = \left( \frac{m_w}{m_a} \right) \frac{6h_d}{\rho_w u_{dz} d_d} (w_{sw} - w_a) dz \quad (3.39a)$$

and Mass transfer associated with the control volume

$$\left( dm_w \right)_{control\ volume} = \frac{6h_d m_w}{\rho_w u_{dz} d_d} (w_{sw} - w_a) dz \quad (3.39b)$$

### 3.2.6 Heat transfers on the wall of the tower

Heat is transferred with the wall when the droplets trajectory hits the wall. Similar to earlier analysis here also heat transfer is considered due to convective and evaporative heat transfer.

$$dQ = dQ_c + dQ_e$$

where,



$dQ_c$  , is the convective heat transfer and is given by

$$dQ_c = h_{cw} (T_{wmean} - T_a) dA_w \quad (3.40)$$

$$dQ_e = i_v h_{dw} (w_{sw(T_{wmean})} - w_a) dA_w \quad (3.41)$$

$h_{cw}$  is the convective heat transfer coefficient of the wall

$h_{dw}$  is the coefficient of mass transfer

$T_{wmean}$  is the mean temperature of the wall

$dA_w$  Area of contact with the wall in height  $dz$

$w_{sw(T_{wmean})}$  Specific humidity at mean wall temperature

Therefore change in enthalpy due to wall interactions

$$(di_{ma})_{wall} = \frac{[h_{cw} (T_{wmean} - T_a) + h_{dw} i_v (w_{sw} - w_a)] K_w dz}{m_a} \quad (3.42)$$

Where

$$dA_w = K_w dz \quad (3.43)$$

For derivation of  $K_w$  see **article 5** of appendix

Mass transfer associated with the wall

$$(dm_w)_{wall} = h_{dw} (w_{sw} - w_a) K_w dz \quad (3.44)$$

Adding the mass transfer we get

$$dm_w = (dm_w)_{control\ volume} + (dm_w)_{wall}$$

$$dm_w = \frac{6h_d m_w}{\rho_w u_{dz} d_d} (w_{sw} - w_a) dz + h_{dw} (w_{sw} - w_a) K_w dz \quad (3.45)$$

now

$$dw_a = \frac{dm_w}{m_a}$$

therefore,

$$\frac{dw_a}{dz} = \frac{6h_d m_w}{\rho_w u_{dz} d_d m_a} (w_{sw} - w_a) + \frac{h_{dw} (w_{sw} - w_a) K_w}{m_a} \quad (3.46)$$

for enthalpy of air

$$di_{ma} = (di_{ma})_{controlvolume} + (di_{ma})_{wall} \quad (3.47)$$

rearranging

$$\begin{aligned} \frac{di_{ma}}{dz} = & \left( \frac{m_w}{m_a} \right) \frac{6h_d}{\rho_w u_{dz} d_d} [L_{ef} (i_{masw} - i_{ma}) + (1 - L_{ef}) i_v (w_{sw} - w_a)] \\ & + \frac{[h_{cd} (T_{wmean} - T_a) + h_d i_v (w_{sw} - w_a)] K_w}{m_a} \end{aligned} \quad (3.48)$$

### 3.2.7 Multi Droplet Diameter Model based on Rosin-Rammler distribution

Up to this level, all the previous analysis is concerned with a single droplet. But in a practical scenario, a spray in an SCT constitutes poly droplets in different fractions. A smaller droplet results in more cooling compared to a large sized droplet due to

- a) More surface area per unit volume
- b) High retention time.

In the Multi Droplet Model, a matrix of Droplet is created. This matrix contains the following information regarding the Droplet:

- a) Diameter of Droplet
- b) Fractional contribution.

In this work a simple distribution pattern based on the Rosin-Rammler distribution is used to describe the droplet size distribution. The Rosin Rammler distribution curve [24] is based on an exponential relationship that exists between the drop diameter,  $d$  and the mass fraction of drop with diameter greater than  $d$ , namely  $Y_d$ . The Rosin-Rammler mean diameter  $d_{RR}$  is defined as the diameter at which  $Y_d = e^{-1} = 0.368$  and was also used in the data analysis process. The spread parameter ( $n$ ) can be obtained by taking the mean of all the intervals spread parameters.

Hence the distribution is described in terms of two parameters,  $d_{RR}$  and  $n$

$d_{RR}$  is a representative diameter, commonly chosen such that 63.2% of the total volume is contained in particles smaller than  $d$ .

The exponent  $n$  provides a measure of the spread of drop sizes. The higher the value of  $n$ , the more uniform the spray. If  $n$  is infinite the drops in the spray are all the same size.

For typical sprays, the value of  $n$  is between 1.5 and 4.

The conventional Rosin-Rammler function is described by

$$Y_d = e^{-(d/d_{RR})^n} \tag{3.49}$$

Referring to the work of Terblanche et al [22], a Rosin –Rammler distribution curve representing droplet size distribution with Droplet Diameter is obtained which is shown below in Fig.4.7, for diameter drop range 50micron to 975 micron in the step of 50 micron with RR- mean diameter of 517.52 micron and for  $n=3.9242$ .

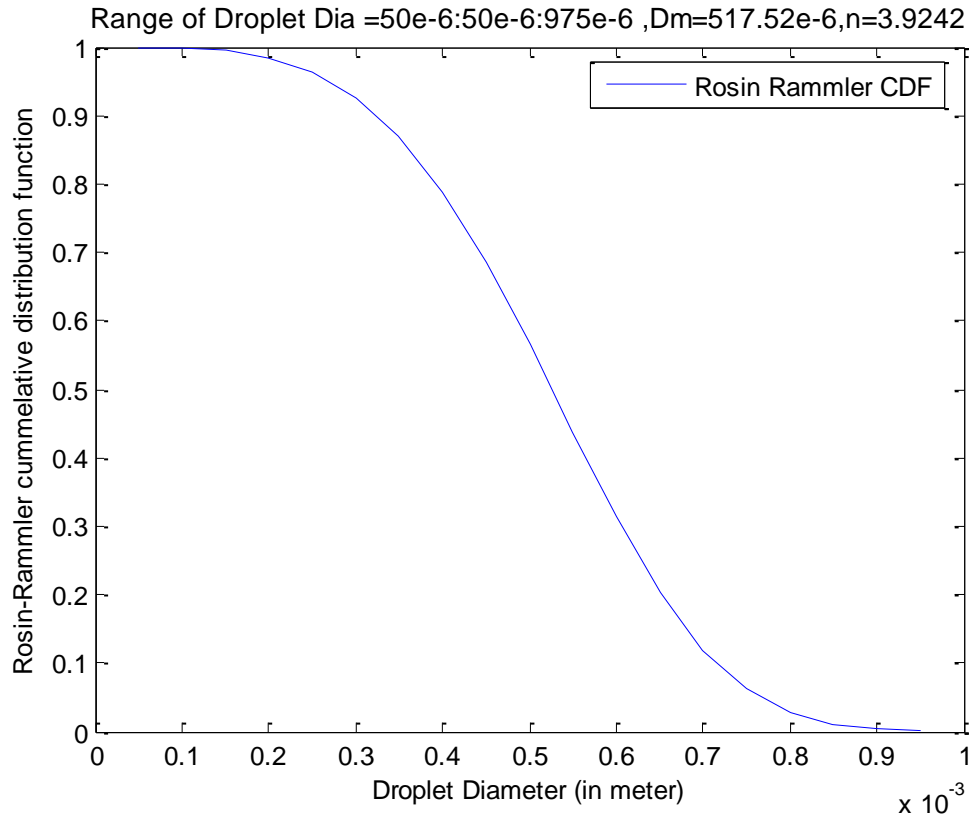


Fig. 3.7 A typical Rosin–Rammler distribution curve for droplet diameter range

From the Rosin-Rammler distribution the other mean diameter can also be calculated which are as following:

The mean or arithmetic mean diameter is used for comparisons and evaporation studies [24].The mean diameter is defined by:

$$d_{dm} = \left[ \frac{\sum_{i=1}^n N_i d_i}{N} \right] \quad (3.50)$$

The sauter mean diameter  $d_{sm}$  is defined as the sum of drop volumes per interval divided by the sum of drop surface per interval. The sauter mean diameter is used for combustion, mass transfer and efficiency studies [24]. The sauter mean diameter is defined as:

$$d_{sm} = \left[ \frac{\sum_{i=1}^n N_i d_i^3}{\sum_{i=1}^n N_i d_i^2} \right] \quad (3.51)$$

Inputs require to generate droplet distribution curve:

- a) Drop diameter range (0- $D_{max}$ )
- b) Rosin-Rammler mean diameter ( $d_{RR}$ )
- c) Spread parameter (n)

### 3.2.8 Total number of equations due to distribution of droplet's diameter

The net change in enthalpy is the summation of changes in enthalpy due to each class of droplets. Therefore

$$\frac{di_{ma}}{dz} = \left[ \frac{di_{ma}}{dz} \right]_{i=1} + \left[ \frac{di_{ma}}{dz} \right]_{i=2} \dots \dots \dots \left[ \frac{di_{ma}}{dz} \right]_{i=n} = \sum_{i=1}^{i=n} \left[ \frac{di_{ma}}{dz} \right]_{i=n} \quad (3.52)$$

where,

$\left[ \frac{di_{ma}}{dz} \right]_{i=n}$  is the change of enthalpy with height due to the  $i^{th}$  set of droplets.

Similarly

$$\frac{d\omega_a}{dz} = \left[ \frac{d\omega_a}{dz} \right]_{i=1} + \left[ \frac{d\omega_a}{dz} \right]_{i=2} \dots \dots \dots \left[ \frac{d\omega_a}{dz} \right]_{i=n} = \sum_{i=1}^{i=n} \left[ \frac{d\omega_a}{dz} \right]_{i=n} \quad (3.53)$$

where,

$\frac{d\omega_a}{dz}$  is the change of humidity with height due to  $i^{th}$  set of droplets.

The solution of this distribution is done with the help of Matlab using ODE45 solver.

Following equations are numerically integrated using Runge-kutta method of fourth order with fifth order correction using Matlab.

**1. The variation of droplet diameter( $d_d$ ) with height,**

$$\frac{d(d_{d,i})}{dz} = \left[ -\frac{2h_{d,i}}{u_{dz,i}\rho_w} (\omega_{sw} - \omega_a)_i \right] \quad (3.54(a))$$

**2. The variation of bulk temperature ,( $T_w$ ) of water droplets with height,**

$$\frac{dT_w}{dz} = \left[ \left( -\frac{6h_d [Le_f (i_{masw} - i_{ma}) + (1 - Le_f)(w_{sw} - w)_i]}{u_{dz} c_{pw} d_d \rho_w} \right)_i \right] \quad (3.54(b))$$

**3. The variation of vertical component of droplet velocity ( $u_{dz}$ ) with height,**

$$\left[ \left[ \frac{du_{dz,i}}{dz} = \left( \frac{\left\{ g(\rho_w - \rho_a) - \frac{3(C_d \rho_a u (u_{dz} - u_a))}{4d} \right\}}{\rho_w u_{dz}} \right)_i \right] \right] \quad (3.54(c))$$

**4. Horizontal component of droplet velocity ( $u_{dx}$ ) with height,**

$$\frac{du_{dz,i}}{dz} = \left[ -\left( \frac{3(C_d \rho_a u u_{dx})}{4d_d \rho_w u_{dz}} \right)_i \right] \quad (3.54(d))$$

**5. Ratio of trajectory equation for  $i^{\text{th}}$  category of droplets**

$$\frac{dx}{dz} = \frac{dx}{dt} \frac{dt}{dz} = \left[ \left( \frac{u_{dx}}{u_{dz}} \right)_i \right] \quad (3.54(e))$$

**6. The net variation of enthalpy of air ( $i_{ma}$ ) with height,**

$$\frac{di_{ma,i}}{dz} = \sum_{i=1}^{i=n} \left[ \left\{ \left( \frac{m_w}{m_a} \right) \frac{6h_d}{\rho_w u_{dz} d_d} [L_{ef}(i_{masw} - i_{ma}) + (1 - L_{ef})i_v(w_{sw} - w_a)] + \frac{[h_{cw}(T_{wmean} - T_a) + h_{dw}i_v(w_{sw} - w_a)]K_w}{m_a} \right\}_i \right] \quad (3.54(f))$$

### 7. The net variation of humidity ratio of the air ( $w_a$ ) with height,

$$\frac{dw_a}{dz} = \sum_{i=1}^{i=n} \left[ \left\{ \frac{6h_d m_w}{\rho_w u_{dz} d_d m_a} (w_{sw} - w_a) + \frac{h_{dw}(w_{sw} - w_a)K_w}{m_a} \right\}_i \right] \quad (3.54(g))$$

### 3.3 Heat and mass transfer formulation in Counter flow shower cooling tower

The analysis of counter flow is more or less similar to that of downward vertical counter flow except the air movement is here from bottom to top. The investigation here also involves the heat exchanges at droplet level, force analysis of droplet and thermal balance in control volume. The difference in the schematic representation of droplet heat exchanges is shown in figure 3.8 and 3.9.

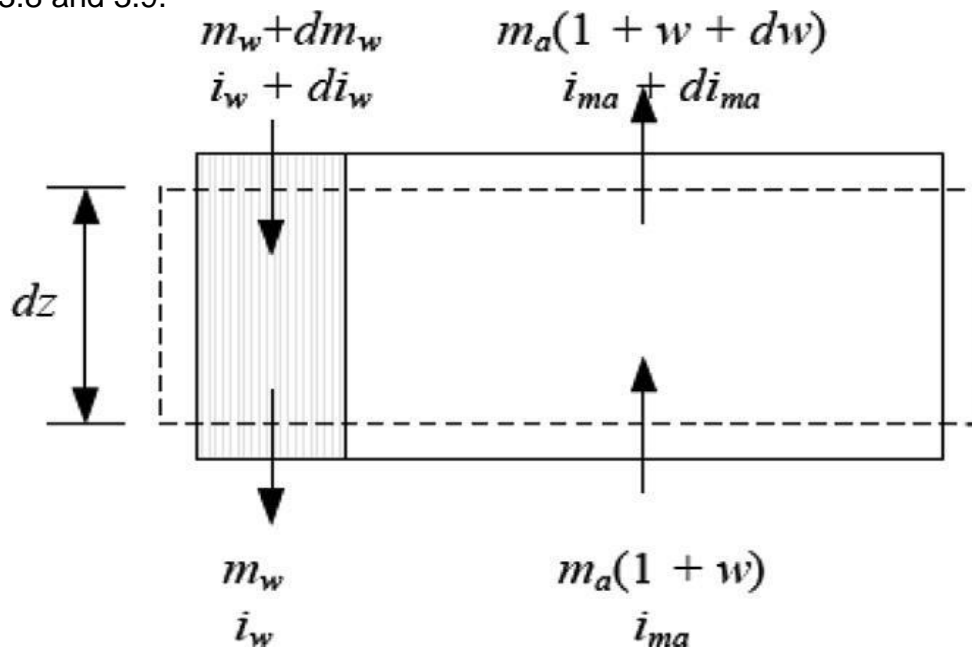
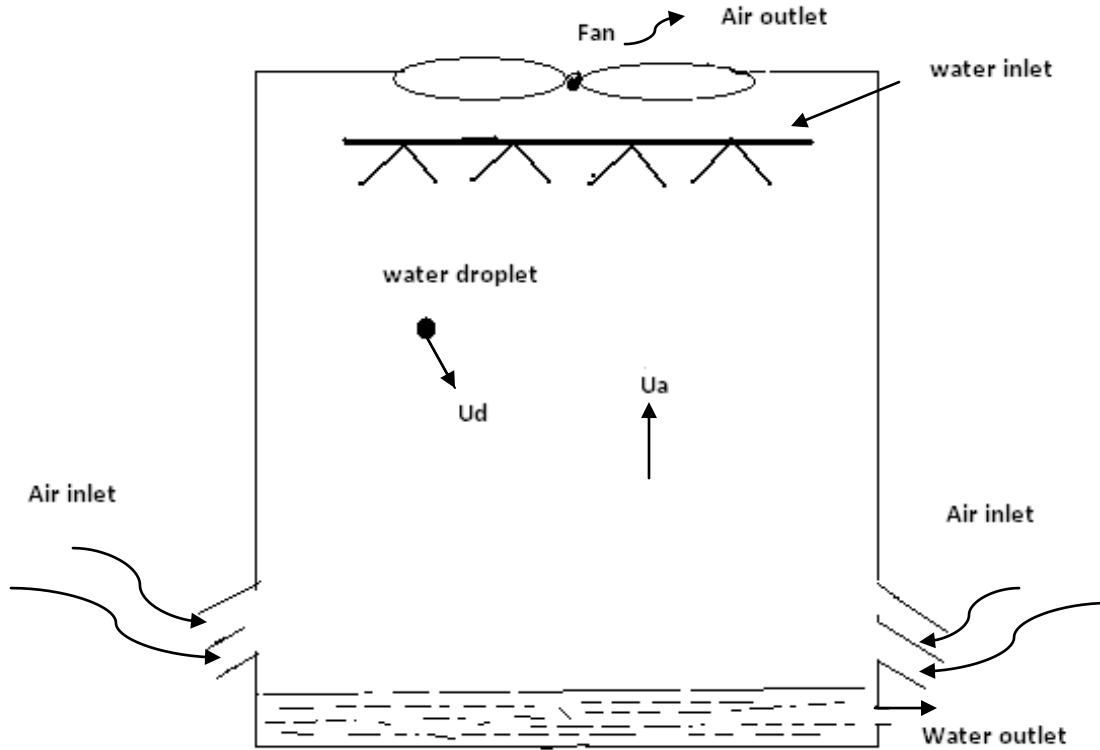


Fig. 3.8 Control volume in counter flow shower cooling tower



**Fig. 3.9 Schematic representation of counter flow Shower Cooling Tower**

### **3.3.1) Governing equations in counter flow for unsaturated air**

The important result of this configuration is summarized below.

#### **1.The variation of droplet diameter( $d_d$ ) with height,**

$$\frac{d(d_{d,i})}{dz} = \left[ -\frac{2h_{d,i}}{u_{dz,i}\rho_{w,i}} (\omega_{sw} - \omega_a)_i \right] \quad (3.55(a))$$

#### **2.The variation of bulk temperature ,( $T_w$ ) of water droplets with height,**

$$\frac{dT_w}{dz} = \left[ \left( -\frac{6h_d [Le_f (i_{masw} - i_{ma}) + (1 - Le_f)(w_{sw} - w)_i]}{u_{dz} c_{pw} d_d \rho_w} \right)_i \right] \quad (3.55(b))$$



**3.The variation of vertical component of droplet velocity ( $u_{dz}$ ) with height,**

$$\frac{du_{dz,i}}{dz} = \left[ \left( \frac{\left\{ g(\rho_w - \rho_a) - \frac{3(C_d \rho_a u (u_{dz} + u_a))}{4d_d} \right\}}{\rho_w u_{dz}} \right) \right]_i \quad (3.55(c))$$

**4.Horizontal component of droplet velocity( $u_{dx}$ ) with height,**

$$\frac{du_{dx,i}}{dz} = \left[ - \left( \frac{3(C_d \rho_a u u_{dx})}{4d_d \rho_w u_{dz}} \right) \right]_i \quad (3.55(d))$$

**5. Ratio of horizontal velocity to vertical velocity for different sized droplets**

$$\frac{dx}{dz} = \frac{dx}{dt} \frac{dt}{dz} = \left[ \left( \frac{u_{dx}}{u_{dz}} \right) \right]_i \quad (3.55(e))$$

**6.The net variation of enthalpy of air ( $i_{ma}$ ) with height,**

$$\frac{di_{ma,i}}{dz} = \sum_{i=1}^{i=n} \left[ \left\{ \left( \frac{m_w}{m_a} \right) \frac{6h_d}{\rho_w u_{dz} d_d} [L_{ef} (i_{masw} - i_{ma}) + (1 - L_{ef}) i_v (w_{sw} - w_a)] + \frac{[h_{cw} (T_{wmean} - T_a) + h_{dw} i_v (w_{sw} - w_a)] K_w}{m_a} \right\} \right]_i \quad (3.55(f))$$

**7. The net variation of humidity ratio of the air( $w_a$ )with height,**

$$\frac{dw_{a,i}}{dz} = \sum_{i=1}^{i=n} \left[ \left\{ \frac{6h_d m_w}{\rho_w u_{dz} d_d m_a} (w_{sw} - w_a) + \frac{h_{dw} (w_{sw} - w_a) K_w}{m_a} \right\} \right]_i \quad (3.55(g))$$

The solution of this distribution is done with the help of Matlab. Above equations is numerically integrated using Range-kutta method of fourth order using Matlab.

### 3.3.2) Governing equations in Counter flow for supersaturated flow

In supersaturated flow air is in supersaturated state at the outlet of cooling tower. Thus the excess water vapor is condensed as a mist, the enthalpy of supersaturated air [16] is expressed by

$$i_{ss} = C_{pa} T_a + \omega_{sa} (i_{fgw0} + C_{pv} T_a) + (\omega_a - \omega_{sa}) C_{pw} T_a \quad (3.66)$$

where

$\omega_{sa}$  = humidity ratio of supersaturated air (kg/kg of dry air)

Using article 3 of appendix and the empirical relation of Bosnjakovic [24] , the Lewis factor for supersaturated air can be represented by ,

$$Le_f = 0.865^{0.667} \left( \frac{w_{sw} + 0.622}{w_{sa} + 0.622} - 1 \right) / \left[ \ln \left( \frac{w_{sw} + 0.622}{w_{sa} + 0.622} \right) \right] \quad (3.67)$$

$$Le_f = \frac{h}{C_{pmas} h_d} \quad (3.68)$$

Where  $C_{pmas}$  the specific heat of is supersaturated air and is defined by

$$C_{pmas} = C_{pa} + \omega_{sa} C_{pv} + (\omega_a - \omega_{sa}) i_v \quad (3.69)$$

Assuming that the heat and mass transfer coefficients for supersaturated and saturated air are same [16], the driving potential for mass transfer is humidity ratio difference between the saturated air at the air water interface and the supersaturated free stream air, thus

$$dm_w = h_d(w_{sw} - w_{sa})dA \quad (3.70)$$

The enthalpy driving potential for supersaturated air is obtained by subtracting Eq. (3.66)

from Eq. (2b) of appendix gives

$$T_w - T_a = \frac{(i_{masw} - i_{ss}) - (\omega_{sw} - \omega_{sa})i_v + (\omega_a - \omega_{sa})C_{pw}T_w}{C_{pmas}} \quad (3.71)$$

and

$$dQ = h(T_w - T_a)dA + i_v h_d(w_{sw} - w_{sa})dA \quad (3.72)$$

rearranging Eq. (3.70), (3.71) and (3.72) yields,

$$\frac{di_{ma}}{dz} = \left(\frac{m_w}{m_a}\right) \frac{6h_d}{\rho_w u_d d_d} [Le_f \{ (i_{masw} - i_{ss}) - i_v(w_{sw} - w_{sa}) + (\omega_a - \omega_{sa})C_{pw}T_w \} + i_v(w_{sw} - w_{sa})] \quad (3.73)$$

Proceeding along the same line as in the case of unsaturated air, the other governing equations for supersaturated air are as following

$$\frac{dT_w}{dz} = \frac{6h_d}{C_{pw} \rho_w u_d d_d} [Le_f \{ (i_{masw} - i_{ss}) - i_v(w_{sw} - w_{sa}) + (\omega_a - \omega_{sa})C_{pw}T_w \} + i_v(w_{sw} - w_{sa}) - (\omega_{sw} - \omega_{sa})C_{pw}T_w] \quad (3.74)$$

$$\frac{d\omega_a}{dz} = \left(\frac{m_w}{m_a}\right) \frac{6h_d}{\rho_w u_d d_d} (\omega_{sw} - \omega_{sa}) \quad (3.75)$$

$$\frac{d(d_d)}{dz} = -\frac{2h_d}{u_{dz} \rho_w} (\omega_{sw} - \omega_{sa}) \quad (3.76)$$

$$\frac{du_{dz}}{dz} = \left[ g(\rho_w - \rho_a) - \frac{3(C_d \rho_a u (u_{dz} + u_a))}{4d_d} \right] \frac{1}{\rho_w u_{dz}} \quad (3.77)$$

The above five equations (3.73 to 3.77) are numerically solved by using Runge-Kutta method in Matlab

### 3.4 Exergy Formulation

Cooling towers are used to extract waste heat from water to atmosphere. An energy analysis alone is not sufficient to describe some important viewpoints on energy utilization and the quality of energy involved. Hence an exergy analysis is required.

Exergy can be defined as the maximum useful work obtainable when a system reaches the restricted dead state, referred to as '0' state. It can be understood as the quality of energy or availability of energy.

The Exergy can be divided into two terms

- Thermo-mechanical exergy- it is the exergy or the quality of energy due to difference in the temperature between the system state and the restricted dead state.
- Chemical exergy- it is the exergy due to the concentration difference.

It can be noted that the specific exergy,  $\psi$ , for any psychrometric process is a measure of thermo-mechanical exergy, changed from actual system state to the restricted dead state plus the chemical exergy, changed from restricted dead state to the environment state [19,20]

Thus

$$\psi = \psi_{tm} + \psi_{ch} \quad (3.78)$$

where

$$\psi_{tm} = (h - h_0) - T_0 (s - s_0) \text{ is the thermo-mechanical exergy} \quad (3.79)$$

$$\psi_{ch} = \sum_{k=1}^n x_k (\mu_{k0} - \mu_{k00}) \text{ is the total chemical exergy in a chemical mixture of } n \text{ elements [19,20]} \quad (3.80)$$

$h$  = enthalpy at the system state

$h_0$  = enthalpy at the restricted dead state

$T_0$  = temperature at the restricted dead state

$s$  = entropy at the system state

$s_0$  = entropy at the restricted dead state

$x_k$  = mole fraction of the  $k^{\text{th}}$  element in the mixture at the system state

$\mu_{k0}$  = chemical potential or Gibbs free energy at the restricted state

$\mu_{k00}$  = chemical potential or Gibbs free energy of the environment

The process in a shower cooling tower is a constant pressure process. As the pressure inside the tower always equals to for a constant pressure process we have

$$(h - h_0) = c_p (T - T_0) \quad (3.81)$$

and

$$s - s_0 = c_p \log_e \left( \frac{T}{T_0} \right) \quad (3.82)$$

Therefore we can rewrite the equation (3.79) as

$$\psi_{tm} = c_p (T - T_0) - T_0 c_p \ln \left( \frac{T}{T_0} \right) \quad (3.83)$$

Using **article 10** from appendix the equation (3.80) can be rewrite as

$$\psi_{ch} = \sum_{k=1}^n R_k T_0 \ln \left( \frac{x_{k0}}{x_{k00}} \right) \quad (3.84)$$

Where

$R_k$  = Gas constant per unit molecular mass of  $k^{\text{th}}$  element in the mixture

By adding the above equations (3.83) and (3.84) the total specific exergy for any psychometric process at the given system state can be calculated, it is also assumed that mole fraction at the restricted dead state approximately equals to that at any given state in the tower.

Therefore

$$\psi_{total} = c_p (T - T_0) - T_0 c_p \ln \left( \frac{T}{T_0} \right) + \sum_{k=1}^n R_k T_0 \ln \left( \frac{x_k}{x_{k00}} \right) \quad (3.85)$$

In the shower cooling tower three distinct working fluids (viz. dry air, water vapor and water) are participating in the operation. Therefore is important to write the exergy equations for them separately to be applied in the analysis.

Specific exergy of **dry air** can be written using equation (3.85) derived above

$$\psi_a = c_{pa} (T - T_0) - T_0 c_{pa} \ln \left( \frac{T}{T_0} \right) + R_a T_0 \ln \left( \frac{x_a}{x_{a00}} \right) \quad (3.86)$$

where

$\psi_a$  is the total specific exergy of dry air

$c_{pa}$  = specific heat capacity of dry air at constant pressure

$x_a$  = mole fraction of the air at the system state

$x_{a00}$  = mole fraction of the air at the environment state

$R_a$  = gas constant for dry air per unit molecular weight of air

using **article 11** from appendix we can write the mole fraction of dry air in terms of specific humidity as

$$x_a = \left( \frac{1}{1 + 1.608 w_a} \right) \quad (3.87)$$

and

$$x_{a00} = \left( \frac{1}{1 + 1.608 w_{00}} \right) \quad (3.88)$$

now substituting equations (3.87) and (3.88) in equation (3.86) we get

$$\psi_a = c_{pa} (T - T_0) - T_0 c_{pa} \ln \left( \frac{T}{T_0} \right) + R_a T_0 \ln \left( \frac{1 + 1.608 w_{00}}{1 + 1.608 w_a} \right) \quad (3.88)$$

where

$w_a$  = humidity ratio of moist air at  $T_a$

$w_{00}$  = humidity ratio in the atmosphere

The total exergy/unit time can be expressed as specific exergy times the mass flow rate.

Therefore

$$X_a = G \psi_a$$

where

$X_a$  = total exergy of dry air

$G$  = mass flow rate of dry air

or

$$X_a = G \left[ c_{pa} (T - T_0) - T_0 c_{pa} \ln \left( \frac{T}{T_0} \right) + R_a T_0 \ln \left( \frac{1 + 1.608 w_{00}}{1 + 1.608 w_a} \right) \right] \quad (3.89)$$

The above analysis calculates the total exergy of only dry air in the system at any given state. In the similar fashion we can write the specific exergy of **vapor**

$$\psi_v = c_{pv} (T - T_0) - T_0 c_{pv} \ln \left( \frac{T}{T_0} \right) + R_v T_0 \ln \left( \frac{x_v}{x_{v00}} \right) \quad (3.90)$$

where



$\psi_v$  = total specific exergy of vapor

$c_{pv}$  = specific heat capacity of vapor at constant pressure

$x_v$  = mole fraction of the vapor at the system state

$x_{v00}$  = mole fraction of the vapor at the restricted dead state

$R_v$  = gas constant per unit molecular weight for dry vapor

using **article 11** from appendix we can write the mole fraction of vapor in terms of specific humidity as

$$x_v = \frac{1.608w_a}{1+1.608w_a} \quad (3.91)$$

therefore, by substituting  $x_v$  in equation (3.90) we get

$$\psi_v = C_{pv}(T - T_0) - T_0 C_{pv} \ln\left(\frac{T}{T_0}\right) + R_v T_0 \ln\left(\frac{w_a(1+1.608w_{00})}{w_{00}(1+1.608w_a)}\right) \quad (3.91)$$

mass flow rate of vapor will be specific humidity times the mass flow rate of dry air because the vapor is flowing the air water mixture

Therefore

$$m_v = m_a \omega_a \quad (3.92)$$

where

$m_v$  is the mass flow rate of vapor at the system state

Total exergy of vapor/unit time,  $X_v$ , can be expressed as

$$X_v = m_a w \psi_v$$

or

$$\psi_v = m_a w_a \left[ C_{pv} (T - T_0) - T_0 C_{pv} \ln \left( \frac{T}{T_0} \right) + R_v T_0 \ln \left( \frac{w_a (1 + 1.608 w_{00})}{w_{00} (1 + 1.608 w_a)} \right) \right] \quad (3.93)$$

The exergy analysis for the **water** can be preceded in the similar fashion as that for dry air and water vapor. The specific exergy of water, considering it as an incompressible liquid, can be written as

$$\psi_w = (h_w - h_0) - T_0 (s_w - s_0) + R_v \ln \left( \frac{x_{w0}}{x_{w00}} \right) \quad (3.94)$$

Where

$\psi_w$  = total specific exergy of water

$x_w$  = mole fraction of the water at the system state

$x_{w00}$  = mole fraction of the water at the environment state

$h_w$  = specific enthalpy of water at any system state

$s_w$  = specific entropy of water at any system state

The ratio of mole fraction of water at atmosphere to that at the dead state can be equated to relative humidity at the dead state (see **article 12** from appendix )

Therefore

$$\frac{x_{w00}}{x_{w0}} = \theta_0 = \text{relative humidity of air at dead state}$$

Substituting the above equation in equation (3.74) and rearranging using **article 13** from appendix we get

$$\psi_w = (h_{fw} - h_{f0}) + v_{fw} (p - p_{sat}) - T_0 (s_{fw} - s_{f0}) - R_v \ln(\theta_0) \quad (3.95)$$

where

$h_{fw}$  = specific enthalpy of saturated water at temperature of system state

$h_{f0}$  = specific enthalpy of saturated water at temperature of restricted dead state

$v_{fw}$  = specific volume of water at temperature of system state

$p$  = partial pressure of water at system state

$p_{sat}$  = partial pressure of water at saturation

Now we make an assumption that at dead state the specific enthalpy of saturated water and saturated vapor are approximately equal and similarly the specific entropy of saturated water and saturated vapor are approximately equal [19,20]

Or in other words

$$h_{f0} \cong h_{g0}$$

$$s_{f0} \cong s_{g0}$$

therefore

$$\psi_w = (h_{fw} - h_{g0}) + v_{fw} (p - p_{sat}) - T_0 (s_{fw} - s_{g0}) - R_v \ln(\theta_0) \quad (3.96)$$

Total exergy of water/unit time,  $X_w$ , can be expressed as

$$X_w = (\psi_w m_w)$$

where

$m_w$  is the mass flow rate of water

Or

$$X_w = m_w \left( (h_{fw} - h_{g0}) + v_{fw} (p - p_{sat}) - T_0 (s_{fw} - s_{g0}) - R_v \ln(\theta_0) \right) \quad (3.97)$$

Now the total exergy/unit time of the system will be the summation of exergy of all the components viz. dry air, vapor and water. Therefore adding equations (3.89) (3.93) and (3.97). We get total exergy of the system as

Exergy of air vapor mixture is represented by adding Exergy of air and vapor.

$$X_{air} = X_v + X_a$$

Therefore

$$\begin{aligned}
 X_{air} = m_a w & \left[ c_{pv} (T - T_0) - T_0 c_{pv} \ln \left( \frac{T}{T_0} \right) + R_v T_0 \ln \left( \frac{w(1 + 1.608w_{00})}{w_{00}(1 + 1.608w)} \right) \right] \\
 & + m_a \left[ c_{pa} (T - T_0) - T_0 c_{pa} \ln \left( \frac{T}{T_0} \right) + R_a T_0 \ln \left( \frac{1 + 1.608w_{00}}{1 + 1.608w_a} \right) \right] \quad (3.98)
 \end{aligned}$$

In the above equation, Exergy due to convection

$$X_{conv} = m_a \left[ c_{pa} (T - T_0) - T_0 c_{pa} \ln \left( \frac{T}{T_0} \right) + w_a \left\{ c_{pv} (T - T_0) - T_0 c_{pv} \ln \left( \frac{T}{T_0} \right) \right\} \right]$$

Exergy due to evaporation can be written as

$$X_{evap} = m_a \left[ R_a T_0 \ln \left( \frac{1 + 1.608w_{00}}{1 + 1.608w_a} \right) + w_a R_v T_0 \ln \left( \frac{w(1 + 1.608w_{00})}{w_{00}(1 + 1.608w)} \right) \right]$$

$$X_{total} = X_w + X_{air}$$

$$X_{total} = X_w + X_v + X_a \quad (3.99)$$

$$\begin{aligned}
 X_{total} = m_w & \left( (h_{fw} - h_{g0}) + v_{fw} (p - p_{sat}) - T_0 (s_{fw} - s_{g0}) - R_v \ln(\theta_0) \right) \\
 & + m_a w \left[ c_{pv} (T - T_0) - T_0 c_{pv} \ln \left( \frac{T}{T_0} \right) + R_v T_0 \ln \left( \frac{w(1 + 1.608w_{00})}{w_{00}(1 + 1.608w)} \right) \right] \quad (3.100) \\
 & + m_a \left[ c_{pa} (T - T_0) - T_0 c_{pa} \ln \left( \frac{T}{T_0} \right) + R_a T_0 \ln \left( \frac{1 + 1.608w_{00}}{1 + 1.608w_a} \right) \right]
 \end{aligned}$$

the term  $v_{fw} (P - P_{sat})$  is very small in terms of other terms therefore can be neglected

hence the equation becomes

$$\begin{aligned}
 X_{total} = & m_w \left( (h_{fw} - h_{g0}) - T_0 (s_{fw} - s_{g0}) - R_v \ln(\theta_0) \right) \\
 & + m_a w \left[ c_{pv} (T - T_0) - T_0 c_{pv} \ln\left(\frac{T}{T_0}\right) + R_v T_0 \ln\left(\frac{w(1 + 1.608w_{00})}{w_{00}(1 + 1.608w)}\right) \right] \\
 & + m_a \left[ c_{pa} (T - T_0) - T_0 c_{pa} \ln\left(\frac{T}{T_0}\right) + R_a T_0 \ln\left(\frac{1 + 1.608w_{00}}{1 + 1.608w_a}\right) \right]
 \end{aligned} \tag{3.101}$$

### 3.5 Exergy Destruction

For determining the rate of exergy destruction i.e, the loss of potential of air to recover exergy supplied by the water, can be constructed from the control volume exergy balance equation. Assuming the air water properties are known at discrete points along the tower at height dz. Taking the case of vertical downward parallel flow and applying the exergy balance on the control volume we get

$$\underbrace{X_{total,z(j)}}_{\text{total exergy/unit time entering at height } z(j)} = \underbrace{X_{total,z(j+1)}}_{\text{total exergy/unit time leaving at height } z(j+1)} + \underbrace{I}_{\text{total exergy/unit time destroyed}}$$

where

$$z(j+1) - z(j) = dz$$

Therefore after rearrangement, the exergy destruction for discrete height dz will be

$$I = X_{total,z(j)} - X_{total,z(j+1)} \tag{3.102}$$

---

### **SIMULATION STUDIES & DISCUSSIONS**

The present chapter describes the solution procedure of the mathematical formulation given in Chapter 4 followed by results and discussions for both parallel flow and counter flow cooling towers.

#### **4.1 Simulation studies for parallel flow downward shower cooling tower**

For the purpose of numerical integration of the differential equations, Runge Kutta method of fourth order with fifth order correction is employed. The system of differential equations for downward vertical parallel configuration is represented by set of equations [3.54(a) to 3.54(g)]. A set of initial values are supplied as input by the user.

#### **4.1.1 Boundary conditions**

The input is boundary conditions which for parallel downward flow are:

- a) Tower geometry: Height, cross section area and shape of the tower.
- b) Spray characteristics: Droplet velocity, angle of projection, mean droplet diameter in mono droplet model and diameter range, mean diameter and droplet spread parameter for poly droplet model.
- c) Inlet air conditions: Air velocity, flow rate, dry bulb temperature and relative humidity at inlet.
- d) Water condition: Mass flow rate and its temperature at inlet

#### **4.1.2 Simulation procedure**

The first step in the approach towards solution procedure is to divide the tower height  $H$ , into a number of divisions ( $div$ ), the numerical integration is carried out in each division to find the variation of the main parameters with height. The main parameters are those parameters that change during the course of the integration. Seven main parameters are used in this analysis. These parameters are  $T_a$  – Temperature of air,  $T_w$  – Temperature of water,  $I_{ma}$  - Specific Enthalpy of air ,  $D_d$ -Diameter of droplets,  $W_a$ -Specific Humidity of air,  $U_y$  and  $U_x$  – Velocity of droplets in X and Y axes respectively



The lagging parameters on the other hand are assumed to be constant during the individual elements of integration. These parameters include kinematic viscosity, density of air, heat transfer coefficient, Lewis factor etc. The lagging parameters are recalculated using the main parameters at every division. These parameters along with the main parameters serve as a fresh input to the solver for the subsequent interval or division. This process is continued for every division till the properties at every height is known. The solution for the main parameters is stored in a result matrix. The result matrix contains the main parameters along with the tower height at which they are calculated.

The above discussion holds good for single as well as multi-diameter droplets model. In multi-diameter droplets model, the different equations of main parameters for different droplets are numerically integrated separately. The main parameters such as enthalpy and specific humidity due to each droplet can be added to give the net enthalpy and net specific humidity at any height. The program automatically build matrix of differential equations according to the range of droplets provided as input.

A brief description of the algorithm is mentioned in the Figure 4.1 and the outline of mathematical model is represented in Figure 4.2

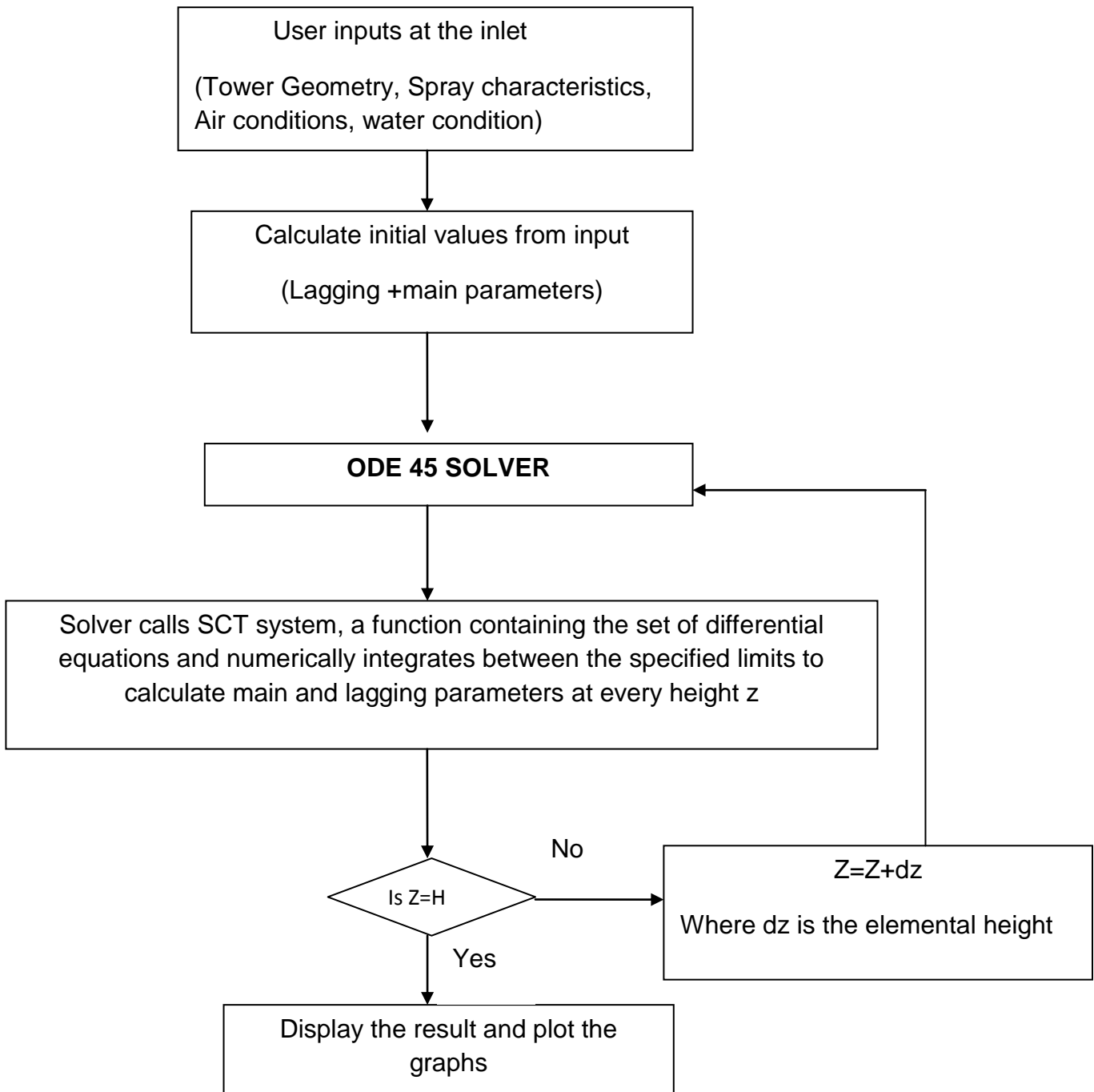


**Figure 4.1 Flow chart of numerical solution**

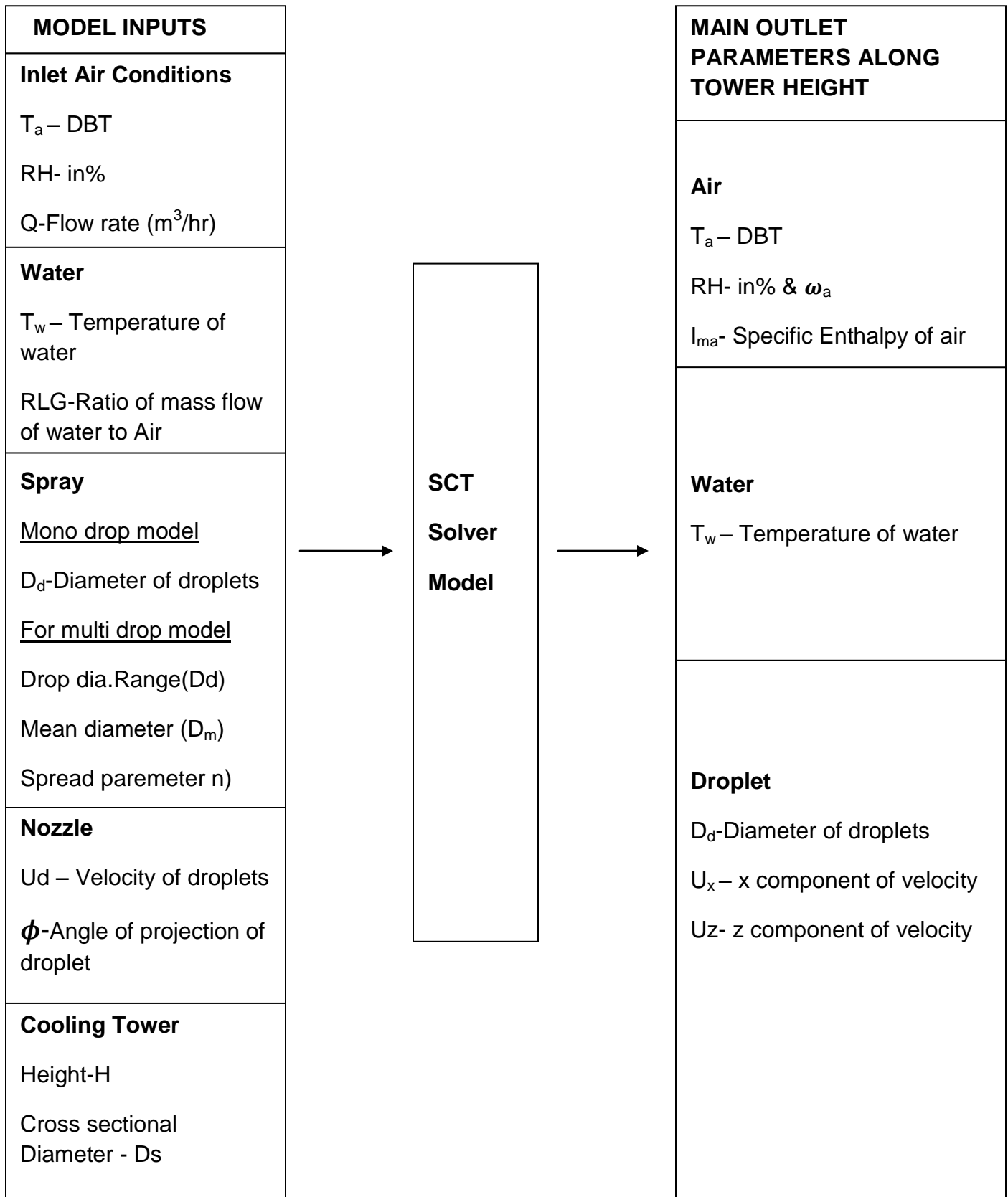


**Figure 4.2 Flow chart of mathematical model**

### 4.1.3 Model validation

The equations obtained in the Chapter 4 and the discussion on their numerical simulation in the previous section seems a rational way of approaching the problem of finding the results for a vertically downward parallel flow Shower Cooling Tower.

The work carried out by *Pearlmutter et al* [4] on a similar active down draft Shower cooling Tower has been used for model validation. The performance of the tower was monitored by measuring the air DBT and relative humidity with the help of electronic temperature and humidity sensors at its inlet and outlet. The air flow rate was calculated according to measured air speed and effective opening area of the air supply system. The air stream passed through a system of spray of water droplets, which are directed downwards together with the air. The results of their work is summarized in the following table

Table 4.1 Field testing and result [4]

configuration	Water supply	Air flow rate (m <sup>3</sup> /hr)	DBT depressions (Celsius)	Predicted DBT depression
1	Coarse spray (1.5mm,assumed)	1150	5.8	5.93
2	Fine spray (800micron)	1150	10.2	10.8

As the mass flow rate of water is not mention in their work, the mass flow rate is adjusted keeping the other parameters constant. The value of water mass flow to air which gives close to the experimental value is 0.245.

Two checks are implemented for validating the differential equation used in this simulation program using the inlet conditions of table 4.1

**i) Mass Balance**

The total mass of water in the system must remain constant. Referring to Figure 4.3 & 4.4, it can be seen that the change of mass flow rate of water at every step is equal to change of Mass Flow rate of vapor added in Air. Hence the mass of water remains conserved validating the derived equations.

**ii) Energy Balance**

The net enthalpy of system must remain conserved. Referring to Figure 4.5, it can be clearly seen that the net enthalpy of System remains nearly constant throughout. An error of 0.2% was observed during the enthalpy balance which is very small and can be neglected.

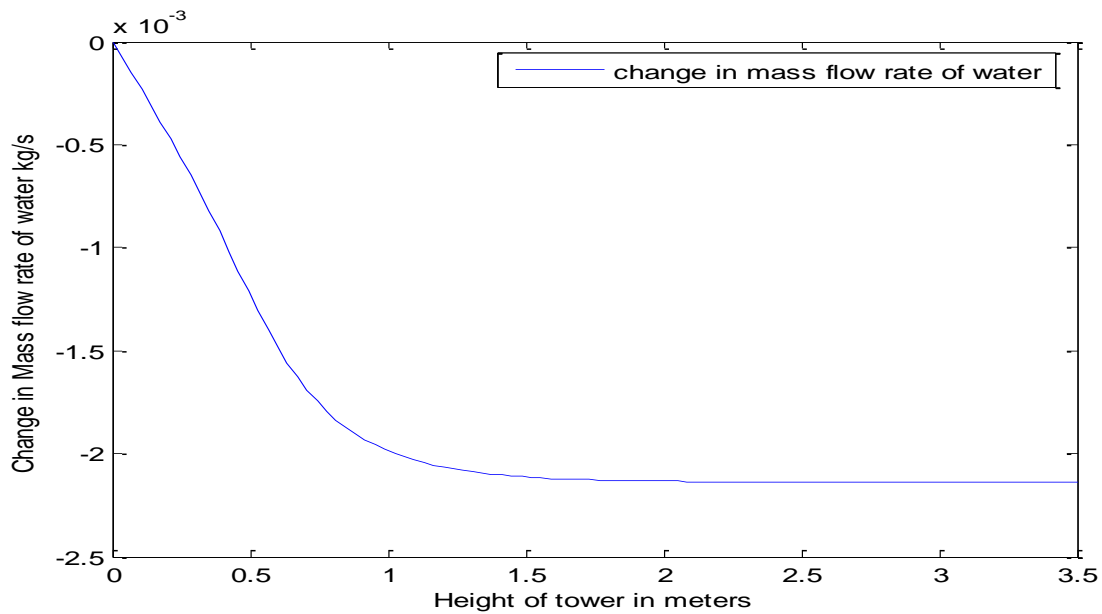


Fig 4.3 Variation of rate of flow of water with height of the tower

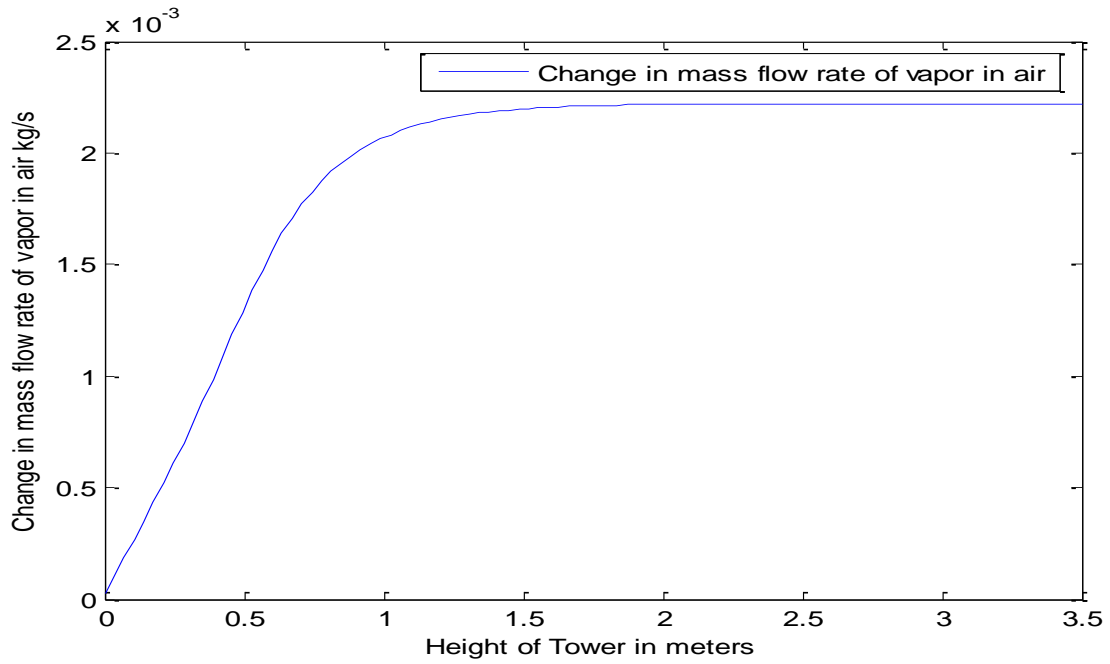


Fig 4.4 Variation of rate of water vapor added in air with height of the tower

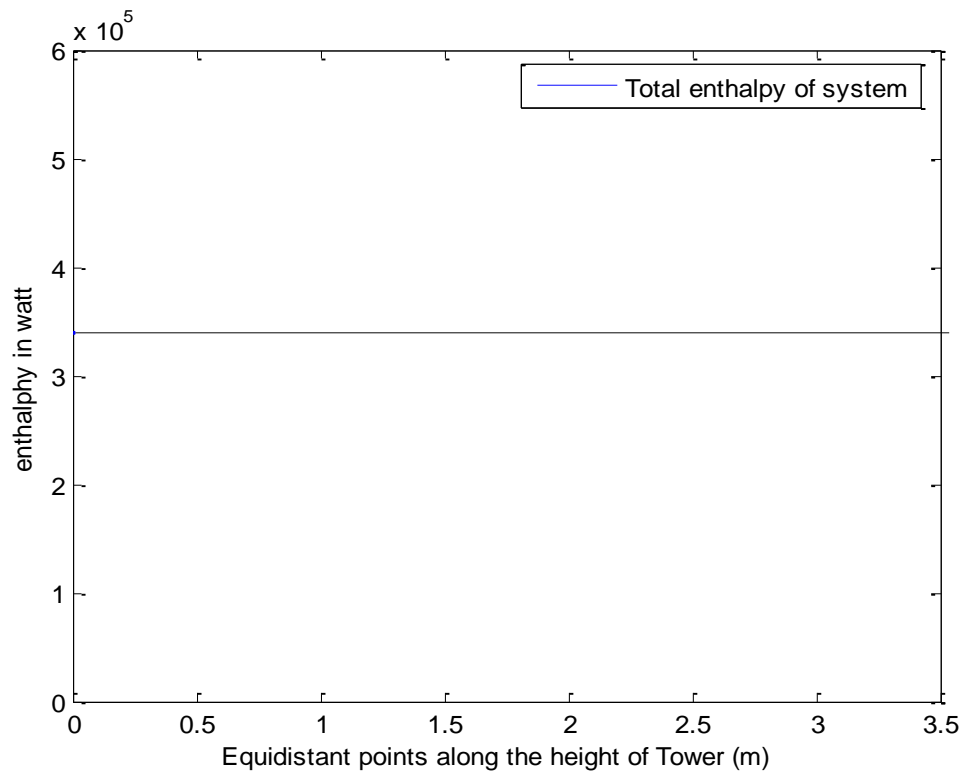


Figure 4.5. Net enthalpy with height of tower

#### 4.1.4 Parametric Study

The various parameters and their ranges used as inputs for mono droplet and multi droplet model are:

- 1) **Droplet Size:** droplet diameter range for mono droplet is 0.25, 0.8 and 1.5 mm and for multi droplet model diameter range is 0.225 mm to 0.975 mm in the step of 0.50 mm (15 droplets), mean diameter 0.51752 mm (calculated from Rosin-rammler distribution) and spread parameter is 3.9242.
- 2) **Inlet water temperature:** 18<sup>0</sup>C, 20<sup>0</sup>C and 25<sup>0</sup>C
- 3) **Droplet projection angle :** 54 degree and 70 degree
- 4) **Droplet injected speed :** 6 m/s and 15.84 m/s
- 5) **Inlet air temperature :** 36<sup>0</sup>C, 40<sup>0</sup>C and 45<sup>0</sup>C

#### a) Initial conditions

The detailed initial conditions used for this computer simulation program are shown in Table 4.1.

Table 4.2 Initial conditions used for simulation program.

<b>Input Parameters</b>	
<b><u>Air/water conditions</u></b>	
Inlet temperature of Air ,Ta ( K)	36+273.15
Inlet air Relative Humidity, RH (%)	20
Inlet air flow rate, Q (m <sup>3</sup> /hr)	1150
Inlet water temperature(K), T <sub>w</sub>	20+273.15
Ratio of mass flow rate of water to air(RLG)	0.425
<b><u>Dimensional parameters</u></b>	

Tower height (m),H	3.5
Cross section diameter(m),D <sub>s</sub>	1.28
Number of division over height	100
<b><u>Droplet input condition</u></b>	
Mono Droplet diameter(m),D <sub>di</sub>	250×10 <sup>-6</sup>
Droplet range (m) (15 droplets)	225×10 <sup>-6</sup> : 50×10 <sup>-6</sup> : 975×10 <sup>-6</sup>
Rosin- Rammler Mean Diameter(m),D <sub>m</sub>	517.52×10 <sup>-6</sup>
Rosin- Rammler Spread Parameter (a scalar),n	3.9342
Droplet velocity (m/s), u <sub>d</sub>	15.84
Droplet angle of Projection(Degree) at inlet ,θ	54 <sup>0</sup>
<b><u>Inlet position parameters</u></b>	
X coordinate	0
Z coordinate	0
<b><u>Other specifications</u></b>	
Acceleration due to gravity(m/s <sup>2</sup> )	9.81

**b) Effect of variation in initial droplet diameter**

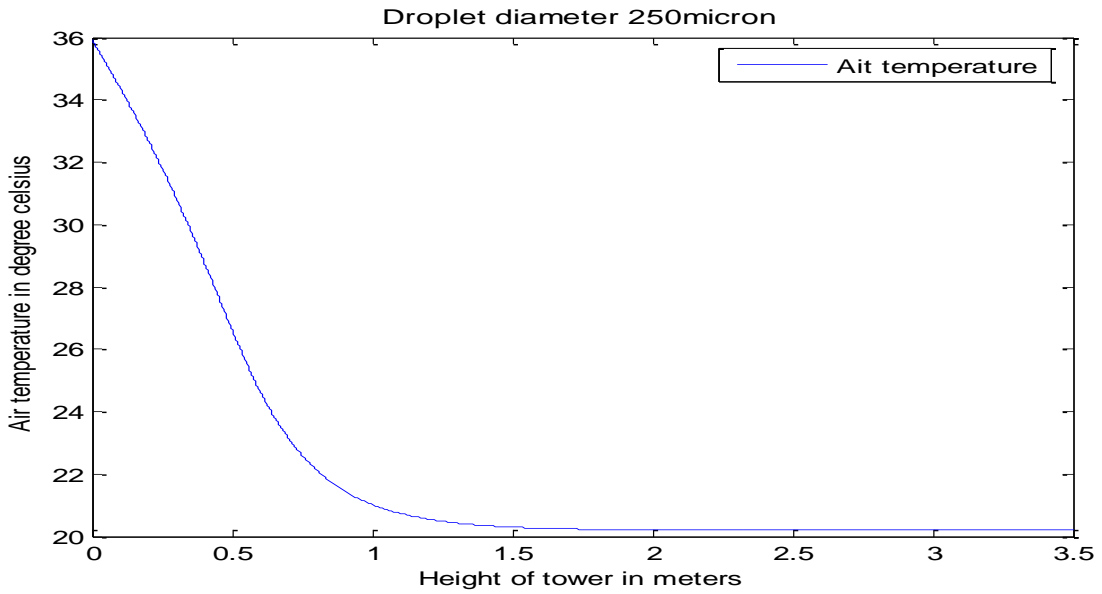
Table 4.3 shows the effect of variation of initial droplet diameter on exit air condition

Table 4.3 Effect on exit air by variation in inlet droplet diameter

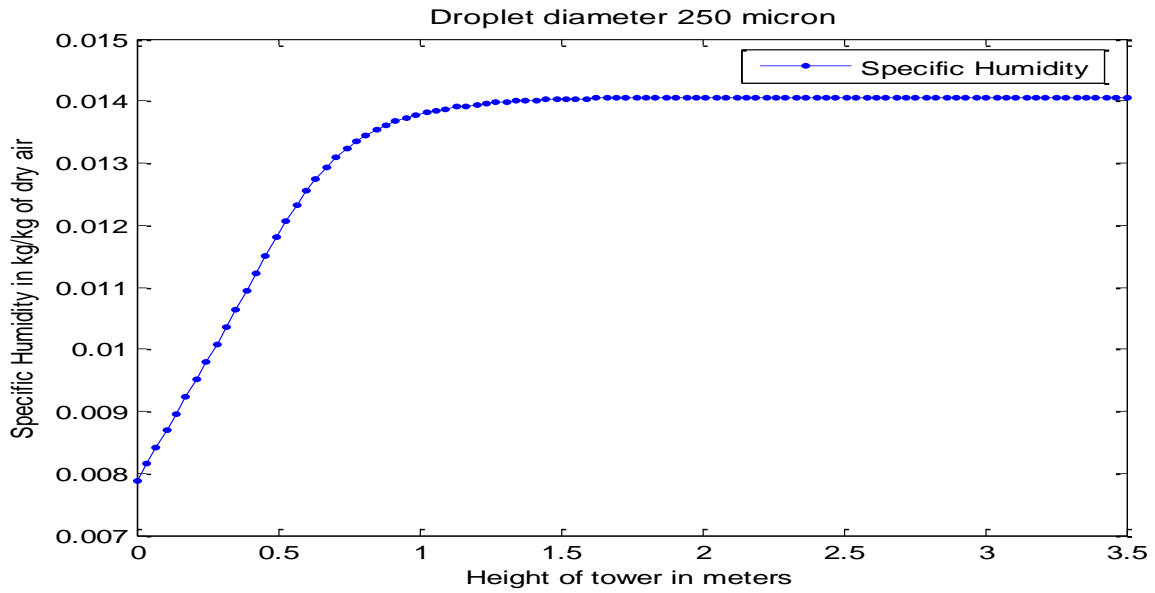
	<b>Inlet drop diameter D<sub>d</sub> (m)</b>	<b>Outlet Air temperature t<sub>a</sub> (°C)</b>	<b>Outlet Specific humidity(ω<sub>a</sub>)</b>	<b>Outlet RH (%)</b>	<b>DBT depression (Δt<sub>a</sub>) (°C)</b>	<b>Cooling capacity (kw)</b>
Run 1	Fine spray 250×10 <sup>-6</sup>	20.4	0.0141	99.953	15.6	3.2
Run 2	Fine spray 800×10 <sup>-6</sup>	25.2	0.0120	59.8	10.8	2.7
Run 3	Coarse spray 1.5×10 <sup>-3</sup>	28.8	0.0108	40	5.9	1.7



Run 4	Multi droplet range and dia. from table 4.2	21	0.0145	90	14.2	3.0
-------	---	----	--------	----	------	-----

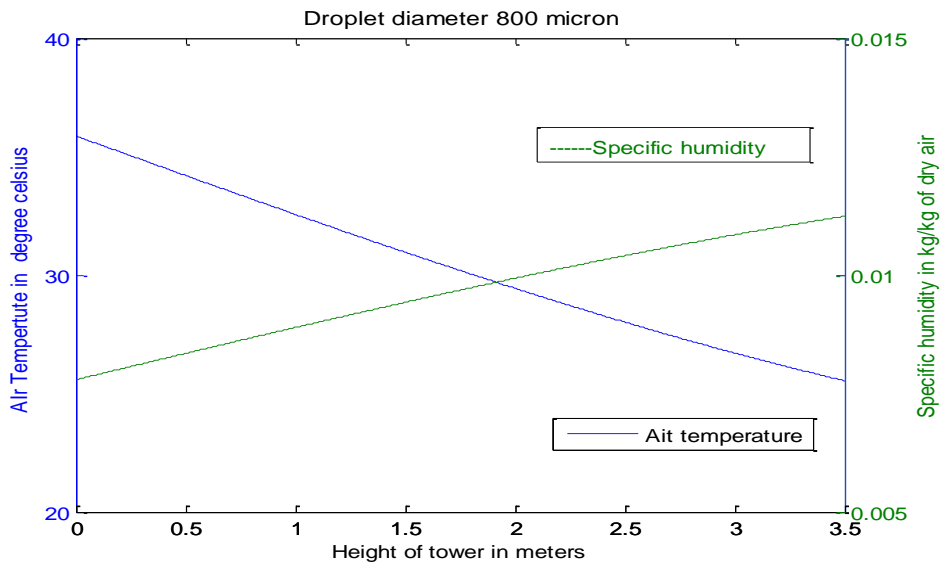


4.6 Air temperature along tower height

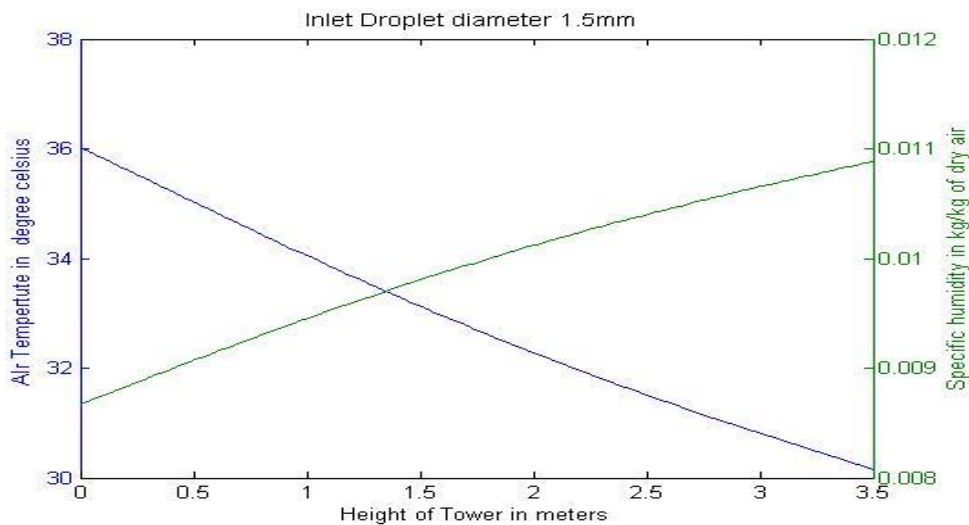


4.7 Specific humidity along tower height

It is clear from Fig. 4.6 that the air temperature decreases along the height of the tower up to around 1.5 to 1.7 m, after that its temperature does not change because of 99.95 % RH (Fig 4.7) and the air is saturated at this height. Beyond this height there is no further cooling of air takes place.

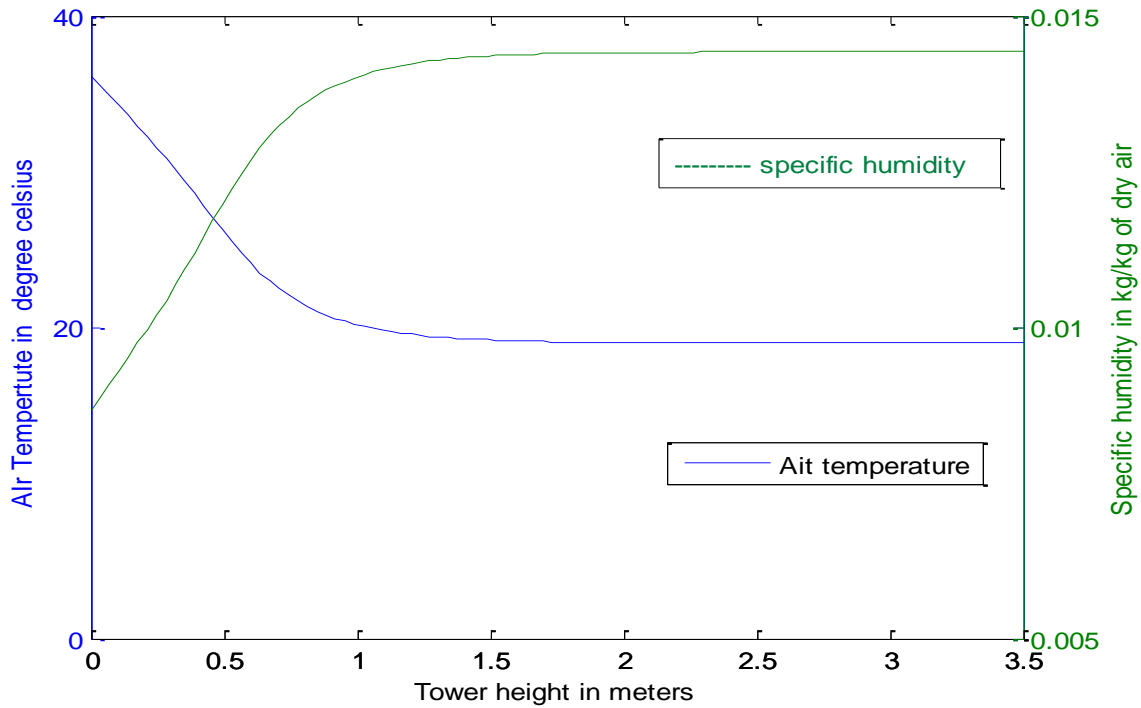


4.8 Air temperature and Specific humidity along tower height



4.9 Air temperature and Specific humidity along tower height

As shown in Figure 4.8 to 4.9 as diameter of droplet increases the outlet air temperature and specific humidity decreases because the retention time and their trajectory path are reduced.



#### 4.10 Air temperature and Specific humidity along tower height for multi droplet model

The Fig 4.10 shows the variation in DBT and specific humidity of air in multi droplet model for the RR mean diameter of droplet range of Table 4.2. It is evident that DBT of air decreases along the height of cooling tower, whereas the specific humidity shows an increase. As shown in Figure 4.11 for the poly droplet injection the retention time for smaller sized droplets is considerably greater than large sized droplets. This is due to the fact that smaller sized droplets have small momentum & the drag force exerted by air is

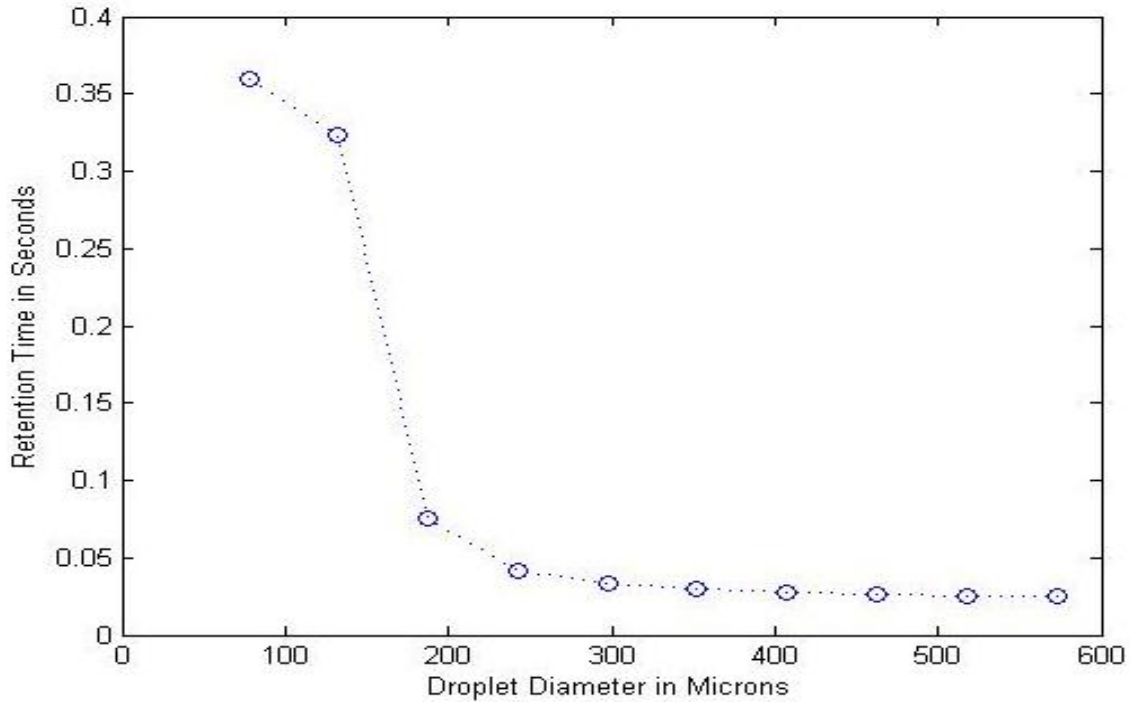


Figure 4.11 Retention Time of Different sized droplets (10 droplets)

able to change their momentum in a very short span of time. Their momentum becomes aligned with the air momentum & is carried with air without striking the wall. This considerably increases their retention time, thereby producing more cooling. From Fig 4.11 it can be observed that retention time sharply reduces between drop size range of 100 to 200 microns.

The present model prediction between 1.5 to 2 meter of tower length the increase in relative humidity and decrease in air temperature is negligible shows that present model matches satisfactory with the series of experiment performed by Pearlmutter et al [4]. Thus 90% cooling is achieved within 1.5 to 2 meter of the tower length. It means for saving cost the ideal tower height for same input parameters is 1.5 to 2 meters.

### c) Effect of variation of Inlet water temperature

As in evaporative cooling the inlet water temperature is goes on decreasing until and unless it achieved WBT of air (theoretically). In present study the three water temperature ranges are selected

(i) Near the Wet Bulb Temperature of incoming air at 20<sup>0</sup>

(ii) Above Wet Bulb Temperature (25<sup>0</sup>C) and

(iii) Below Wet Bulb Temperature (18<sup>0</sup>C)

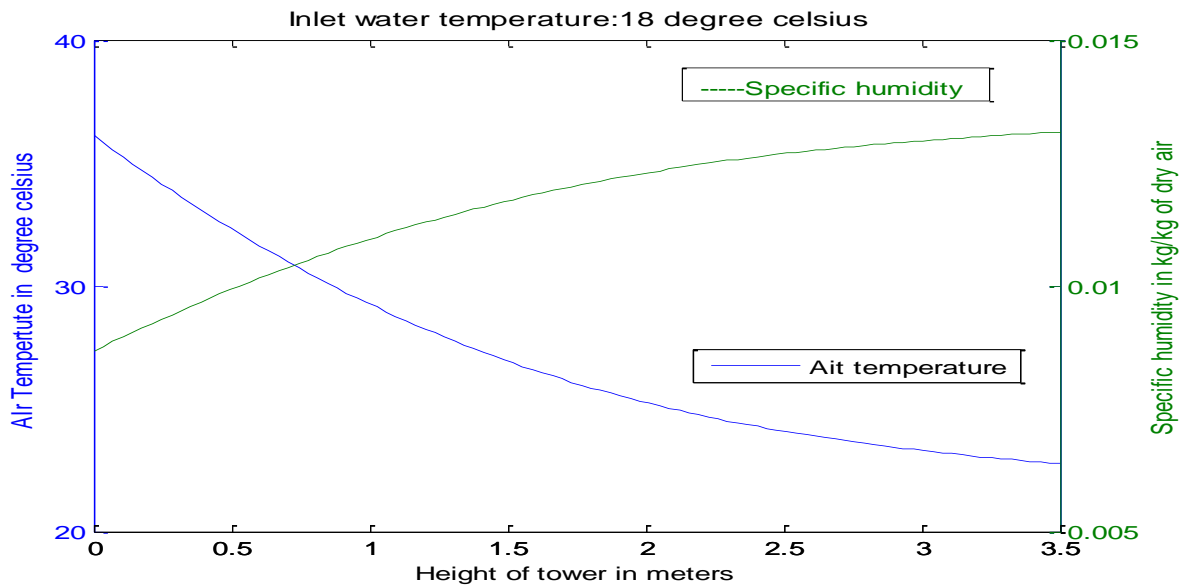
Water temperature below wet bulb can be achieved by using vapor absorption refrigeration system. Table 4.4 shows the effect of water temperature for droplet diameter size equal to 800 microns.

Table 4.4 Effect of variation in inlet water temperature on air outlet condition

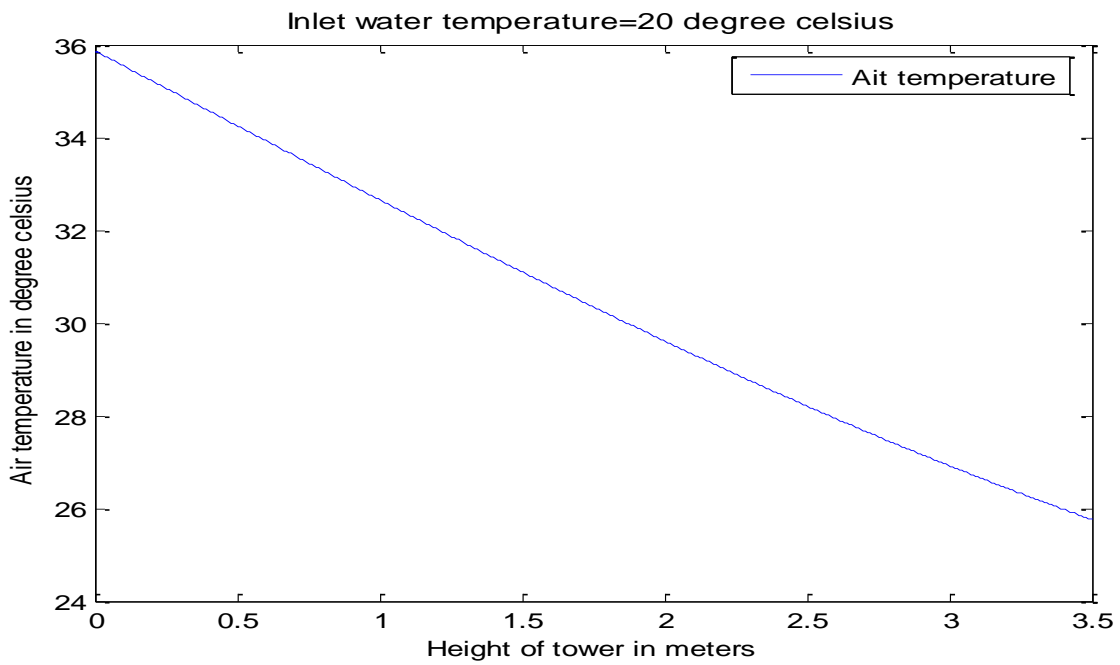
	<b>Inlet <math>t_w</math> (<sup>0</sup>C)</b>	<b>Outlet <math>t_a</math> (<sup>0</sup>C)</b>	<b>Outlet Specific humidity(<math>\omega_a</math>)</b>	<b>DBT depression (<math>\Delta t_a</math>) (<sup>0</sup>C)</b>
Run 1	18	22.7	0.0131	13.3
Run 2	20	25.8	0.0120	10.2
Run 3	25	28.16	0.0130	7.84

(a) Water temperature below WBT of incoming air

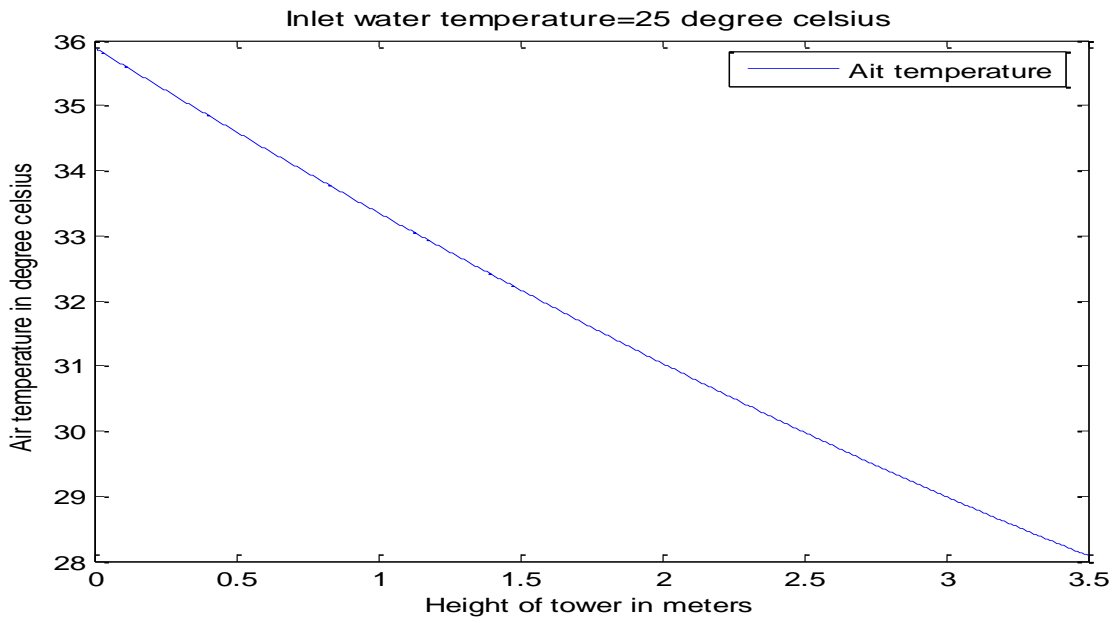
Fig 4.12 shows the variation in air DBT and specific humidity along the height of the tower



4.12 Air temperature and Specific humidity along tower height ( $t_w=18^{\circ}\text{C}$ )



4.13 Air temperature along tower height ( $t_w=20^{\circ}\text{C}$ )



4.14. Air temperature along tower height( $t_w=25^{\circ}\text{C}$ )

Fig 4.12 and 4.13 shows air temperature variation at water temperature of  $18^{\circ}\text{C}$  and  $25^{\circ}\text{C}$

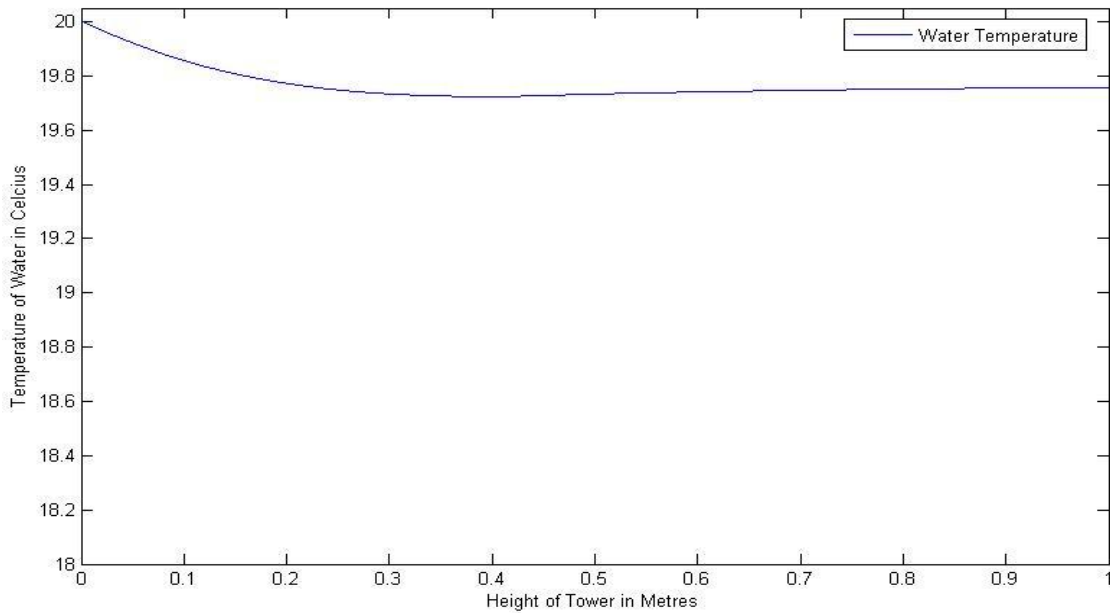


Figure 4.15 Water temperature variations

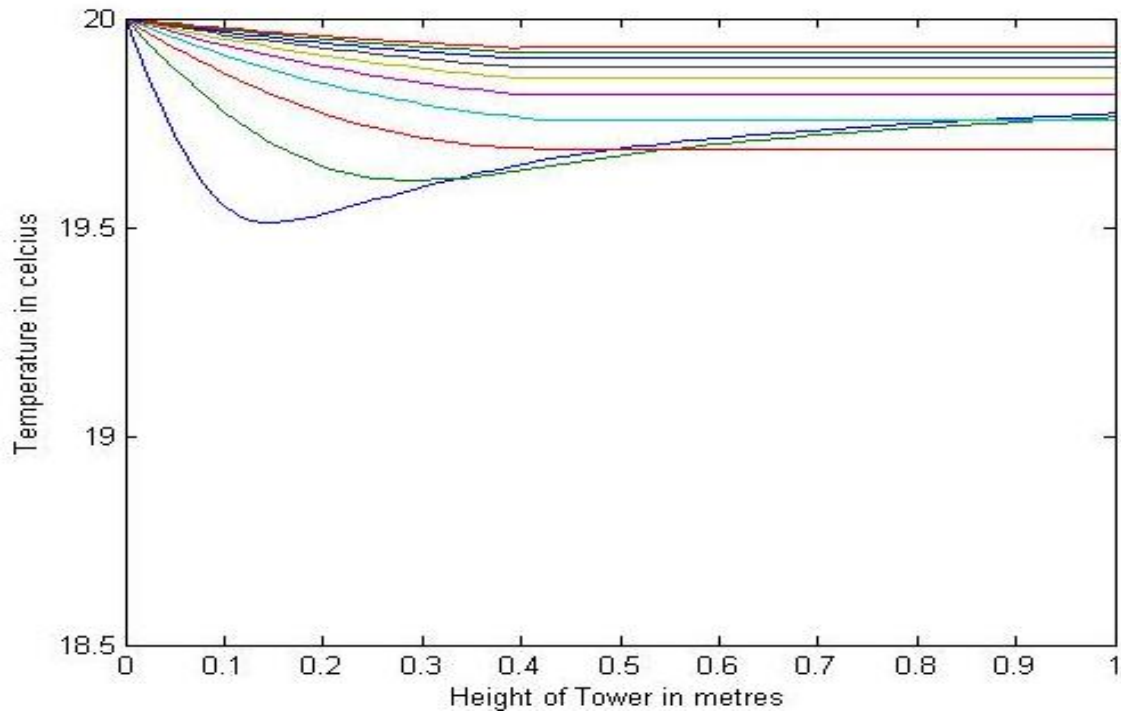


Figure 4.16 Water temperature distributions among droplets

Refer to figure 4.15 It can be seen that water temperature also decreases till the wet bulb temperature & becomes nearly constant (19.6°C). Before the point of wet bulb temperature is reached, the latent heat of evaporation taken from droplet is more than heat from convection added to droplet. After the wet bulb temperature, the latent heat of evaporation taken from water becomes equal to the heat of convection added to droplet, hence the water temperature becomes stable at WBT & point of equilibrium for water is reached. The slight variation of .05°C in water temperature after wet bulb temperature can be attributed to simulation computational errors.

Also it can be noted that the spray of water constitutes of different sized droplets & the temperature indicated above represent the mean water temperature. The temperature of water of different sized water droplets would be different at any particular cross section.

(Figure 4.16)



#### d) Droplet projection angle

The angle of projection play an important role in cooling as the retention time of droplets and the air water interaction is depends on it. Two range of projection angle is selected [23] at  $54^{\circ}$  and  $70^{\circ}$ .

Table 4.5 Effect of variation of projection angle on air outlet properties

	Projection Angle( $\theta$ )	Outlet $t_a$ ( $^{\circ}\text{C}$ )	Outlet Specific humidity( $\omega_a$ )	DBT depression ( $\Delta t_a$ ) ( $^{\circ}\text{C}$ )
Run 1	$54^{\circ}$	25.8	0.0120	10.2
Run 2	$70^{\circ}$	22.26	0.0132	13.74

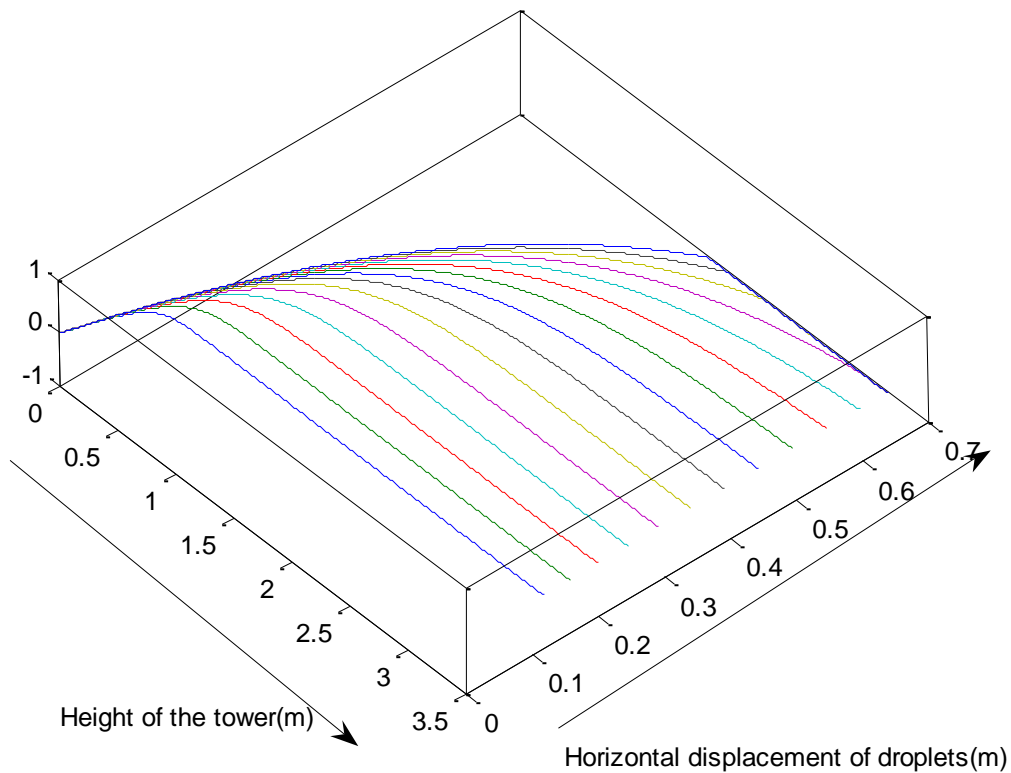


Figure4.17 Droplet trajectories of 15 droplets at an angle  $54^{\circ}$  from horizontal (Increasing size from left to right)

As refer to Fig.4.17 droplets are injected at an angle of  $54^{\circ}$  from horizontal at the absolute speed of 6 m/s, out of 15 droplets injected only biggest four drops striking with wall having diameters 825,875,925 and 975 (micron)respectively, and all other cover full length of cooling tower and play major contribution in cooling .

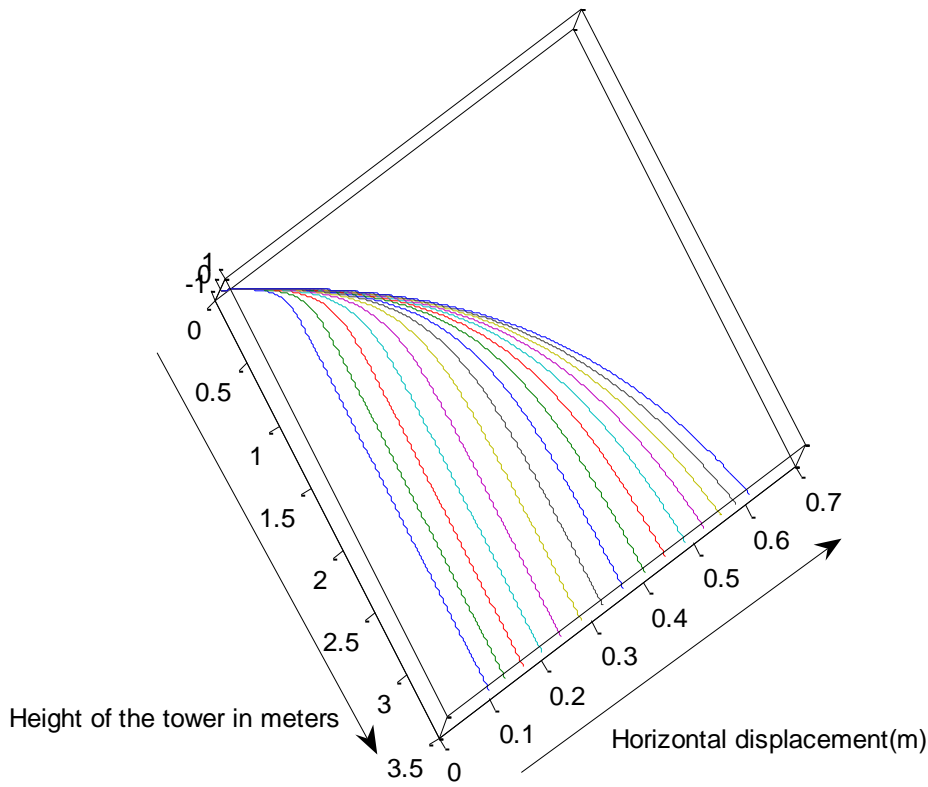


Figure4.18. Droplet trajectories of 15 droplets at an angle  $70^{\circ}$  from horizontal,  
Droplet injected speed=6m/s  
(Increasing size from left to right)

Refer to Figure 4.18 projection angle is  $70^\circ$  at the same speed, here all the injected droplets are covering whole tower length and thereby increasing cooling output.

Theoretically projection angle is same for all the droplets injected but in practical the spray angle increases with the pressure and diameter. Moreover the influence of surrounding air flow is that it deflects the spray; the tendency is to decrease the spray angle, in an experimental set up at IIT, Delhi by Kumar et al [23] a maximum of  $9^\circ$  deflections in half cone angle is observed for 4mm diameter nozzle for air velocities between 0 and 3m/s (in this simulation program air speed is 0.2482 m/s).

#### d) Droplets injected speed

A trajectory of droplet at drop inlet speed of 15.84 is shown in Fig. 4.19 at this speed only

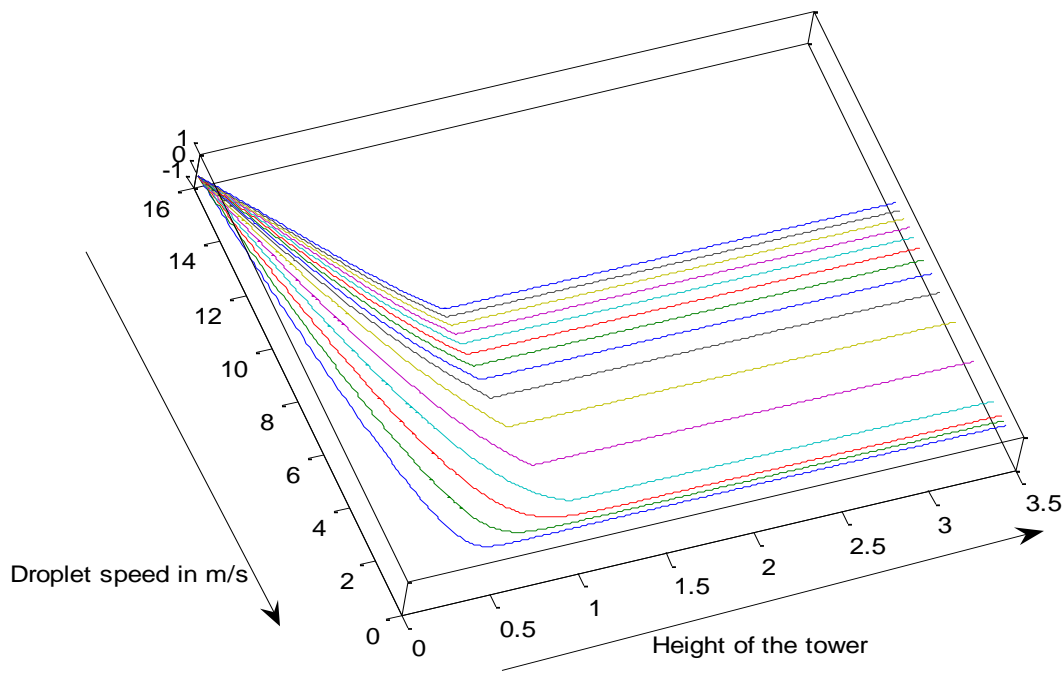


Figure4.19. Absolute Speed of Droplets with height  $\theta=54^\circ$ , droplets injected speed  $u_d=15.84\text{m/s}$  (Increasing size from bottom to top).

Only three smallest droplets completed their whole journey up to the end of the tower and rest of the bigger droplets strike to the wall, but at the droplet speed of 6m/s (Fig 4.20) at least 10 to 12 droplets cover the whole journey. The reason of that is more the speed of the droplet less is the chance that incoming air reduced their angle.

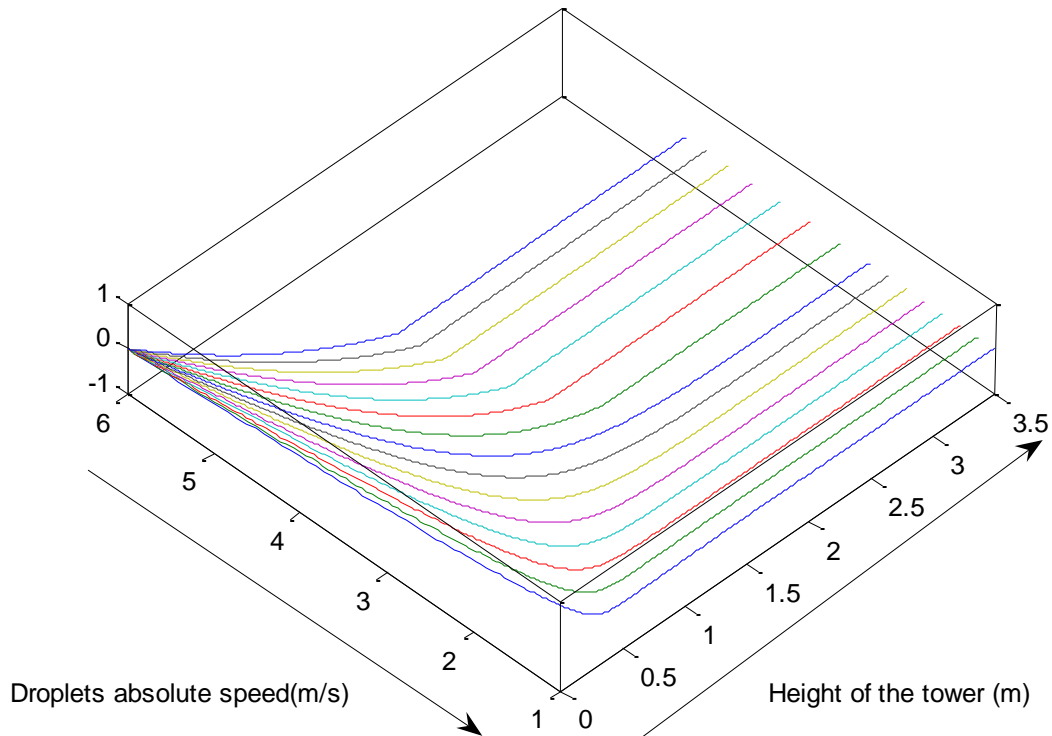


Figure4.20 Absolute Speed of Droplets with height  $\theta=54^{\circ}$ , droplets injected speed  $u_d=6\text{m/s}$  (Increasing size from bottom to top).

It is clear that, the speed of smaller sized droplets is drastically reduced due to air drag & becomes almost equal to air speed. Thus increasing their retention time, this indicates that small sized droplets result more cooling than bigger size droplets.

#### e) Inlet air temperature

In the case of an evaporative cooling system, the energy is supplied primarily by intake

air, whose heat content and capacity to hold the vapor is indicated by its DBT and RH.

Considering this fact three temperature range is selected 45<sup>0</sup>C, 40<sup>0</sup>C and 36<sup>0</sup>C.

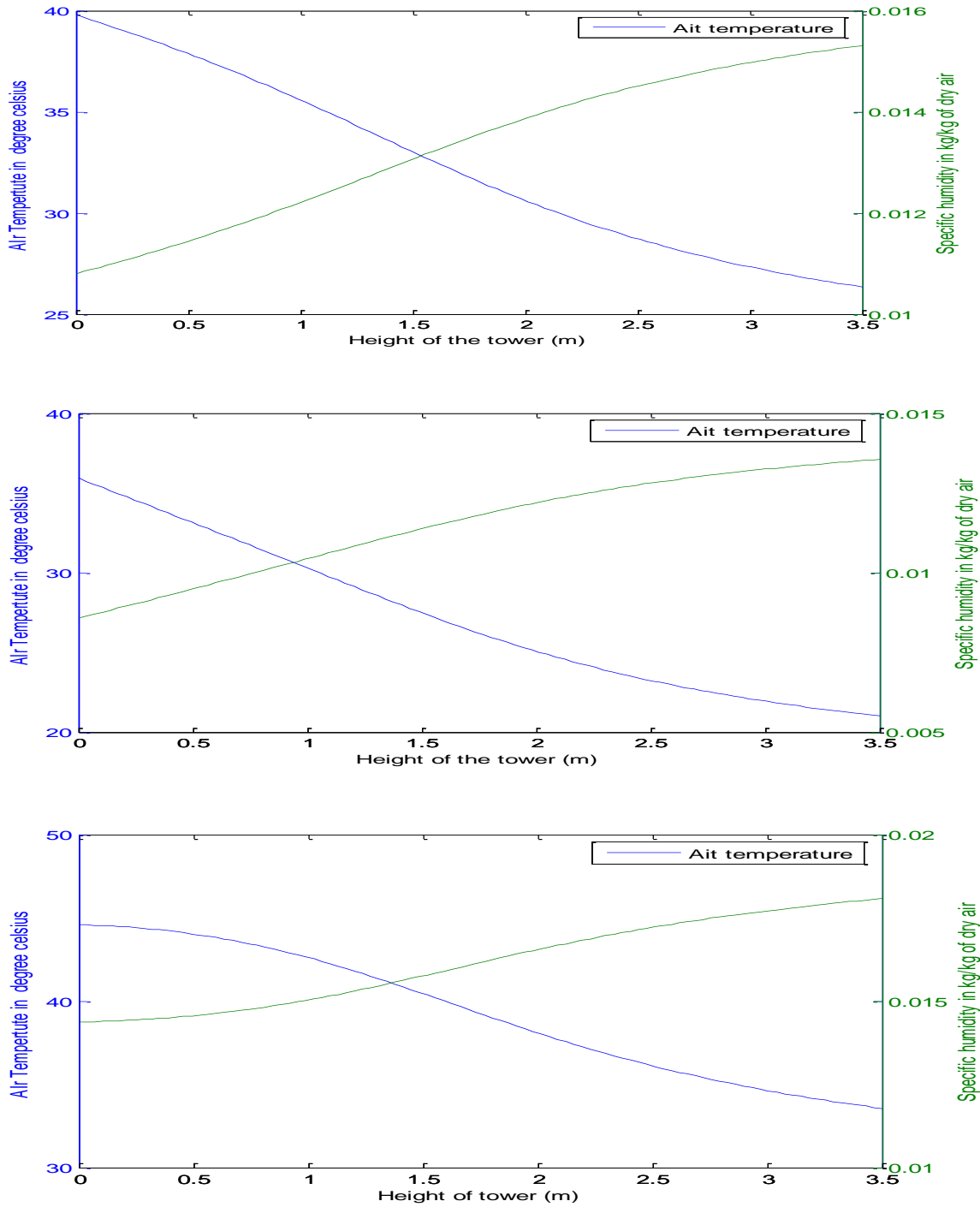


Figure 4.21 Air temperature and specific humidity along tower height

Figure 4.21 shows the effect of change in inlet air temperature while RH is at 22%.

#### 4.1.5. Exergy analysis

The reference condition used for exergy analysis are at  $T_0=293\text{K}$  and  $\text{RH}_{00}=80\%$

##### a) Exergy of Water

Fig. 4.22 shows water exergy,  $X_w$  and mass flow rate of water. Water exergy defined as the available energy carried by supplied water. From the exergy formulation in Chapter 3

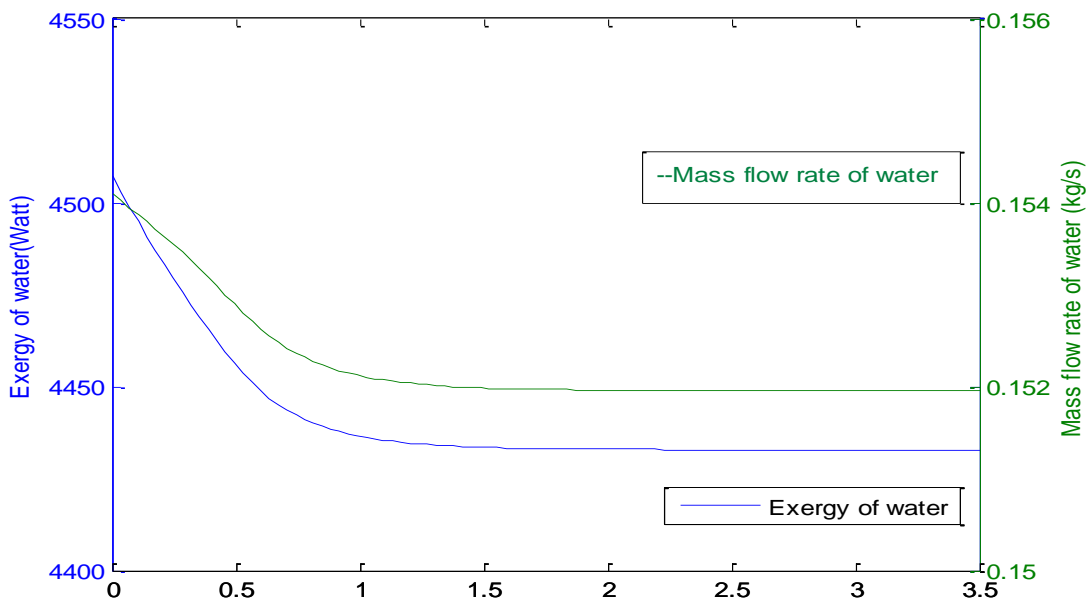


Figure 4.22 Exergy and mass flow rate of water

it is observed that total exergy of water in an SCT is a function of Temperature & mass flow rate. Since the temperature variation of water is very small (Figure 4.16), hence exergy becomes dependent on mass flow rate of water. It is clear from the figure that as mass flow

rate of water decreases the exergy of water decreases. Another interesting point to note is that after height of 2 meter as the decrease of mass flow rate of water is unchanged due to saturation condition. The exergy of water is constant. Hence the exergy of water in this case remains dependent mainly on mass flow rate of water.

## b) Exergy of air

### Convective Exergy

Convective exergy is dependent on magnitude of Temperature difference of air with the reference temperature. Hence Convective exergy should be proportional to the temperature difference of air & reference temperature.

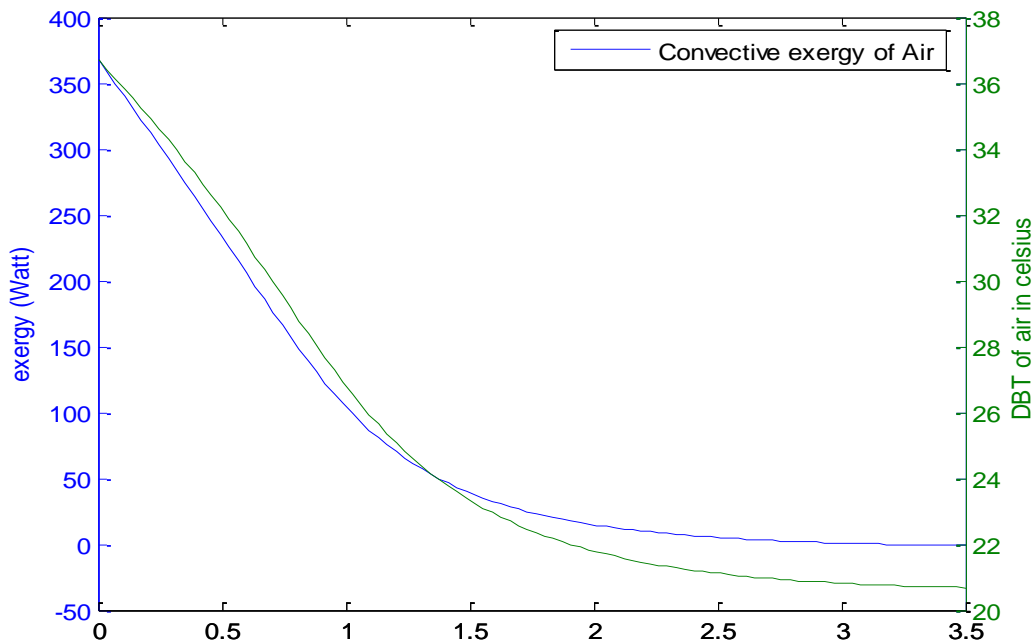


Figure 4.23 Convective exergy of air

In figure 4.23, it can be seen that convective exergy of air follows temperature difference between air temperature and reference temperature. As in the end of the tower temperature difference between air & reference temperature approaches zero so does convective exergy.

### Evaporative Exergy

From the formulation of exergy derived in Chapter 3, it was evident that evaporative exergy is proportional to absolute difference of specific humidity at reference & air specific humidity at any instant. Therefore the magnitude of difference between specific humidity of air & reference humidity should decrease with height & so does evaporative exergy. Refer to figure 4.24, it can be observed that evaporative exergy decreases with increasing specific humidity.

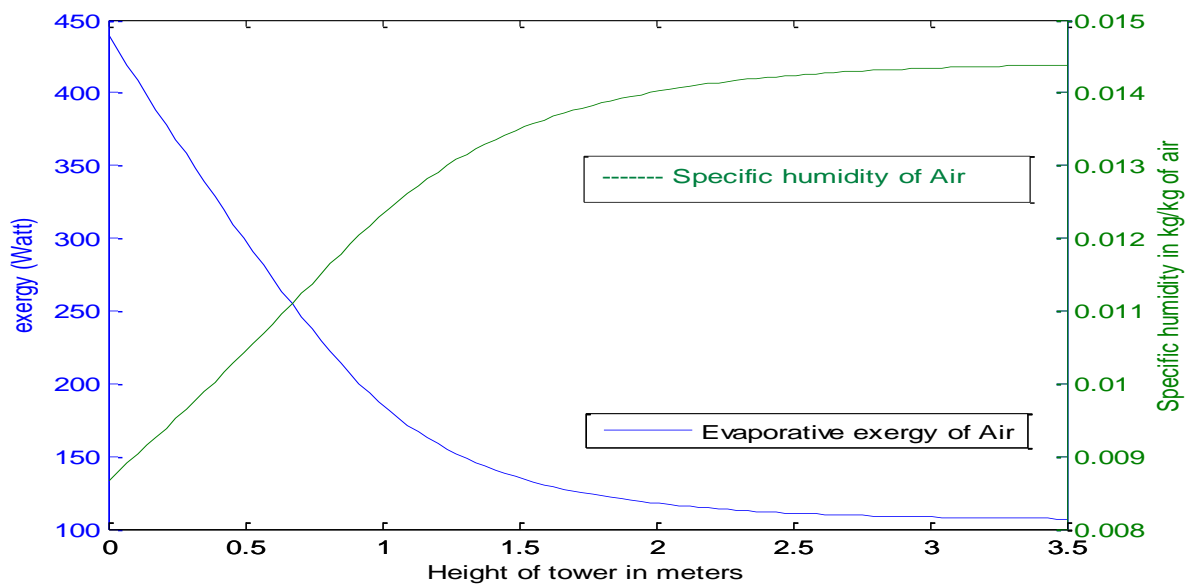


Fig.4.24 Evaporative exergy of Air



Also as the rate of increase of specific humidity decreases at around 2 m & so does the rate of decrease of exergy ..

The total exergy of air is the sum of evaporative & convective exergy & it can be clearly said that reference temperature & reference humidity will play an important role in deciding the value of total exergy of air.

**c) Exergy Destruction**

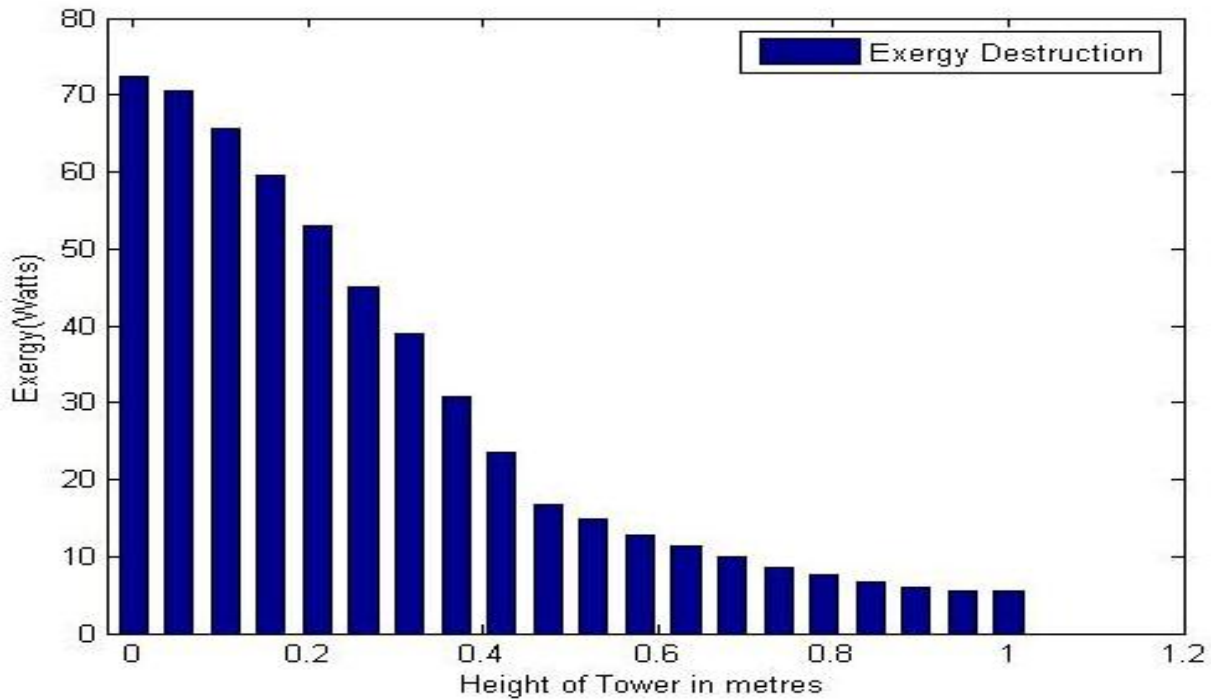


Figure 4.25 Exergy Destruction

Exergy Destruction which is  $(\text{Exergy of Air} + \text{Exergy of Water})_i - (\text{Exergy of Air} + \text{Exergy of Water})_{i+1}$  is calculated at discrete steps to know the overall sense of exergy

destruction(Figure 4.25). From the above figure it can be inferred that exergy destruction is maximum at the entry i.e. at bottom & goes on decreasing with height of tower(only 1 m tower length is consider as the maximum exergy destruction is within this area). This can be explained as the rate of maximum potential or exergy exists at the inlet, therefore the rate of destruction is proportional to the magnitude of exergy available. Also from Figure 4.25., it is evident that the steepness of the total exergy decreases from top to bottom of shower cooling tower.

From the above discussion of exergy destruction it is clear that maximum exergy destruction takes place at the inlet, hence the cooling towers should be designed focusing on inlet section. Higher attention should be given to the design of cooling tower at the inlet to reduce the exergy destruction.

## 4.2 Simulation studies for counter flow shower cooling tower

The formulation described in chapter 3 consists of governing equations for various parameters in the counter flow shower cooling tower. These equations are solved at every interval along height of cooling tower starting from top to get various properties of air and water at every level.

### 4.2.1 Simulation procedure

The procedure for solving these equations is an iterative method. Initially the exit conditions of air i.e. DBT and humidity of air at the exit of cooling tower is assumed. The first part of the solution is to solve the governing equations up to whole length of tower. If the convergence criteria is not satisfied after the first iterations the changes in the assumed values are made accordingly. When the predicted air values and the actual values are in close approximation to each other ( $\Delta e=10^{-3}$ ) i.e. they satisfy the convergence criteria the solution is obtained.

For the purpose of numerical integration of the differential equations, Runge Kutta method of fourth order with fifth order correction is employed. The system of differential equations for counter flow configuration is represented by set of equations (3.73 to 3.77). A set of initial values are supplied as input by the user.

The above procedure can be better understood through the flow diagram (Fig 4.26):

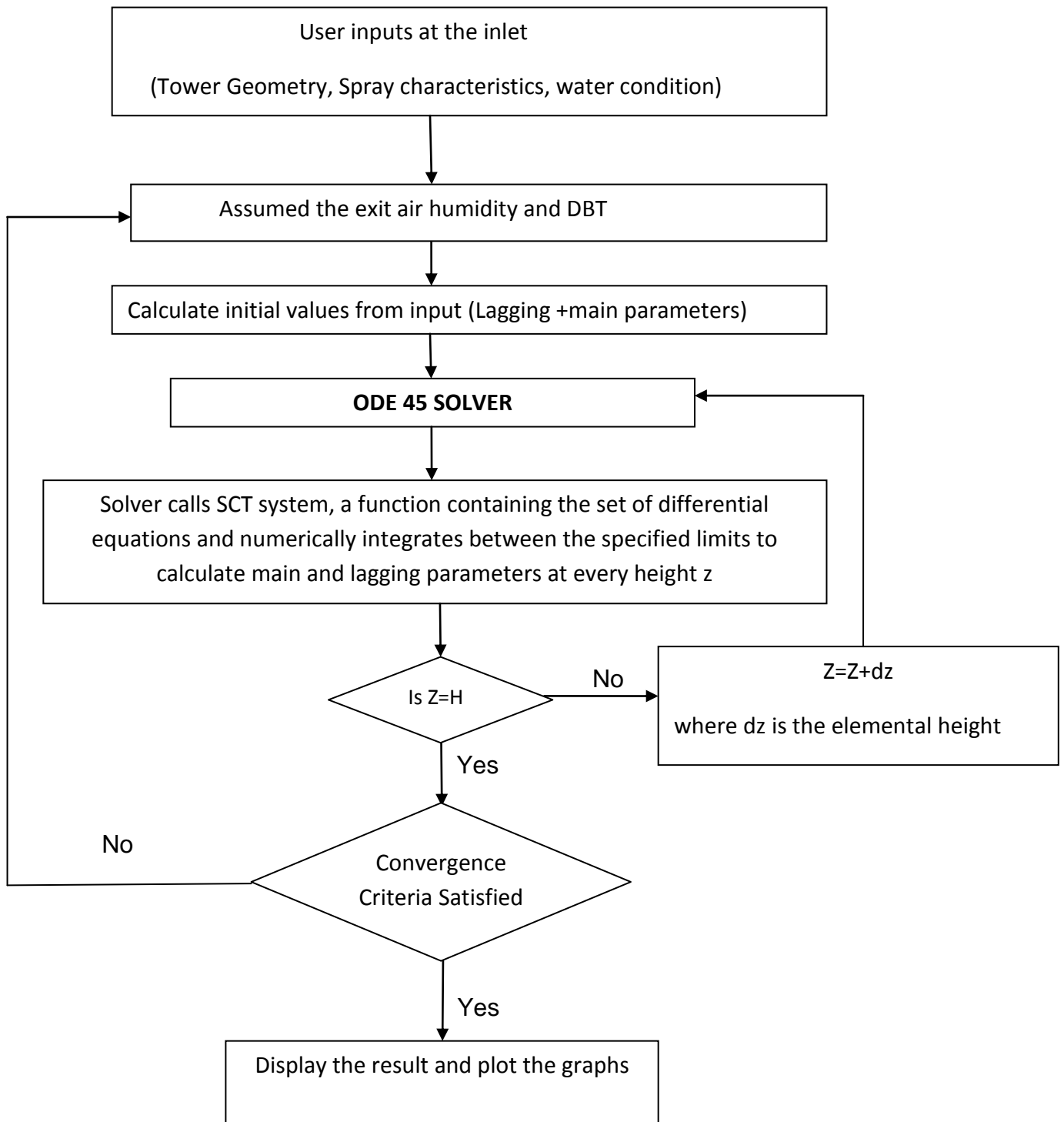


**Figure 4.26 Flow chart of numerical solution of counter flow**

#### 4.2.2 Boundary conditions

The input is boundary conditions which for parallel downward flow are:

- a) Tower geometry: Height, cross section area and shape of the tower.
- b) Spray characteristics: Droplet velocity, angle of projection, mean droplet diameter.
- c) Inlet air conditions: Air velocity, flow rate, assumed dry bulb temperature and relative humidity at air exit (Air enters from the bottom).
- d) Water condition: Mass flow rate and its temperature at inlet

#### 4.2.3 Model validation

The work carried out by Xiaoni et al [16] on a similar counter flow shower cooling tower has been used for model validation. The following assumptions are made:

- 1) The wall effect is neglected.
- 2) Only one dimensional motion of droplets is considered.
- 3) For same RGL, the air velocity is changed in steps and its affect on cooling tower performance is analyzed.
- 4) The minimum droplet diameter is selected from 0.7mm as below this diameter, droplets entrained out of tower for the selected air speed (6m/s).

The performance and operating parameters of the experimental SCT by Xianoi et al (16) are arranged in the following table 4.6

DBT of inlet air ( $^{\circ}\text{C}$ )	31.5
WBT of inlet air ( $^{\circ}\text{C}$ )	28
Tower basic dimensions (m)	9×9

Tower height(m)	5
Air flow rate (kg/s)	3.4
Volumetric flow rate (m <sup>3</sup> /s)	1000
Initial velocity of droplet(m/s)	6
Inlet water temperature( <sup>0</sup> C)	43
Outlet water temperature( <sup>0</sup> C)	33
<b>Predicted outlet temperature(<sup>0</sup>C)</b>	<b>34</b>

This simulation program achieved the predicted water temperature drop in the range of 34<sup>0</sup>C which is very closed to 33.4<sup>0</sup>C achieved by Xiaoni et al. this validate our model.

#### 4.2.4 Parametric Study

The various parameters selected as inputs are:

- 1) **Droplet Size:** droplet diameter range is selected from 0.7 ,0.8, 0.9 and 1.0 mm
- 2) **Inlet water temperature:** 43<sup>0</sup>C
- 3) **Droplet injected speed :** 5, 6, 7 and 8 m/s
- 4) **Inlet air temperature :** DBT 31.5<sup>0</sup>C, WBT28<sup>0</sup>C
- 5) **Tower geometry:** height 5m, Area 81m<sup>2</sup>
- 6) **Air inlet speed:** 1 , 2 and, 3m/s

##### **a) Influence of equivalent diameter of water droplets**

Figure 4.27 shows the variation of water outlet temperatures with the equivalent diameter of the water droplets for different initial velocities. It is clear that the influence

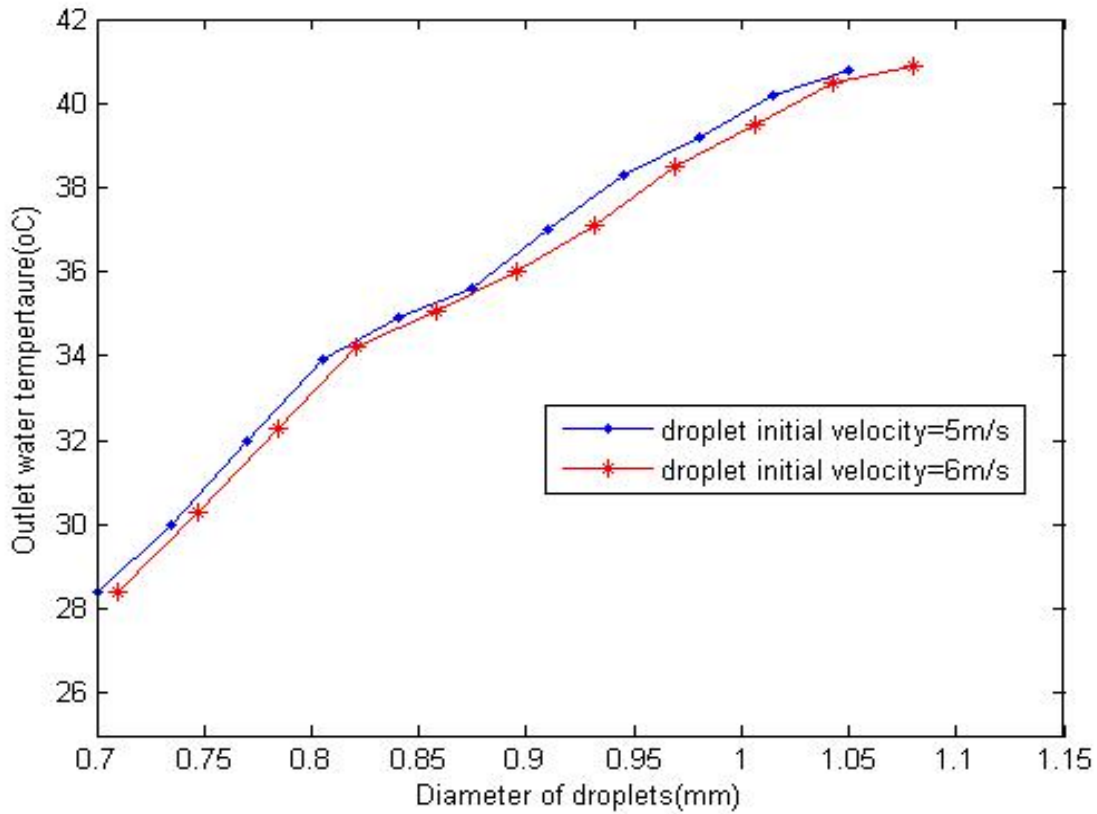


Figure 4.27 Influence of initial velocity and diameter on the outlet temperature for air  
Velocity 3 m/s

of the diameter on the result of the heat transfer is significant, The smaller is the diameter the more cooling of water is possible. It is clear from the figure that the greater the initial velocity, the better is the cooling effect, but at the same time if the initial velocity is much smaller, the droplets are easy to be entrained out of the tower by the air. So the initial velocity and the diameter of the water droplets should be chosen carefully, otherwise cooling effect may reduce.

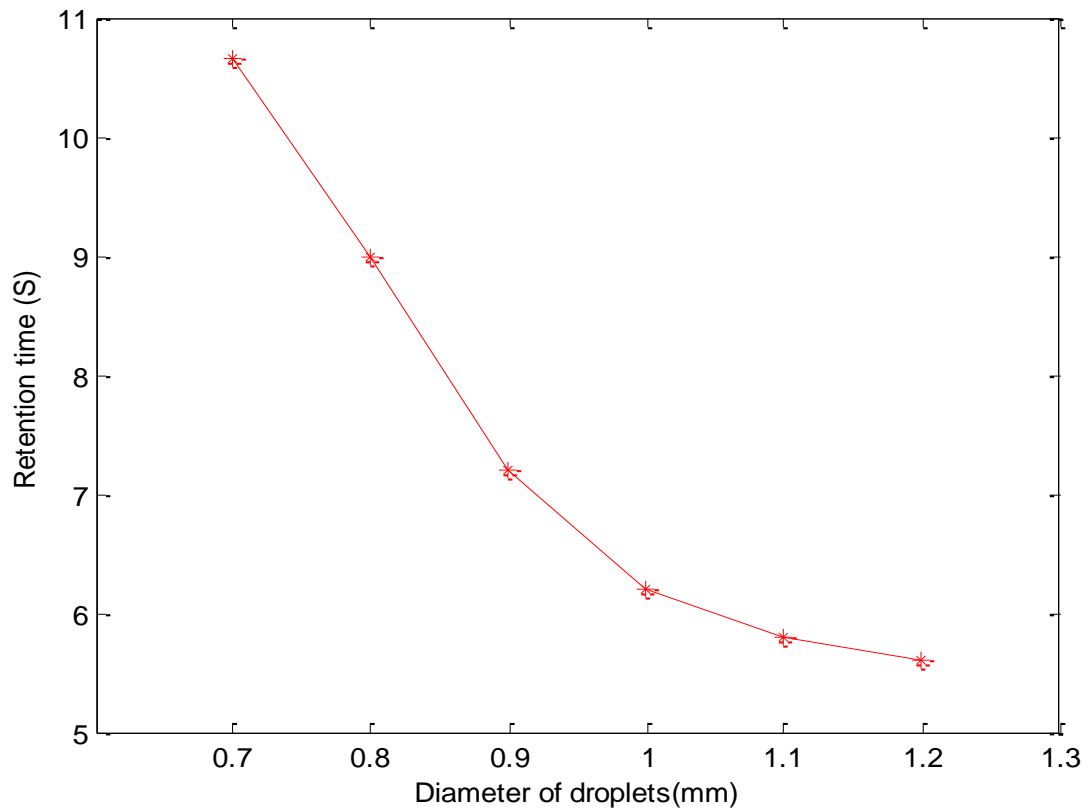


Figure 4.28 Effect of mean diameter on the retention time of the water droplet

Figure 4.28 shows as the diameter increases from 0.7 mm to 1.2 mm, the retention time decreases from 10.6s to 5.8s. So the smaller is the diameter, the greater is the cooling effect.



### Conclusions & Future Scope

This chapter describes the conclusion drawn from the results and discussions given in Chapter 4 followed by recommendations for the future work.

#### 5.1 Conclusions

A reliable computational model based on Pope equation [6] and modified by Xiaoni et al [16] is developed which is based on kinetic and thermodynamic analysis between the air and water droplet in a shower cooling tower. The model developed is applicable for downward parallel flow and counter flow cooling tower. A fourth order Runge-Kutta method is employed to solve the system of ordinary differential equations for both mono and multi droplets.

***The following conclusion can be drawn for parallel flow downward shower cooling tower:***

- 1) The model explain the air water interaction with variable properties along the whole length of cooling tower, .
- 2) The model gives satisfactory results with experimental data by Pearl Mutter et al [4] considering the uncertainty of test results, high sensitivity to droplet distribution of model & model approximations, the results obtained are found to be reasonably good.
- 3) The model is compared for different number of droplets & found to be highly sensitive for droplet distribution & for number of different sized droplets.

4) Exergy analysis of the model is also conducted and it is found that exergy is a strong function of reference conditions. .

***The following conclusion can be drawn for counter flow cooling tower***

1) A one dimensional heat and mass transfer computer model is developed which studied the heat and mass transfer mechanism of a water droplet as it moves from the top to the bottom of the tower with the air lift upward.

2) The factors affecting the cooling result have been studied.

3) It is clear from the simulation study that as small a mean diameter as possible is desirable for high performance. The factors of diameter, velocity have been studied in this model which helps to decide the proper size of the droplet to prevent the droplets being entrained out of the tower.

4) The model is validated within range by using data from the research paper of Xiaoni et al.

**Recommendation of Future work**

1) The existing counter flow model can be extended to multi droplet model includes wall effect and backward flow of droplets

2) As the model is highly sensitive to droplet distribution, future effort should be directed to analyze droplet distribution & improve input parameters of droplet distribution

3) A more rigorous software program can be developed in CFD.

## APPENDIX

### 1. Mass of droplet ,

Surface area of droplet,  $A_d = \pi d_d^2$  ,

$$\text{therefore, } \frac{m_d}{A_d} = \rho \frac{d_d}{6} .$$

### 2. The enthalpy of the water vapor at the bulk water temperature,

$$i_v = i_{fgw0} + c_{pv} T_w \quad (2a)$$

The enthalpy of saturated air evaluated at the local bulk water temperature,  $T_w$  , is given by

$$i_{masw} = c_{pa} T_w + w_{sw} (i_{fgw0} + c_{pv} T_w)$$

Using above two equations and rearranging find,

$$i_{masw} = c_{pa} T_w + w i_v + (w_{sw} - w) i_v \quad (2b)$$

The enthalpy of air-water vapor mixture per unit mass of dry air is expressed by

$$i_{ma} = c_{pa} T_a + w (i_{fgw0} + c_{pv} T_a) \quad (2c)$$

Taking the difference of the last two equations , the resultant equation can be simplified if the small differences in specific heats, which are evaluated at different temperatures are ignored,

$$T_w - T_a = \frac{(i_{masw} - i_{ma}) - (w_{sw} - w)i_v}{c_{pma}} \quad (2d)$$

3. **Lewis factor**,  $Le_f = \frac{h}{c_{pma} h_d}$ , is an indication of the relative rates of heat and mass transfer in an evaporative process. *Bonjakovic* developed an empirical relation for the Lewis factor  $Le_f$  for air-water vapor systems. The Lewis factor for unsaturated air, according to *Bosnjakovic*[24] is given by

$$Le_f = 0.865^{0.667} \frac{\left( \frac{w_{sw} + 0.662}{w_a + 0.622} - 1 \right)}{\left[ \ln \left( \frac{w_{sw} + 0.622}{w_a + 0.622} \right) \right]}$$

For droplet air interaction we have

$$L_{efwd} = \text{lewis factor} = L_e [W_{sw}(T_{wmean}), W]_a$$

which is a function of humidity ratio at bulk water temperature

4. According to the motion condition, **the drag coefficient,  $C_d$** , is expressed as[24]:

$$C_d = \left( \frac{24}{Re} \right) \left( 1 + \frac{Re^{\frac{2}{3}}}{6} \right) \quad Re \leq 1.9169 \quad (\text{laminar flow}) \quad (4a)$$

$$C_d = 18.5 / \text{Re}^{\frac{3}{5}} \quad 1.9169 \leq \text{Re} \leq 508.3917 \text{ (transition flow)} \quad (4b)$$

$$C_d = 0.44 \quad \text{Re} \geq 508.3917 \text{ (turbulent flow)} \quad (4c)$$

5. Consider the **shape of the body** of the tower (frustum of the cylinder)

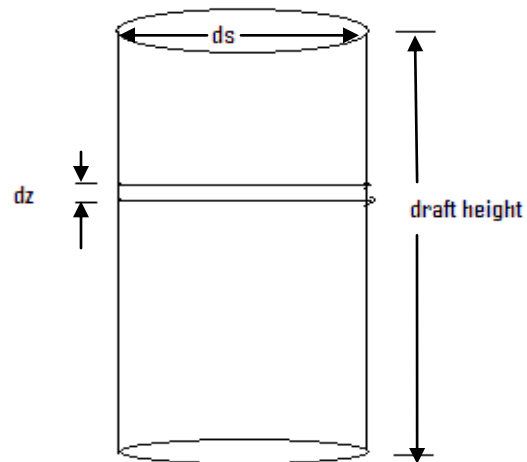


Fig.4.6

$$dA_w = dz \times (K_w)$$

where

$$K_w (\text{Perimeter of the Tower}) = \pi D_s$$

$D_s$  = Diameter of Cooling Tower in meter

$dA_w$  is the small wetted area of the wall

#### 6. Specific heat of water ( $c_p$ ) in J/Kg

$$c_p = 8155.993 - 28.0627 \times T + 5.11283 \times 10^{-2} \times T^2 + 2.17582 \times 10^{-13} \times T^6$$

where T is the Temperature in Kelvin.

#### Specific heat of saturated water in J/Kg

$$c_p = 1.3605 \times 10^3 + 2.31334T - 2.46784 \times 10^{-10} \times T^5 + 5.91332 \times 10^{-13} \times T^6$$

where T is the Temperature in Kelvin.

#### Specific heat of air ( $c_{pa}$ ) in J/Kg

$$c_{pa} = 1.045356 \times 10^3 - 3.161783 \times 10^{-1} \times T + 7.083814 \times 10^{-4} \times T^2 - 2.705209 \times 10^{-7} \times T^3$$

where T is the Temperature in Kelvin.

#### 7. Dynamic viscosity ( $\mu_a$ ) and kinematic viscosity ( $\nu_a$ ) of air are given by,

$$\mu_a = 2.287973 \times 10^{-6} + 6.259793 \times 10^{-8} T - 3.131956 \times 10^{-11} T^2 + 8.15038 \times 10^{-15} T^3$$

$$\nu_a = \frac{\mu_a}{\rho_a}$$

Kinematic Viscosity is in (m<sup>2</sup>/s) & T is in Kelvin.

**8)Dynamic viscosity( $\mu_v$ ) and kinematic viscosity( $\nu_v$ ) of vapor are given by,**

$$\mu_v = 2.562435 \times 10^{-6} + 1.816683 \times 10^{-8} T + 2.579066 \times 10^{-11} T^2 - 1.067299 \times 10^{-14} T^3$$

$$\nu_v = \frac{\mu_v}{\rho_v}$$

Kinematic Viscosity is in (m<sup>2</sup>/s) & T is in Kelvin.

Fraction of air( $x_a$ ),

$$x_a = \frac{1}{(1+1.608w)}$$

Fraction of air( $X_a$ ),

$$X_v = \frac{w}{(w+0.622)}$$

The kinematic viscosity of mixture of air and vapor

$$\nu = \frac{x_a \cdot \mu_a \cdot \sqrt{m_a} + x_v \cdot \mu_v \cdot \sqrt{m_v}}{\rho_a (x_a \sqrt{m_a} + x_v \cdot \sqrt{m_v})}$$

*Relations given by Godridge*

Ref. **General Electric Heat Transfer & Fluid Flow Data Book.**

### 9. Nusselt's number for wall

Since case is assumed to be that of a forced convection internal flow, the relation for Nusselt's no given by Gliensky is used.

**When Reynolds's number,  $Re > 2300$**

$$Nu = \left[ \frac{\frac{f}{8} (Re - 1000) Pr \left( 1 + \left( \frac{Dh}{height} \right)^{0.66} \right)}{1 + 12.7 \left( \frac{f}{8} \right)^{1/2} (Pr^{0.66} - 1)} \right]$$

**for  $Re < 2300$**

$$Nu = 3.66$$

**Where  $f$  is the friction factor given by**

$$f = \left[ 1.74 - f^{-0.5} - \log_{10} \left( e + \frac{1.87}{Re \sqrt{f}} \right) \right]$$

and  $e$  is the surface roughness ratio

**Pr is the Prandtl number given by,**

$$Pr = \mu c_p / k$$



And **Re** is **Reynolds's no.** given by

$$\text{Re} = \frac{VD_h}{\nu}$$

Where

$D_h$  = hydraulic diameter

$D_h = \frac{4A_c}{P}$  Where  $A_c$  cross sectional area and  $P$  is the wetted perimeter.

$\nu$  = kinematic viscosity

**10.** The chemical potential integrated between restricted state and the environmental state

at ambient temperature  $T_0$  is given by

$$\mu_{k0} - \mu_{k00} = R_k T_0 \ln \left( \frac{P_{k0}}{P_{k00}} \right)$$

where  $P_{k0}$  and  $P_{k00}$  are the partial pressures of k at restricted dead state and atmosphere respectively

Therefore

$$P_{k0} = x_{k0} P_{total}$$

and

$$P_{k00} = x_{k00} P_{total}$$

where

$P_{total}$  is the total pressure

therefore

$$\mu_{k0} - \mu_{k00} = R_k T_0 \ln \left( \frac{x_{k0}}{x_{k00}} \right)$$

11. Specific humidity of air is defined as the amount of water vapor present in the air per kg of the dry air

$$w = \frac{m_v}{m_a}$$

$$w = \left( \frac{m_v M_a}{M_v m_a} \right) \frac{M_v}{M_a}$$

where  $M_v$  and  $M_a$  are the molecular masses of Water and dry air respectively

therefore

$$w = \left( \frac{x_v}{x_a} \right) 1.608$$

$$\frac{w}{1.608} = \left( \frac{x_v}{x_a} \right) \quad (11a)$$

but we know that sum of the mole fractions of all the elements in the mixture equals to unity therefore

$$x_v + x_a = 1 \quad (11b)$$

hence solving the equations (11a) and (11b) we get.

$$x_a = \left( \frac{1}{1 + 1.608w} \right)$$

and

$$x_v = \left( \frac{1.608w}{1 + 1.608w} \right)$$

**12.** Relative humidity is defined as the ratio of the partial pressure of water vapor in a gaseous mixture of air and water vapor to the saturated vapor pressure of water at a given temperature. Relative humidity  $\theta$  can be expressed as

$$\theta = \frac{P_w}{P_{sat}}$$

also as the dead state for water is assumed to be a saturated state, the partial pressure at the dead state is equal to the saturation pressure of water, therefore

$$p_{w0} = p_{sat} = x_{w0}P$$

Also

$$p_{w00} = x_{w00}P$$

Therefore

$$\theta = \frac{x_{w00}}{x_{w0}}$$

**13)** As the restricted dead state for water is assumed to be saturated state

Therefore

$$h_0 = h_{f0}$$

enthalpy of water at any given state other than saturation state will be given by

$$h_w = h_{fw} + v_f (p - p_{sat})$$

also by above arguments

$$s_0 = s_{f0}$$

And

$$S_w = S_{fw}$$

## References

- 1) B. Givoni, "Semi-empirical model of a building with a passive evaporative cooling tower", Sol. Energy, 50 (1993) 425-434
- 2) Carew Paul and Joubert Gerry, Shower Tower, "Miele Showroom, Johannesburg, South Africa", 23<sup>rd</sup> conference on Passive and low energy, 6-8 Sep 2006.
- 3) Webster A and Mannison, "An innovative approach of Passive cooling using four down draft cooling tower", Charles Sturt University, Australia (2003)
- 4) Pearlmuter D, Erel E, Etzian Y, Meir I. A, Di H, "Refining the use of evaporative cooling in an experimental down draft cooling tower", Energy and buildings 23(1996)
- 5) Jaber, H., and Webb, R. L., "Design of cooling towers by the effectiveness-NTU method," ASME J. Heat Transfer, 111, 837- 843, 1989.
- 6) Kloppers, J.C., D.G Kroger, 2004, "A critical investigation into the heat and mass transfer analysis of counter flow wet-cooling towers," International Journal of Heat and Mass Transfer, 48, 765-777, 2005.
- 7) Kloppers, J.C., D.G Kroger, "Cooling tower performance evaluation-Merkel, Poppe and e-NTU methods of analysis," Trans, ASME: Journal of Engineering for Gas Turbines and Power, 127, 1-7, 2005.

- 8) Kloppers, J.C., D.G Kroger, "The Lewis factor and its influence on the performance prediction of wet-cooling towers," *International Journal of Thermal Sciences*, 44, 879-884, 2005.
- 9) Kloppers, J.C., D.G Kroger, "Loss coefficient correlation for wet cooling towers," *Applied Thermal Engineering*, 23, 2201-11, 2003.
- 10) Naphon P., "Study of heat transfer characteristics of an evaporative cooling tower", *International Communications in Heat and Mass Transfer*, 32, 1066-74, 2005.
- 11) Kachhwaha S.S., Samsher, Sunil Soni, " Heat and mass transfer analysis of a counter flow wet cooling tower", *Proceedings of 14<sup>th</sup> ISME International Conference on Mechanical Engg. in Knowledge Age*, December 12-14,2005 at Delhi College of Engineering, Delhi India, 621-627,2005.
- 12) Sutherland, J. W., "Analysis of Mechanical draft counter flow air water cooling towers," *ASME J. Heat Transfer*, 105, 576-583, 1983.
- 13) Bilal A. Qureshi, Syed M. Zubair, "A complete model of wet cooling towers with fouling in fills", *Applied Thermal Engineering* 26, 1982-1989,2006.
- 14) Bilal A. Qureshi, Syed M. Zubair « Second-law based performance evaluation of cool towers and evaporative heat exchangers », *International Journal of Thermal Science*: 46 (2007) 188-198
- 15) Xiaoni Qi , Zhenyan Liu, Dandan Li "Performance characteristics of a shower cooling tower."
- 16) Xiaoni Qi , Zhenyan Liu "Further investigation on the performance of a shower cooling tower."

tower”

17) Thirapong Muangnoi, Wanchai Asvapoositkul, Somchai Wongwises, “An exergy analysis on the performance of a counterflow wet cooling tower”, Applied Thermal Engineering 27 (2007) 910-917

18) Thirapong Muangnoi, Wanchai Asvapoositkul, Somchai Wongwises, “ Effects of inlet relative humidity and inlet temperature on the performance of counter flow wet cooling tower based on exergy analysis”, (2008) doi 10, 1016

19) A. Bejan , Advanced Engineering Thermodynamics second ed. Wiley 1997

20) M.J. Moran, Availability Analysis: A guide to efficient use, Prentice hall New Jersey, 1982

21) Viljoen D. J, “Evaluation and performance prediction of Cooling Tower spray zones”, M.Sc.(Engineering) thesis, University of Stellenbosch, South Africa, December 2006.

22) Terblanche R, Reuter H.C, Kroger D.G, “Drop size distribution below different cooling tower fills”, Applied Thermal Engineering 29(2009) 1552-1560

23) R. Suresh Kumar, S.R.Kale, P.L.Dhar,” Heat and mass transfer process between water spray and ambient air-I. Experimental data” Applied Thermal Engineering 28(2008)349-360

24) Bosnjakovic F. Technical thermodynamics. Dresden: Theodor Steinkopf Press;1962

25) Levich VG. Physicochemical hydrodynamics. NJ: Prentice-Hall; 1962





